hp66 Protein Paralogs:
SUMO Modification and Complex Formation

Inaugural-Dissertation

zur

Erlangung des Doktorgrades

der Naturwissenshaftlichen Fachbereiche

der Justus-Liebig-Universität Gießen

-Dr.rer.nat.-

vorgelegt von

Zihua Gong

aus China

Gießen, September 2006

Die vorliegende Arbeit wurde am Institut für Genetik des Fachbereiches 08 der Justus-Liebig-Universität Gießen, in der Zeit von March 2003 bis September 2006 unter der Leitung von Prof. Dr. Rainer Renkawitz angefertigt.

PUBLICATIONS

Gong Z, Brackertz M, Renkawitz R.
SUMO modification enhances p66 mediated transcriptional repression of the Mi-2/NuRD complex. *Molecular and Cellular Biology,* 2006, 26: 4519-28.

Brackertz M, **Gong Z**, Leers J, Renkawitz R.
p66 alpha and p66 beta of the Mi-2/NuRD complex mediated MBD2 and histone interaction. *Nucleic Acids Research, 2006,* 34: 397-406.

1. Gutachter:	Prof.Dr.Rainer Renkawitz Institut für Genetik Justus-Liebig-Universität Gießen
2. Gutachter:	Prof.Dr. Ewald Beck Institut für Biochemie Universitätsklinikum Giessen und Marburg GmBH
3. Prüfer:	Prof.Dr. Wolfgang Clauss Institut für Tierphysiologie Justus-Liebig-Universität Gießen

Contents

Zusammenfassung

Die Methylierung von CpG-Dinukleotiden in Eukaryotes ist eine epigenetische Markierung, die eine Unterdrückung der Transkription der Gene in den betroffenen Bereichen des Genoms zur Folge hat. Hierbei rekrutiert das Methyl-CpG bindende Protein MBD2 den reprimierenden Mi2/NuRD Komplex an methylierte Promotoren. Die Proteine p66α und p66β sind Bestandteile dieses Komplexes und fungieren als starke Repressoren, jedoch sind bisher keine Details zum Mechanismus der transkriptionellen Repression durch diese Faktoren beschrieben.

Die vorliegenden Untersuchungen belegen eine Beteiligung der Deacetylierung von Histonen an der transkriptionellen Repression durch p66α und p66β. Zwei Repressions-Domänen in p66α und eine in p66β wurden charakterisiert. Weiterhin zeigte sich, dass die Aminosäure Lysin an Position 149 von p66α essentiell für die Interaktion mit MBD2 und die Lokalisation von p66α innerhalb des Zellkerns ist. Eine Analyse von p66 auf eine mögliche SUMO (small ubiquitin-like modifier)-Modifikation, die in zunehmenden Maße mit der Regulation der Aktivität von Transkriptionsfaktoren in Verbindung gebracht wird, identifiziert p66α und p66β als Zielproteine dieser Modifikation. Sowohl bei p66α, als auch bei p66β führt die SUMO-Modifikation zu einer Verstärkung der transkriptionellen Repression. Die SUMO-Modifikation erfolgt an Lysin 30 und Lysin 487 in p66α und an Lysin 33 in p66β, wobei die Mutation der SUMO-Zielsequenzen verglichen mit den Wildtyp p66 Formen bei beiden Proteinen keine Veränderung der zellulären Lokalisation hervorruft. Darüber hinaus wird HDAC1 (Histonedeacetylase 1) des Mi2/NuRD Komplexes an Lysin 30 von p66α, das eine TSA (Trichostatin A) sensitive Repression aufweist, rekrutiert. Die Mutation von Lysin 33, die keine Sensitivität gegenüber TSA zeigt, hebt die Interaktion zwischen p66β und RbAp46 (Rb Associated protein 46) *in vivo* auf. Zusammenfassend weisen diese Ergebnisse darauf hin, dass sowohl die Interaktion innerhalb des Mi2/NuRD Komplexes, als auch die optimale Repression durch SUMO-Modifikation vermittelt wird.

Zur detaillierten Analyse von p66 enthaltenden Proteinkomplexen wurden stabile Zelllinien, die rekombinante p66 Proteine exprimieren etabliert. Die Isolierung der Proteinkomplexe erfolgte durch zweistufige chromatographischer Trennung und anschließende Reinigung über die mit p66 verknüpfte Affinitätsmarkierung. Western-Blot Analysen zeigten, dass die rekombinanten p66 Proteine mit verschiedenen bekannten Komponenten des Mi2/NuRD Komplexes, wie MBD2 und PRMT5, assoziiert vorliegen und belegen damit die Eignung dieses Systems für eine weitere Charakterisierung der p66 Komplexe.

Summary

Methylation of CpG dinucleotides in eukaryotes is an epigenetic mark that is implicated in transcriptional silencing. Methyl-CpG binding protein MBD2 serves to recruit the Mi-2/NuRD repressive complex to a methylated promoter. Human p66α and p66β, which are components of Mi-2/NuRD complex, are two potent transcriptional repressors that interact with MBD2, but no details concerning the mechanism in hp66 proteins-mediated transcriptional repression have been described.

The current work showed that transcriptional repression mediated by hp66α and hp66β is partially dependent on histone deacetylation. Two major repression domains in hp66α, and one in hp66β were characterized. In addition, the amino acid Lys-149 of hp66α was identified to be essential for the interaction with MBD2 and the nuclear localization of hp66α. Emerging evidence indicated that SUMO (small ubiquitin-like modifier) modification negatively regulates the transcriptional activity of transcription factors. The study gave evidence that both hp66α and hp66β proteins can be SUMOylated, and furthermore that SUMO modification enhances hp66-mediated transcriptional repression. Two major SUMO modification sites at Lys-30 and Lys-487 of hp66α, and one major SUMO modification site at Lys-33 of hp66β were identified. Mutational analysis of the SUMO modification sites in hp66α or hp66β revealed that there is no change in localization in comparison to wild type hp66. But interestingly, the Mi-2/NuRD complex component HDAC1 (histone deacetylase 1) is recruited to the SUMO modification site Lys-30 of hp66α which shows TSA (Trichostatin A) sensitivity, whereas mutation of the SUMO modification site Lys-33, which shows TSA insensitivity, abolishes the interaction between hp66β and RbAp46 (Rb associated protein 46) *in vivo*. Taken together, these results suggest that both, interactions within the Mi-2/NuRD complex as well as optimal repression are mediated by SUMOylation.

Moreover, to gain further insights into protein complexes containing hp66 proteins, stable cell lines expressing individually both hp66 proteins were established. After a two-step chromatographic purification and a subsequent FLAG affinity purification protein complexes were isolated. Western blotting analysis revealed that several subunits of the Mi-2/NuRD complex as well as MBD2, and PRMT5 were found to be associated with FLAG-hp66 proteins.

1 INTRODUCTION

1.1 Molecular mechanisms of gene silencing

1.1.1 Basic principles of gene expression

In general, histones and DNA are organized into chromatin by wrapping DNA around histone proteins octamers. It has long been known that structural changes in the chromatin have an impact on gene expression. Active gene transcription correlates with an open chromatin conformation, whereas inactive gene transcription relates to a closed chromatin conformation (Rountree et al., 2001; Wu and Grunstein, 2000). These dynamic chromatin states are controlled by reversible epigenetic patterns of DNA methylation and histone modifications (Feinberg and Tycko, 2004). Basically, active regions of chromatin have unmethylated DNA and hyperacetylated histones, whereas inactive regions of chromatin contain methylated DNA and deacetylated histones (Peterson and Laniel, 2004).

1.1.2 DNA methylation

The term “Epigenetics” refers to heritable changes in gene expression that occur without alterations in the gene nucleotide sequence (Roloff and Nuber, 2005). Epigenetic events such as DNA methylation play an essential part in regulating gene expression, genomic stability, X chromosome inactivation, and chromatin structure (Jones and Baylin, 2002). Significant advances have been made in elucidating mechanisms underlying DNA methylation and its effects on chromatin structure and gene trancription. DNA methylation occurs at the 5' position of the cytosine ring by covalent addition of a methyl group following production of 5-methylcytosine (Bird, 2002). In mammalian DNA, 5-methylcytosine is primarily at palindromic sequence CpG. Roughly 70% of all CpG dinucleotides in the mammalian genome are methylated. The majority of unmethylated CpG sites locate more frequently within CpG islands (clusters of high-density CpG dinucleotides) found typically in or near the promoter and first exon regions of genes (Herman and Baylin, 2003).

1.1.3 DNA methyltransferases

The addition of methyl groups is carried out by a family of enzymes, DNA methyltransferases (DNMTs). In mouse development, the maintenance methyltransferase DNMT1 appears to copy established methylation patterns onto the new DNA strand, whereas the *de novo* methyltransferase DNMT3a and DNMT3b seem to be responsible for mediating cytosine methylation at previously unmethylated CpG sites during DNA replication (Bestor, 2000; Okano et al., 1999; Okano et al., 1998). Recent evidences have uncovered the mechanisms by which DNMT enzymes are recruited to the targeted DNA sequences for *de novo* methylation. These studies have demonstrated at least three possible pathways by which *de novo* methylation might be targeted. First, DNMT3 enzymes themselves might recognize DNA or chromatin via specific domains. It has been shown that the conserved PWWP domain of DMNT3 is required to target the catalytic activity to regions of pericentromeric heterochromatin of the genome, and further mutation of the PWWP domain of the human DNMT3b protein causes ICF syndrome, a severe autosomal recessive disease in humans (Shirohzu et al., 2002). Second, DNMT3a and DNMT3b might be recruited through interactions with transcription factors. More recent evidence have shown that Myc is required for recruitment of DNMT3a to the $p21^{cip1}$ promoter region, resulting in *de novo* methylation of the $p21^{cip1}$ promoter, which indicates that DNMT3 can be recruited to the targeted DNA sequence via protein–protein interactions with some transcription factors (Brenner et al., 2005). Third, the RNA-mediated interference (RNAi) system might target *de novo* methylation to specific DNA sequences. Two independent studies have reported that the target gene is efficiently silenced concomitant with *de novo* DNA methylation of the corresponding promoter sequence, when double-stranded RNA corresponding to the promoter sequence of a gene is introduced into mammalian cells (Kawasaki and Taira, 2004; Morris et al., 2004). Although initial evidence supports its existence, the mechanism of the RNAi-directed DNA methylation during gene silencing remains poorly understood.

1.1.4 **DNA methylation and gene silencing**

It is well known that DNA methylation is assocated with a repressive chromatin state (Kass et al., 1997; Siegfried et al., 1999). There are several general models by which DNA methylation represses gene transcription (Fig.1.1): first, certain transcriptional activators are unable to bind to cognate DNA recognition sequences when methylated (Watt and Molloy, 1988); and second,

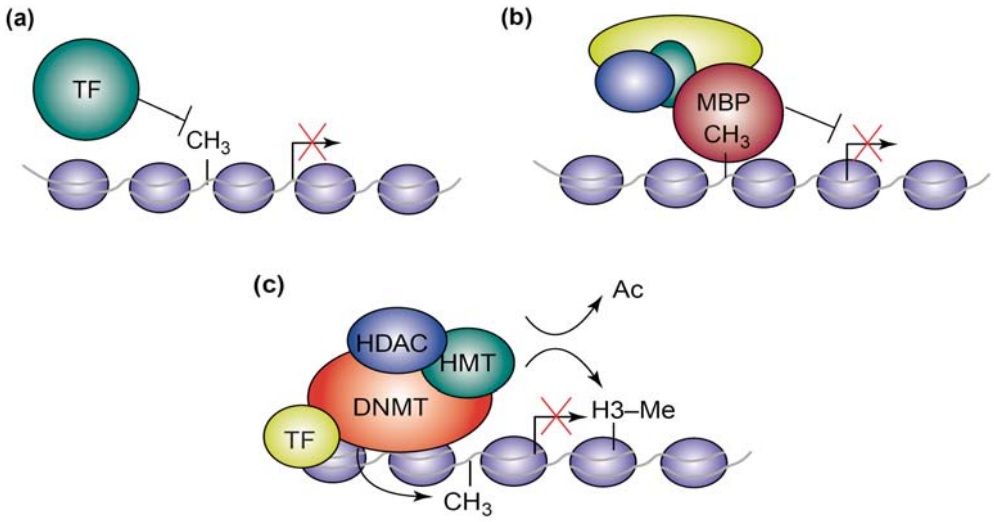

Figure 1.1 Mechanisms of DNA methylation-mediated repression. (a) DNA methylation in the cognate DNA-binding sequences of some transcription factors (TF) can result in inhibition of DNA binding. By blocking activators from binding targets sites, DNA methylation directly inhibits transcriptional activation. **(b)** Methyl-CpG-binding proteins (MBPs) directly recognize methylated DNA and recruit co-repressor molecules to silence transcription and to modify surrounding chromatin. **(c)** In addition to their DNA methyltransferase activities, DNMT enzymes are also physically linked to histone deacetylase (HDAC) and histone methyltransferase (HMT) activities. In this case, the addition of methyl groups to DNA is coupled to transcriptional repression and chromatin modification. Modified after (Klose and Bird, 2006).

Methyl-CpG-binding proteins (MBPs) recognize methyl-CpG and recruit transcriptional co-repressor molecules to repress transcription and to modify local chromatin architecture, indicating a link between DNA methylation and chromatin remodeling and modification (Jones et al., 1998; Nan et al., 1998; Ng et al., 1999; Sarraf and Stancheva, 2004; Wade et al., 1999; Zhang et al., 1999). Furthermore, another pathway of DNA methylation-mediated silencing has recently been discovered. As discussed above, DNMTs can be targeted to specific DNA sequence through interaction with some transcriptional repressors, resulting in methylation of DNA. Recent evidence showed that DNMTs physically interact with histone deacetylases, histone methyltransferases, and ATP-dependent chromatin remodeling protein hSNF2H independent of its catalytic domain, indicating that DNMTs mediate gene silencing through recruitment of transcriptional repressors such as HDAC1 (Bai et al., 2005; Fuks et al., 2000; Fuks et al., 2001; Fuks et al., 2003; Geiman et al., 2004; Lehnertz et al., 2003; Robertson et al., 2000; Rountree et al., 2000).

1.1.5 Methyl-CpG binding proteins (MBPs)

The fact that methylated CpG islands relate to gene silencing led to search for transcription

factors that are able to recognize and interpret these epigenetic events. In the early 1990s, the family of proteins that specifically recognize methyl-CpG were identified. MeCP2 was the first such protein to be purified and characterized (Lewis et al., 1992). An additional four members, MBD1, MBD2, MBD3, and MBD4 have been identified based on conserved amino acid sequences homologous to the methyl-CpG-binding domain (MBD) of MeCP2 (Hendrich and Bird, 1998). Alignment of the MBPs represents that the MBD of MBD1, MBD2 and MBD3 are more similar to each other than to those of either MBD4 or MeCP2, while the MBD of MBD4 is most similar to that of MeCP2 (Ballestar and Wolffe, 2001; Hendrich and Tweedie, 2003). The mammalian MBD proteins (MBPs) are shown in Fig.1.2. With the exception of MBD4 that is well defined for its role in DNA repair (Hendrich et al., 1999; Millar et al., 2002), other members of this family are transcriptional repressor which is associated with histone deacetylases in the context of chromatin remodeling (Feng and Zhang, 2001; Jones et al., 1998; Nan et al., 1998; Ng et al., 1999; Sarraf and Stancheva, 2004; Wade et al., 1999; Zhang et al., 1999). However, more recent evidence suggested that MBD4 might also be a transcriptional repressor (Kondo et al., 2005). Four members of this family, MeCP2, MBD1, MBD2 and MBD4 are able to bind to methylated DNA with the exception of MBD3, which contains amino acid substitutions that prevent binding to methyl-CpG. A novel MBP named Kaiso lacks the MBD, but recognizes methylated CpG islands directly using two of three adjoining zinc-finger motifs near its carboxy terminus (Prokhortchouk et al., 2001). There are several potential mechanisms for transcriptional repression mediated by MBPs. First, as discussed earlier, MBPs binding to methylated DNA leads to local recruitment of histone deacetylases, which in turn results in transcriptional repression. Second, MBPs bind to methylated DNA and physically prevent access to the sequence by transcription factors. Third, MBPs bind to methylated DNA and locally modify chromatin structure (Wade, 2001).

1.1.5.1 MeCP2

MeCP2 is the first member of MBPs that specifically binds to a single, fully symmetrically positioned methylated CpG site (Lewis et al., 1992), however, a recent study has shown that enrichment for A/T base pairs, (A/T)≥4, adjacent to methyl-CpG dinucleotides is essential for high-affinity binding to MeCP2 target sites of its known target genes, *Bdnf* and *Dlx6*, indicating

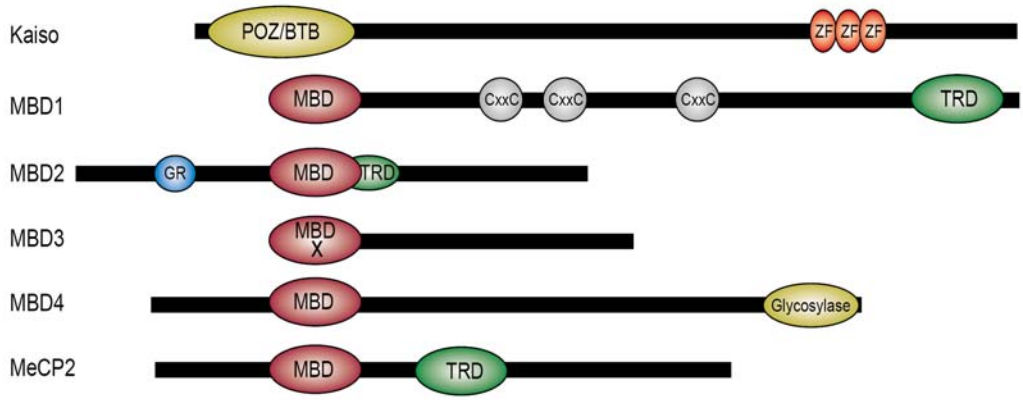

Figure 1.2 A family of methyl-CpG-binding proteins (MBPs). Six mammalian MBPs have been characterized so far. Kaiso is an atypical MBP, because it depends on a zinc-finger domain (ZF) to recognize methylated DNA and a POZ/BTB domain to repress transcription. MBD1 uses its methyl-binding domain (MBD) to bind methylated DNA sequences. In addition, MBD1 contains three zinc-binding domains (CxxC), one of which binds specifically to non-methylated CpG dinucleotides, and a C-terminal transcriptional repression domain (TRD). MBD2 possesses an MBD that overlaps with its TRD domain, and a GR repeat at its N terminus. MBD3 contains a well-conserved MBD domain that does not recognize methylated DNA owing to crucial amino acid changes. MBD4 binds methylated DNA through an MBD domain and has a C-terminal glycosylase domain that is important for is function in DNA repair. MeCP2 is the founding member of the MBD protein family and contains a conserved MBD domain and an adjacent TRD domain (Klose and Bird, 2006).

the target genes of MeCP2 appear to require this additional sequence specificity (Klose et al., 2005). This requirement for specific DNA sequences also applies to other MBPs such as MBD1, MBD4, and Kaiso with the exception of MBD2 that only binds specificly to methyl-CpG sites (Fujita et al., 2000; Klose et al., 2005; Prokhortchouk et al., 2001). MeCP2 is a chromatin associated nuclear protein of molecular weight approximately 55KDa (Nan et al., 1993). Two alternatively spliced MeCP2 transcripts have been identified: MeCP2A and the slightly longer MeCP2B, which differ only in their most 5' regions (Kriaucionis and Bird, 2004; Mnatzakanian et al., 2004). It is also the MeCP2 protein in which the MBD was first well-defined, and providing the molecular link between DNA methylation and histone modification(Fuks et al., 2003; Jones et al., 1998; Nan et al., 1993; Nan et al., 1998). MeCP2 is found to localize to pericentromeric heterochromatin, which contains highly methylated major satellite DNA in mouse cells (Fujita et al., 1999). In fact, it has been shown that MeCP2 is able to bind nucleosomal DNA to form discrete complexes, providing a molecular mechanism by which MeCP2 can gain access to chromatin and recruit corepressor complexes to further modify local chromatin structure (Chandler et al., 1999). Considerable efforts have been put into understanding how MeCP2 repress transription. It has been reported that MeCP2 represses

transcription of methylated promoters, but does not repress non-methylated promoters *in vitro* and *in vivo* (Kaludov and Wolffe, 2000; Nan et al., 1997). A major breakthrough is that the transcriptional repression domain (TRD) of MeCP2 was found to interact with a Sin3A co-repressor complex containing HDACs, thus leads to the establishment and maintenance of repressive chromatin architecture (Jones et al., 1998; Nan et al., 1998). This important finding provided the first link between DNA methylation-mediated transcriptional repression and histone modifications. Histone methylation is another key epigenetic mark for the organization of chromatin structure and the regulation of gene expression (Kouzarides, 2002). In particular, methylation at lysine 9 of histone H3 (H3K9) is associated with gene silencing. MeCP2 has also been shown to repress transcription throuth H3K9 methylation, which is carried out by the histone lysine methyltransferase SUV39H1 (Fuks et al., 2003). Nevertheless, other evidence showed HDAC-independent transcriptional repression by MeCP2 (Yu et al., 2000), indicating that MeCP2 is able to repress transcription via "two layers" mechanisms.

Lines of evidences have been indicated that MeCP2 is required in neurons for normal brain function. Mutations in the *MeCP2* gene cause a RTT-like phenotype in mice (Chen et al., 2001; Guy et al., 2001), and lead to Rett syndrome (RTT) in humans (Amir et al., 1999), which is a progressive neurodevelopmental disorder that occurs almost exclusively in females (Kerr et al., 2001). Take together, aberrent MeCP2 might account for more than 95% of sporadic cases of classical Rett syndrome in females (Archer et al., 2006). Several mouse models have advanced our understanding of the function of MeCP2 in the mechanisms that underlie Rett syndrome (Bienvenu and Chelly, 2006). Microarray-based global gene expression profiling analysis has revealed subtle changes between wild-type and *MeCP2* knockout mice brains (Nuber et al., 2005; Tudor et al., 2002). In addition, recent studies revealed that several imprinted genes such as *Dlx5*, *Dlx6* and *Ube3A*, show loss of normal expression in brain tissue of *MeCP2*-null mice (Horike et al., 2005; Makedonski et al., 2005; Samaco et al., 2005), this is consistent with that DNA methylation is important in the regulation of imprinted gene expression. Recent results suggested that the function of MeCP2 might be more complicated. MeCP2 was shown to have a high-affinity RNA binding activity independent of the MBD, and regulate alternative splicing via an interaction with the RNA-binding protein YB1 (Jeffery and Nakielny, 2004; Young et al., 2005). The finding suggested that MeCP2 regulates transcription and mRNA splicing of some of its targets through multiple layers of epigenetic regulation.

1.1.5.2 MBD1

MBD1 contains, in addition to the MBD and the TRD, a cysteine-rich CXXC sequence, which is similar to DNA methyltransferase 1 (DNMT1) (Cross et al., 1997). Like MeCP2, MBD1 requires only one symmetrically methylated CpG to bind DNA. So far, at least four MBD1 isoforms were identified including MBD1v1-4, which are alternatively spliced with variations in the number of CXXC domains as well as differences at the C-terminus (Fujita et al., 1999; Hendrich and Bird, 1998). Characterization of the CXXC domains in MBD1 revealed that the third CXXC domain has DNA binding capacity, regardless of the methylation status (Fujita et al., 2000). Thus, MBD1 is unique among the MBPs in that it is able to bind both unmethylated promoters via a third CXXC motif and methylated promoters via the MBD domain, which in turn leads to repress transcription (Nakao et al., 2001). The biological significance of this dual DNA-binding capacity of MBD1 is currently unknown. The repression by MBD1 has been reported to be HDAC dependent (Ng et al., 2000). Whether HDAC-independent mechanisms of repression exist for MBD1 remains unclear, since MBD1 has not been placed in a known repressor complex. MBD1 has been demonstrated to form a transient complex with histone H3K9 methyltransferase enzyme SETDB1, and the chromatin assembly factor CAF-1 during S phase of the cell cycle when DNA replication occurs, indicating MBD1 binding to methylated CpG sites associates with the DNA replication machinery (Sarraf and Stancheva, 2004). Also similar to MeCP2, MBD1 is an abundant, chromosomal protein (Ng et al., 2000), and localizes to the hypermethylated regions of chromosome 1q12 (Fujita et al., 1999). As determined from nuclear magnetic resonance (NMR) spectroscopic analysis, the MBD is suggested to interact with a methyl-CpG pair in the major groove of a standard B-form DNA (Wakefield et al., 1999). Further studies will explore the molecular basis of genome regulation by MBD1 and its functional relationship with other MBPs.

1.1.5.3 MBD2

There are two potential forms of MBD2, full-length protein (MBD2a, 43KDa) and N-terminal truncation (MBD2b, 29KDa), which are generated from a single gene that corresponding to alternative translational start codon (Hendrich et al., 1999; Hendrich and Bird, 1998). Recent studies revealed that MBD2a is able to bind methylated cyclic AMP (cAMP)-responsive

element (CRE) and repress its transcription via recruitment of MeCP1 corepressor complex. On the other hand, MBD2a could activate unmethylated CRE transcription through association with the CBP/RNA helicase A/Pol II complex. The results indicated that MBD2a has dual function in gene regulation based on DNA methylation status on CRE (Fujita et al., 2003). The truncated MBD2b protein was originally described as a DNA demethylase (Bhattacharya et al., 1999), however, this discovery failed to be confirmed by others, and rather suggested that it may also function in transcriptional repression (Boeke et al., 2000; Ng et al., 1999; Wade et al., 1999). MBD2 has a transcriptional repression domain that overlaps with the MBD that confers both transcriptional repression as well as the interaction with Sin3A (Boeke et al., 2000). Recently, MBD2-interacting zinc finger (MIZF) was identified as a novel interaction partner of MBD2. MIZF can bind to a specific recognition sequence within the promoter of target gene, and thus repress transcription in an HDAC-dependent manner and enhance MBD2-mediated repression, indicating that MIZF may recruit MBD2, and potentially also the Mi-2/NuRD repressor complex, to mediate transcriptional repression of methylated regions (Sekimata and Homma, 2004; Sekimata et al., 2001). MBD2 has been reported to be a component of MeCP1 complex that consists of additional Mi-2/NuRD chromatin remodeling complex, which represses transcription from methylated reporter gene in an HDAC-dependent manner (Feng and Zhang, 2001; Ng et al., 1999). MBD2 is able to bind a single methyl CpG dinucleotide and overexpression of GFP-MBD2 localizes to major satellite DNA in mouse cells (Hendrich and Bird, 1998). Unlike MBD2, *Mbd3* knockout mice dies during early embryogenesis, whereas *Mbd2*-null mice display a normal methylation pattern and does not show any defect in genomic imprinting or silencing of endogenous transposable elements (Hendrich et al., 2001). Moreover, significantly reduced repression of methylated reporter genes is seen in *Mbd2*-deficient cell lines, further confirming that MBD2 has a role in DNA methylation-mediated gene silencing (Hendrich et al., 2001).

1.1.5.4 MBD3

MBD3, the smallest member of the MBPs family, coding for a protein of about 32KDa, shares extensive sequence similarity to MBD2 outside the MBD motif, differing only in the sizes of their introns in the vertebrates (Hendrich and Bird, 1998). This suggests a recent gene duplication event, which is supported by the fact that MBD2/3 protein is encoded by a single

gene in invertebrate genomes (Hendrich et al., 1999). Due to the point substitutions in two highly conserved amino acids, mammalian MBD3 lacks the ability to recognize methylated DNA (Hendrich and Bird, 1998), whereas *Xenopus* MBD3 is able to bind with high affinity to methylated CpG similar to that of MeCP2 (Wade et al., 1999), suggesting that the capacity to recognize methylated DNA by MBD3 is lost during the evolution of mammals but retained in amphibians. Moreover, overexpressed MBD3-GFP is shown to accumulate in many nuclear foci, and does not associate with the highly methylated major satellite DNA in mouse cells (Hendrich and Bird, 1998). In addition, MBD3 is crucial to normal mammalian development as MBD3 knockout mice leads to embryonic lethality immediately after implantation of the embryo (Hendrich et al., 2001). A recent study showed that embryonic stem cells lacking MBD3 are viable and undergo the initial steps of differentiation, but fail to commit to developmental lineages, indicating MBD3-NuRD mediated gene silencing is not absolutely required for embryonic stem cells differentiation, however, provides a new link between preservation of the undifferentiated states and the capacity to differentiation (Kaji et al., 2006). It is well known that MBD3 is a component of the nucleosome remodeling and histone deacetylation (NuRD) corepressor complex containing HDACs, a chromatin remodeling ATPase and other proteins (Le Guezennec et al., 2006; Wade et al., 1999; Zhang et al., 1999). It has not yet been proved that MBD3 represses transcription through mechanisms similar to those described for MeCP2, but it is likely that similar mechanism to that observed for MBD2 and MeCP1 complex based on association of MBD3 with HDACs. Another possible mechanism is that MBD2 can form heterodimers with MBD3, thus results in binding hemimethylated DNA and recruiting HDACs as well as DNA methytransferase protein 1 (Tatematsu et al., 2000).

1.1.5.5 MBD4

MBD4 is a 62-kDa protein of the MBD family that consists of two well-conserved, functional domains, an N-terminal MBD and a C-terminal DNA glycosylase catalytic domain with homology to bacterial DNA glycosylases, which appears to coordinate DNA repair with DNA methylation events (Hendrich et al., 1999). It has been shown to be involved in DNA repair rather than transcriptional repression (Bellacosa et al., 1999; Hendrich and Bird, 1998). The MBD of MBD4 binds preferentially to methyl-CpG/TpG mismatches, which originate from spontaneous deamination at methyl-CpG in the genome, although its MBD can bind

symmetrically methylated CpG sites *in vitro* (Hendrich et al., 1999). MBD4 then efficiently removes thymine or uracil from a mismatch CpG site with the glycosylase domain, suggesting that the combination of binding and catalysis of MBD4 may function to minimize mutation at methyl-CpG (Hendrich et al., 1999). The function was further confirmed by using transgenic MBD4-mutant mice. As expected, an increase in 5 methylcytosine to T mutations at CpG sites was found in *Mbd4*-mutant mice, and leads to reduced survival and an increased occurrence of tumour, indicating that MBD4 has a role in reducing mutation at methylated CpG sites *in vivo* (Millar et al., 2002; Wong et al., 2002). Besides G-T mismatch repair activity, MBD4 also has the activity of 5-methylcytosine DNA glycosylase, however, the biological significance of MBD4 has not yet been elucidated. Like MBD1, overexpressed GFP-MBD4 localizes at the foci of hypermethylated satellite DNA and this localization is impaired in DNMT-deficient emobryonic stem cells that have a reduced level of DNA methyltion (Hendrich and Bird, 1998). More recently, MBD4 appears to be involved in transcriptional repression through methyl-CpG. Transcriptional repression by the MBD4 is HDAC dependent, and MBD4 directly binds to Sin3A and HDAC1. Further evidence showed that both MBD and the glycosylase catalytic domain are tethered within the hypermethylated promoter in $p16^{INK4a}$, suggesting that the glycosylase catalytic domain may be the maintenance of mCpG sites to allow preferential binding by MBD of MBD4 (Kondo et al., 2005).

1.1.5.6 Kaiso

Kaiso, is a unique methyl-DNA-binding protein, belongs to the BTB/poxvirus and zinc finger (POZ) protein family (Collins et al., 2001). Many evidences have shown that many members of this family repress gene transcription through recognition of specific DNA sequence by zinc finger (van Roy and McCrea, 2005). Kaiso does not have a classical methyl-DNA-binding domain, and is the only known member of this family that binds two distinct DNA motifs: two or more adjoining methylated CpG islands (Prokhortchouk et al., 2001; Yoon et al., 2003), and sequence-specific consensus sites with six core nucleotides (CTGCNA, where N indicates any nucleotide) (Daniel et al., 2002). It has been presumed, but not shown that both sites might work together to creat a stronger and more integrated repression complex in some gene-regulatory context. Kaiso represses transcription of target genes by virture of its directly binding to methylated DNA using zinc finger motif, and by recruiting transcriptional

corepressors such as nuclear receptor co-repressor (NCoR) by its amino-terminal POZ domain, which in turn recruits histone deacetylases containing NCoR complex (Daniel et al., 2002; Yoon et al., 2003). Furthermore, a double-point mutation in POZ domain abolishes its association with NCoR, indicating that co-repressor NCoR is essential for Kaiso's repression function (Park et al., 2005). Moreover, Kaiso in a complex with NCoR represses the MTA2 gene locus in a methylation-dependent manner (Yoon et al., 2003). Recently, the analysis of gene-array data has indicated that a number of methylated genes are upregulated following the depletion of Kaiso during early *Xenopus* embryonic stages (Ruzov et al., 2004), further indicating that Kaiso functions as a methylation-dependent transcriptional repressor. The mechanisms that regulate the functions of Kaiso seem to be complex and require to further investigation.

1.1.6 NuRD complex and MeCP1 complex

The vertebrate Mi-2/NuRD (nucleosome remodeling histone deacetylase) complex is a multi-subunit protein complex with both chromatin remodeling and histone deacetylase activity, although the compostion of the complex remains controversial (Tong et al., 1998; Tyler and Kadonaga, 1999; Wade et al., 1998; Xue et al., 1998; Zhang et al., 1998). It has been established that the two histone deacetylses HDAC1 and HDAC2, and the two histone binding proteins RbAp46 and RbAp48 form a core complex and exist in most of the histone deacetylase complexes examined to date (Guschin et al., 2000; Le Guezennec et al., 2006; Yao and Yang, 2003). It has been reported that Mi-2, which is an autoantigen associated with human disease dermatomyositis (Ge et al., 1995) and a member of the SWI2/SNF2 family of ATP-dependent chromatin remodeling proteins (Eisen et al., 1995), is the largest subunit of the Mi-2/NuRD complex (Tong et al., 1998; Wade et al., 1998; Xue et al., 1998; Zhang et al., 1998). There are two isoforms of human Mi-2: Mi-2α and Mi-2β. However, Mi-2 isoforms seem to be present in the complex differently in terms of different context (Bowen et al., 2004). One possibility is that Mi-2β represents the sole Mi-2 isoform present in the complex (Zhang et al., 1998), amd the second is that both Mi-2α and Mi-2β are present, although Mi-2β is abundant (Le Guezennec et al., 2006; Tong et al., 1998). Surprisingly, recent studies showed that Mi-2 is not present in the so called "metastasis associated protein 1 (MTA1) complex", which also contains core complex and MBD3 (Yao and Yang, 2003). It might be that the above differences likely

result from different purification strategies employed. MTA1, which is associated with invasion and metastasis of tumor, was first identified as a component of Mi-2/NuRD complex (Xue et al., 1998). Shortly after this finding, MTA2, an MTA1 homologue, was reported to be a subunit of Mi-2/NuRD complex (Zhang et al., 1999). Recently, the third isoform of MTA family was also found to be associated with the Mi-2/NuRD complex by immunoprecipitation. Interestingly, there was no physical interactions between MTA3 and either MTA2 or MTA1 (Fujita et al., 2003). Other findings further revealed that MTA2 complex is remarkably similar to the Mi-2/NuRD complex, whereas MTA1 complex does not contain Mi-2 but contains specific MTA1-associated proteins, although both MTA1 and MTA2 complex share core complex and MBD3. These studies suggested that different Mi-2/NuRD complexes with distinct subunits of MTA family members exist. The other component of Mi-2/NuRD complex that may bring the complex to methylated DNA is MBD3, a member of MBPs family, suggesting a possible connection between methylated DNA and histone deacetylation. But due to the point substitutions in two highly conserved amino acids, mammalian MBD3 lacks the ability to recognize methylated DNA (Hendrich and Bird, 1998), although *Xenopus* MBD3 is able to bind with high affinity to methylated CpG (Wade et al., 1999). However, it was shown that the Mi-2/NuRD complex can be recruited to methylated DNA through interaction with MBD2 (Zhang et al., 1999), which is known to bind methylated DNA and but is not an integral component of Mi-2/NuRD complex. Thus NuRD complex connects DNA methylation, chromatin remodeling and histone deacetylation (Bird and Wolffe, 1999).

This MBD2 containing Mi-2/NuRD complex has been called MeCP1 complex (Feng and Zhang, 2001; Ng et al., 1999). MeCP1 was originally identified as a methyl-CpG binding activity that requires 15 or more symmetrically methylated CpG pairs (Meehan et al., 1989). In a later study, MeCP1 seems to be a large multi-subunit complex, which conatins 10 major polypeptides including MBD2, seven characterized NuRD components and two polypeptides of 66 and 68 KDa (Feng and Zhang, 2001; Ng et al., 1999). In addition, MeCP1 complex is able to repress transcription through preferentially binding, remodeling, and deacetylation of methylated nucleosomes (Feng and Zhang, 2001). In another independent study, HDAC1 complex was shown to contain all known components of Mi-2/NuRD complex and MBD2. In contrast, HDAC2 complex contains no detectable MBD2 (Humphrey et al., 2001). The results seem to confirm the existence of MeCP1 complex. However, more recent study have revealed that MBD2 and MBD3 assemble into mutually exclusive distinct Mi-2/NuRD-like complexes,

termed as MBD2/NuRD complex and MBD3/NuRD. Both complexes contain an additional component DOC-1, which is a putative tumor repressor, besides known subunits of Mi-2/NuRD complex. In addition, arginine methyltransferase PRMT5 and its cofactor MEP50 were identified as specific components of MBD2/NuRD complex but not MBD3/NuRD complex. It is proposed that previous MeCP1 complex may in fact be a mixture of Mi-2/NuRD complexes, some containing MBD2 and others containing MBD3. Taken together, it seems that HDAC1/2, MTA1/2 or MBD2/3 may assemble into distinct protein complexes (Table 1.1).

Table 1.1 Difference in composition of known subunits of NuRD formed complexes

Mi-2β[c,e]	MTA1[d]	MTA2[d]	MBD2[b]	MBD3[b]	HDAC1[a,f]	HDAC2[e]
Mi-2α		Mi-2	Mi-2α	Mi-2α	Mi-2	Mi-2
Mi-2β			Mi-2β	Mi-2β		
MTA1[c]	MTA1		MTA1	MTA1		
MTA2[e]		MTA2	MTA2	MTA2	MTA2	MTA2
MTA3			MTA3	MTA3		
p66 (?)	p66	p66	p66α	p66α	p66	p66
p68 (?)	p68	p68	p66β	p66β		
HDAC1	HDAC1	HDAC1	HDAC1	HDAC1	HDAC1	HDAC1
HDAC2	HDAC2	HDAC2	HDAC2	HDAC2	HDAC2	HDAC2
RbAp46	RbAp46	RbAp46	RbAp46	RbAp46	RbAp46	RbAp46
RbAp48	RbAp48	RbAp48	RbAp48	RbAp48	RbAp48	RbAp48
			MBD2		MBD2	
MBD3	MBD3	MBD3		MBD3	MBD3	MBD3
	MTA1 associated proteins		DOC-1	DOC-1		
			PRMT5		mSin3A	
			MEP50		CoREST	

Proteins identified as components of the various complexes as indicated. Speculative identifications of these proteins are indicated as query in parentheses (a, Humphrey et al., 2001; b, Le Guezennec et al., 2006; c, Xue et al., 1998; d, Yao and Yang, 2003; Zhang et al., 1998; e, Zhang et al., 1999).

1.1.7 hp66 protein paralogs: hp66α and hp66β

p66 protein was first identified as a component of *Xenopus* Mi-2/NuRD complex (Wade et al., 1999; Wade et al., 1998). Meanwhile, as described above in the table, several groups reported that human p66 is also a subunit of Mammalian Mi-2/NuRD complex. It was first reported that two novel polypeptides of p66 and p68, are components of MeCP1 complex. Further research revealed that p66 and p68 represent the same protein and that p68 is a modified form of p66 (Feng et al., 2002; Feng and Zhang, 2001). Since MBD2 has been shown to associate with Mi-2

/NuRD complex within the MeCP1 complex (Ng et al., 1999), our group identified two highly related 66KDa proteins in a yeast two-hybrid screen with MBD2b as a bait (Brackertz et al., 2002). Sequence comparison of both proteins to the p66 component of *Xenopus* Mi-2/NuRD complex demonstrated that one p66 proteins is the human orthologue of the *Xenopus* p66 protein (Wade et al., 1999), refered as human p66α (hp66α), another p66 protein is identical to the previous identified p66/68 of human MeCP1 complex (Feng et al., 2002), refered as human p66β (hp66β). Thus, hp66α and hp66β, also named as GATAD2A and GATAD2B, are encoded by two different genes comprising a novel gene family. Functional characterization of both hp66α and hp66β was carried out, and is summarized in the Table 1.2.

Table 1.2 functional characterization of hp66α and hp66β

	hp66α	**hp66β**
homology	chromosome 19p13.11	chromosome 1q23.1
	52%	
	conserved region 1 (CR1) 75%, conserved region 2 (CR2) 72%	
expression	ubiquitously expressed in cell lines, fetal and adult tissues	
	expression of both p66 proteins are independent from one another	
localization	?	colocalizes with MBD3 and dependent on CR2
	identical distribution of both proteins in a nuclear speckle pattern	
	colocalize with MBD2 and depends on CR2 and MBD2	
repression	?	CR1 is major repressive domain
	?	partially dependent on histone deacetylation
	repress transcription in Gal-fusion system in a dose dependent manner	
	functional interplay for the repression of both proteins	
	enhance/reduce MBD2-mediated repression by overexpression/knockdown	
	MBD2 is not essential for the repression of both proteins	
interaction	stronger interaction with MBD2 and MBD3 than hp66β	weaker interaction with MBD2 and MBD3 than hp66α
	C-terminus including CR2 binds to MBD2 and MBD3	C-terminus including CR2 doesnt bind to MBD2 and MBD3
	CR1interacts with MBD2 interact with MeCP1 complex ?	CR1 ineracts with components of MeCP1 complex
	strong affinity for all histone tails H2A, H2B, H3 and H4	
	interact with PCAF and p300	
	acetylation of histone tails by PCAF or p300 specifically reduces its association with both hp66 proteins	

Functional characterization of hp66 proteins was summarized from several publications (Brackertz et al., 2002; Brackertz et al., 2006; Feng et al., 2002). Modified after Brackertz's thesis.

1.2 SUMO: a history of protein modification

Reversible posttranslational protein modifications are acetylation, methylation, phosphorylation, glycosylation, carboxylation, poly(ADP-ribosyl)ation, as well as ubiquitination. The most well-known example of posttranslational modification is ubiquitination, which was first characterized at 1987 (Shanklin et al., 1987) and has been extensively studied in the previous years (Shcherbik and Haines, 2004). Ubiquitination is a highly conserved post-translational protein modification process in which ubiquitin is covalently attached to lysine residues of the targeted substrates (Pickart, 2001). It should be noted that this process is reversible and is carried out by deubiquitinating enzymes (Hochstrasser, 1996). Ubiquitination requires three different enzymes, the ubiquitin-activating enzyme (E1), ubiquitin-conjugating enzyme (E2), and ubiquitin ligase (E3). Although most of the known examples of ubiquitination involve proteasome-dependent degradation of transcriptional regulators, ubiquitin-modified proteins also perform other important functions in cell cycle progression, signal transduction, DNA repair, apoptosis, and transcriptional regulation (Hershko and Ciechanover, 1998; Hochstrasser, 1996; Pickart, 2001). In addition to ubiquitin, there are several ubiqutin-like polypeptides which acts as posttranslational protein modifiers have been identified (Schwartz and Hochstrasser, 2003; Seeler and Dejean, 2003). One member of this ubiquitin-like protein family is a 97 amino acid mature polypeptide, termed as small ubiquitin-like modifier (SUMO). SUMO is covalently attached to the lysine residues of target proteins via a "three-enzyme-step" mechanism analogous to, but distinct from, ubiquitin (Johnson, 2004). The significance of SUMO was first discorved in studies on nuclear import as a covalent modification of RanGAP1 (Matunis et al., 1996). In recent years, a plethora of substrate proteins for SUMO modification have been identified. However, the consequences of SUMO modification seems to vary with the particular target protein. SUMO modification of target proteins has diverse effects on cell cycle, subcellular transport, DNA repair, regulation of transcription factor activity (Gill, 2005; Hay, 2005).

1.2.1 The family of SUMO proteins

To date, four different SUMO isoforms termed SUMO-1, SUMO-2, SUMO-3, and SUMO-4 have been identified in mammals. Of these, SUMO-2 and SUMO-3 are closely related and

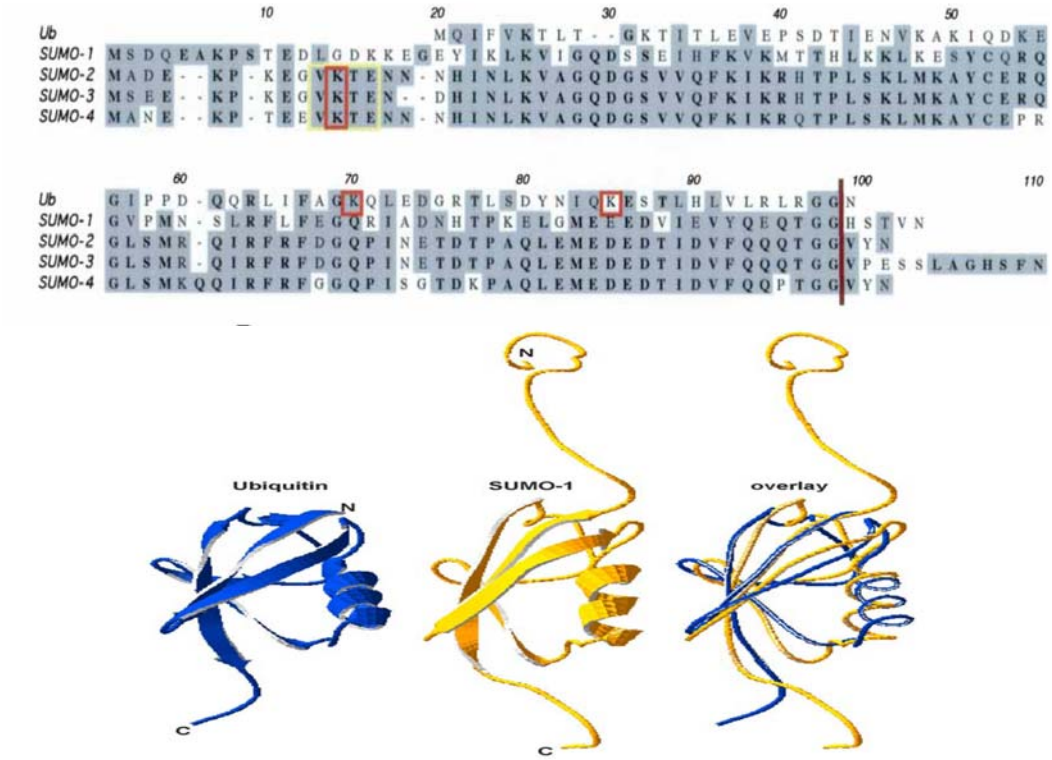

Fig.1.3 SUMO is highly related to ubiquitin. (A) amino acid sequence of ubiqutin and the four SUMO isoforms from human. Identities are indicated in bold and similarities are shaded. A consensus motif for SUMOylation present in SUMO-2/3/4 is boxed in yellow; the SUMO acceptor lysine (K) in this motif is boxed in red. Ubiquitin Lys 48 and Lys 63, which serve as common sites for ubiquitin polymerization, are boxed in red. The site of cleavage to produce the mature proteins with C-terminal di-glycine residues is also indicated. (B) Structure comparison of ubiquitin and human SUMO-1. Both proteins share a characteristic tightly packed ββαββαβ fold, and a C-terminal di-glycine motif. SUMO is distinguished by a long and flexible N-terminal extension (Dohmen, 2004; Gill, 2004).

share about 95% amino acid sequence identity, in contrast to sharing about a 50% identity with SUMO-1 (Kim et al., 2002; Saitoh and Hinchey, 2000; Schwartz and Hochstrasser, 2003). Profiles of fractionated SUMO-1 and SUMO-2/3-modified proteins demonstrate that SUMO isofroms appear to modify common and also different substrates. There are examples of substrates such as RanGAP1 that is predominantly modified by SUMO-1, whereas Topoisomerase II and CAAT/enhancer-binding protein-β are specifically modified by SUMO-2/3 (Azuma et al., 2003; Eaton and Sealy, 2003; Vertegaal et al., 2004). Recent evidence supported the concept of important distinctions between the SUMO-2/3 and SUMO-1 pathways, with SUMO-1 conjugated to proteins as a monomer, while SUMO-2 and SUMO-3 are conjugated to proteins as higher molecular weight polymers with SUMO-1 terminating further SUMO addition (Tatham et al., 2001). The fourth isoform SUMO-4 which was recently described a restricted expression pattern with strongest levels reported in kidney cells (Bohren et al., 2004). Further research will focus on establishing the expression profile of this gene in

different tissues. So far, the mechanisms that determine specific SUMO isoforms for modification of certain protein is presently unclear, and the functional consequences of modification by specific SUMO isoforms also remains to be found out. The SUMO-1 protein is highly conserved from yeast to human, which is 18% identical to ubiquitin., but has a similar three-dimensional structure as shown by NMR studies (Fig.1.3). The distribution of charged residues on the surface of SUMO-1, however, is quite different from that of ubiquitin. Furthermore, SUMO-1 has a flexible N-terminal extension, which is absent in ubiquitin. These differences suggest that both SUMO-1 and ubiquitin interact specifically with distinct enzymes and substrates. Another important feature is a di-glycine motif at the C-terminus in the mature forms of SUMO and ubiqutin, which is very critical for SUMO conjugation.

1.2.2 The SUMOylation machinery

Over the past 10 years, significant progress has been made in understanding the molecular mechanism of the SUMOylation pathway. Similar to ubiquitination, SUMOs are conjugated to target substrates via a conserved enzymatic cascade requiring the E1 activating enzymes, E2 conjugating enzymes, and in most cases, also requires an E3 ligases (Fig.1.4). SUMO is first activated by formation of a high energy thioester bond between its C-terminal glycine and the catalytic cysteine residue (C173) of the SUMO E1 activating enzyme, which is a heterodimer containing SAE1 and SAE2 subunits (also named Aos1/Uba2) (Desterro et al., 1999; Gong et al., 1999; Johnson et al., 1997; Okuma et al., 1999). This step requires ATP hydrolysis. The SUMO moiety is then transesterified from SAE2 to E2 conjugating enzyme Ubc9, forming the Ubc9-SUMO thioester complex through cysteine 93 of Ubc9, which is the only known SUMO E2 conjugating enzyme (Bernier-Villamor et al., 2002; Desterro et al., 1999; Johnson et al., 1997; Lin et al., 2002). Unlike many other E2 enzymes responsible for ubiquitin conjugation, Ubc9 is able to recognize substrate proteins. Thus, Ubc9-SUMO thioester complex can catalyze formation of an isopeptide bond between glycine 97 of SUMO and the ε–amino group of the target lysine residue. This specific lysine residue is usually found within a SUMO modification consensus motif ψKXE, where ψ is a large hydrophobic residue and X is any residue (Rodriguez et al., 2001), which is also recognized by the Ubc9 active site (Bernier-Villamor et al., 2002; Lin et al., 2002). It should be noted that certain substrates are modified on lysine residues where the surrounding sequence does not conform to this consensus, and not all

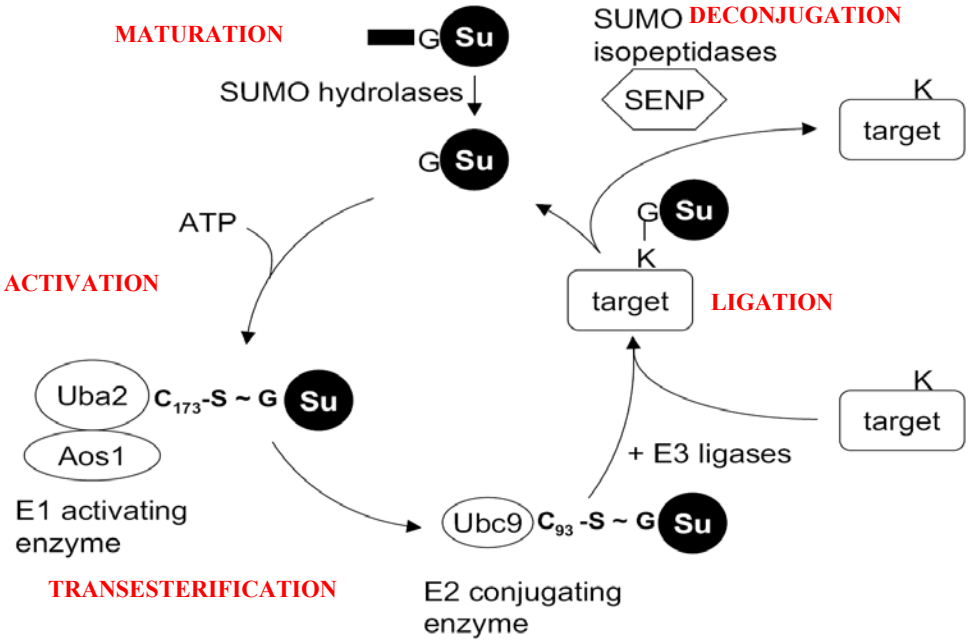

Fig.1.4. The SUMO cycle. The SUMO precursor is processed by a SUMO specific protease to reveal the C-terminal di-glycine that is activated by formation of a thioester bond with the catalytic cysteine (C173) of the Uba2 subunit from the E1 activating enzyme (AoS1/Uba2). This step requires ATP hydrolysis. SUMO is then transferred to the catalytic cysteine (C93) of the E2 conjugating enzyme Ubc9., the protein target is selected., and with the help of E3 ligases, the SUMO from Ubc9 is transferred to the lysine side chain of the substrates. SUMO can be deconjugated from the target proteins due to the presence of SUMO-specific protease. Modified after (Bossis and Melchior, 2006; Hay, 2005).

proteins containing this consensus motif are modified by SUMO. Although SUMO E1 activating enzyme and E2 conjugating enzyme are shown to be sufficient for SUMO modification of various substrates *in vitro*, recent evidence demonstrated that additional components are required to increase the efficiency of transfer SUMO from Ubc9 to target proteins *in vivo*. Such proteins are known as E3 ligases (Pickart, 2001). To date, three different types of SUMO E3 ligases have been identified: the PIAS protein, RanBP2, and the polycomb group protein Pc2. These SUMO E3 ligases most likely function as adaptors rather than "ligases". They bind to SUMO E2 conjugating enzyme Ubc9 and increase transfer of SUMO from Ubc9 to target proteins (Johnson and Gupta, 2001; Pichler et al., 2002; Takahashi et al., 2001). The PIAS proteins contain RING-finger domain similar to ubiquitin E3 ligases, whereas RanBP2 and Pc2 have no sequence similarity with the ubiquitin E3 liagses. PIAS proteins were initially described as protein inhibitors of activated STAT, and at least five PIAS proteins (PIAS1, PIASxα, PIASxβ, PIASγ, and PIAS3) were characterized with the RING-finger domain in mammalians (Chung et al., 1997; Liu et al., 1998; Moilanen et al., 1999; Tan et al., 2002). During the past few years, extensive studies have demonstrated that PIAS proteins

influence the activity of many transcription factors either by inhibiting their binding to DNA, by acting as co-repressors or co-activators, or by recruiting histone deacetylases (Jackson, 2001; Schwartz and Hochstrasser, 2003). Another type of SUMO E3 ligase is the nucleoporin RanBP2/Nup358, which is located the cytoplasmic filaments of the nuclear pore complexes, and was one of the first SUMO targets to be identified (Pichler et al., 2002). This distinct localization could contribute to functional speicificity of SUMO E3 liagses.

SUMO modification of target proteins is dynamic and reversible. SUMO-speicific proteases play critical roles in both processing SUMO precursor to the mature form and deconjugating SUMO moiety from target proteins. Two SUMO proteases, Ulp1 and Ulp2, have been identified as cysteine proteases by structural analysis and sequence comparisons in yeast (Li and Hochstrasser, 1999; Li and Hochstrasser, 2000). So far, eight mammalian homologs of Ulp1 have been characterized and are referred to as SENP proteins (1-8) (Yeh et al., 2000). Of these proteases, SENP1 (Bailey and O'Hare, 2004), SENP2 (Best et al., 2002; Nishida et al., 2001), SENP3 (Gong and Yeh, 2006; Nishida and Yasuda, 2002), SENP5 (Gong et al., 2006), and SENP6 (Kim et al., 2000) have been shown to have SUMO-specific protease activity, whereas, SENP8 has been found to be a NEDD8 specific protease (Mendoza et al., 2003; Wu et al., 2003). Very importantly, the mammalian SUMO-specific proteases have distinct subcellular localization that allows selection of modified substrates for deconjugation by the SUMO proteases *in vivo*. SENP1 is in nuleoplasm and nuclear bodies, SENP2 is cytoplasmic and nuclear pore, SENP3 is nucleolar, and SENP6 is cytoplasmic (Bailey and O'Hare, 2004; Gong et al., 2000; Hang and Dasso, 2002; Kim et al., 2000; Nishida et al., 2000). In general, most SUMO modified substrates are at very low steady state levels in vivo. Dynamic and reversible SUMO conjugation/deconjugation cycles could be responsible for the frequently observed scenario: only a small fraction of a given target protein is SUMOylated at steady state, even in the presence of inhibitors of SUMO-specific proteases (Hay, 2005).

1.2.3 Functions of SUMO modification

The first protein be identified as a SUMO-modified substrate was RanGAP (Matunis et al., 1996). Since this finding, the number of proteins identified as substrates of SUMO modification has greatly increased and new SUMO-moidified target proteins continue to be identified all the time. SUMO modification affects the functions of target proteins in many

ways and plays important roles in diverse processes such as subcellular transport (Lin et al., 2003; Matunis et al., 1996; Zhong et al., 2000), inhibition of ubiquitin-mediated degradation (Desterro et al., 1998), and transcriptional regulation (Gomez-del Arco et al., 2005; Terui et al., 2004; Tiefenbach et al., 2006). Furthermore, SUMOylation regulates cell cycle (Azuma et al., 2003; Bachant et al., 2002), DNA damage repair (Hoege et al., 2002; Stelter and Ulrich, 2003; Ulrich, 2005), signal transduction (Lee et al., 2003; Lin et al., 2003; Lin et al., 2003), protein-protein interactions (Yang et al., 2003), protein-DNA binding activity (Goodson et al., 2001) and enzymatic activity (Hardeland et al., 2002).

1.2.3.1 SUMO modification and nuclear localization

SUMO modification is involved in regulating subcellular localization of many proteins, including the first identified SUMO substrate RanGAP1 (Matunis et al., 1996). Unmodified RanGAP1 resides exclusively in the cytoplasm, whereas SUMO-modified RanGAP1 is associated with nuclear pore complex mediated by an interaction with RanBP2/Nup358, which is component of nuclear pore complex and a SUMO E3 ligase (Mahajan et al., 1997; Matunis et al., 1998; Pichler et al., 2002). Another well-characterized example in understanding SUMO-dependent regulation in subcellular localization comes from studies of the protein, promyelocytic leukaemia (PML), which is major component of PML nuclear bodies (also named ND10) (Zhong et al., 2000). SUMOylated forms of PML is observed predominantly in the PML nuclear body. Mutation of the SUMO modification sites in PML leads to nuclear body components such as Sp100 to relocalize in the nucleus (Best et al., 2002; Sternsdorf et al., 1999; Zhong et al., 2000). These observations indicated that SUMO modification of PML provides protein-protein interaction surface for assembly or stablility of PML nuclear body. On the other hand, some recent studies found that mutation of SUMO modification site of the transcriptional repressor CtBP leads to a cytoplasmic localization and a loss of repression activity, while wild type CtBP normally localizes in the nucleus (Lin et al., 2003). SUMO modification also targets subcellular localization of other substrates such as NF-κB (Desterro et al., 1998). Taken together, SUMO modification is involved in promoting subcellular localization of substrates. The function of SUMO modification in nuclear cytoplasmic transport remains a subject of further investigation.

1.2.3.2 SUMO modification and ubiquitination

Lysine residues are not only targets for SUMOylation, but also for methylation, acetylation and ubiquitination. Over the past years, it has been demonstrated that several modification system could communicate and mutually influence the functions of common substrate proteins, and in some cases even involving the same lysine residue. A number of substrates have been identified to be modified by both SUMOylation and ubiquitination. The first example is IκBα inhibitor proteins in the context of transcription factor NF-κB siganling pathway (Desterro et al., 1998). Phosphorylation of residues Ser32/36 of IκBα leads to poly-ubiquitination, subsequently results in degradation of IκBα by the 26S proteasome, thus allows NF-κB to reenter the nucleus and to activate transcription of its target gens (Baldwin, 1996; Karin and Ben-Neriah, 2000). In the absence of phosphorylation, SUMO modification takes place on the same lysine residue 21 of IκBα, and protects IκBα from ubiquitination-mediated degradation by direct competition for the same modification site. In addition, SUMOyaltion of IκBα also indirectly leads to repression of NF-κB–dependent transcription. This paradigm was first reported to show the antagonistic relationship between SUMO modification and ubiquitination (Fig.1.5). As indicated above, other target proteins such as cAMP-reponse element binding protein (CREB) is also subjected to ubiquitination that leads to degradation of CREB and promotes expression of target genes, whereas SUMO modification of CREB results in stablization and nuclear localization of CREB (Comerford et al., 2003). Recent insights into NEMO, the kinase (IKK) regulator, demonstrated that NEMO is also modified by both SUMO and ubiquitin. Ubiquitin and SUMO, however, don't counteract each other in this context. SUMO modification of NEMO results in retention of NEMO in the nucleus, and IKK remains in an inactive state. After removal of SUMO, NEMO is ubiquitinated and translocated back to the cytoplasm, where it activates IKK and subsequently induces NF-κB (Huang et al., 2003). This scenario suggests that SUMOylation and ubiquitination are successive events, and in some cases, need to coexist on the common substrate proteins such as NEMO and and proliferating cell nuclear antigen (PCNA) protein (Hoege et al., 2002; Stelter and Ulrich, 2003; Ulrich, 2005). In conclusion, opposing effects of SUMOylation and ubiquitination on same target protein might be due to stablization of substrates via relocalization or sequestration of the substrates by SUMO modification that competes with ubiquitination-mediated degradation of

substrates. Nevertheless, SUMO and ubiquitin modification could cooperate to exert distinct functions of target proteins. Besides ubiquitination, research insights into other modifications such as acetylation (Bouras et al., 2005; Sapetschnig et al., 2002), phosphorylation (Bossis et al., 2005; Gregoire et al., 2006; Kang et al., 2006; Muller et al., 2000; Yang et al., 2003), indicated crosstalk between SUMO and other modifications.

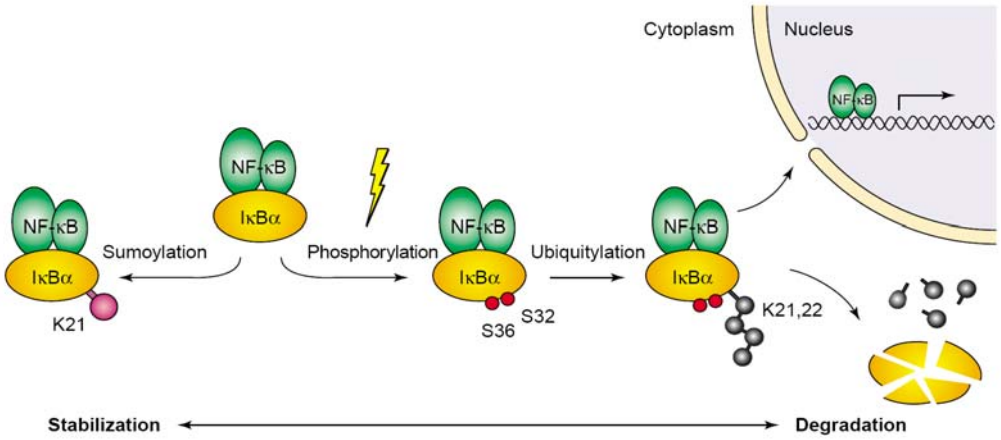

Fig.1.5. Opposing effects of ubiquitin and SUMO on IκBα. Signaling from cell-surface receptors (shown in yellow) leads to phosphorylation and subsequent ubiquitylation of IκBα. Proteasome-mediated degradation then releases active NF-κB, which translocates into the nucleus and activates its target genes. In contrast to ubiquitination, sumoylation stabilizes IκBα, thereby preventing the release of NF-κB. Ubiquitin are shown in gray, SUMO moieties are shwn in pink. Phosphate moieties are represented in red, and lysine and serine residues relevant to the modifications are indicated (Ulrich, 2005).

1.2.3.3 SUMO modification and transcriptional regulation

Among the many known targets of SUMOylation, over half of the recently identified SUMO target proteins are regulators of gene expression, and in particular transcriptional activators, repressors, coactivators or corepressors. Thus, SUMO modification of transcription factors have diverse functional consequences -both activation and repression transcription. In most of these cases, however, SUMO modification of transcription factors results in inhibiton of transcription. SUMOylation of a limited number of transcription factors correlates with positive effects on transcriptional activity. SUMO modification of the heat-shock transcription factors HSF1 and HSF2 with SUMO-1 leads to increased DNA-binding activity and mutation of the target lysine decreases the HSF1 transcriptional activity (Goodson et al., 2001; Hong et al., 2001). Also SUMO modification of nuclear factor of activated T (NAFT), Ikaros has been

shown to increase its transcriptional activity (Gomez-del Arco et al., 2005; Terui et al., 2004), although the mechanisms underlying these events remains obscure. Nevertheless, it has been described to date, SUMO modification of transcription factors is more often associated with transcriptional repression. Several evidences have been reported that the SUMO modification sites in many transcription factors such as Elk-1 are mapped within previously defined inhibitory or negative regulatory domains or the so called "synergy control" motifs, mutation of target lysines has been found to enhance transcriptional activity of transcription factors (Holmstrom et al., 2003; Iniguez-Lluhi and Pearce, 2000; Kim et al., 2002). In addition, overexpression of SUMO-1 or Ubc9 is able to increase SUMO subtrate mediated transcriptional represson (Tiefenbach et al., 2006; Verger et al., 2003). Consistent with these findings, blocking SUMOylation pathway by co-expression of a C93S dominant negative version of Ubc9 (Eloranta and Hurst, 2002; Girdwood et al., 2003; Yang et al., 2003) or removal of SUMO from substrates by SUMO-specific proteases (Kim et al., 2002; Long et al., 2004; Poukka et al., 2000; Ross et al., 2002; Sapetschnig et al., 2002; Subramanian et al., 2003; Yang et al., 2003) has been shown to derepress SUMO-dependent transcriptional repression of transcription factors, therefore suggesting a mechanism for regulating transcription. Recent studies provided new insights into the molecular mechanisms by which SUMO modification regulates transcriptional repression of transcription factors. There are several models to explain SUMO dependent transcriptional repression, but are not mutually exclusive. First, SUMO modification of transcription factors may repress transcription by recruitment of transcriptional co-repressors (Gill, 2004; Gill, 2005; Hay, 2005; Zhang et al., 2004). It is well known that acetylated histone tails correlates with active gene transcription, whereas deacetylated histone tails correlates with inactive gene transcription (Wu and Grunstein, 2000). Recent studies demonstrated that corepressor HDACs might play an important role in transcriptional repression mediated by SUMO modification. Consistent with this idea, Yang and coworkers found that SUMO modification of Elk-1 recruits HDAC2 to responsive promoters and decreases levels of histone acetylation at an Elk-1-regulated promoter using chromatin immunoprecipitation assay (Yang and Sharrocks, 2004). Similarly it was shown that SUMO modification of the transcriptional co-regulator p300 mediates transcriptional repression by recruiting HDAC6 (Girdwood et al., 2003). Moreover, SUMO modification of histone H4 was found to repress transcription, mediated by HDAC1 and HP1 (Shiio and Eisenman, 2003). These findings suggested that SUMO modified transcription factors repress transcription by

recruitment of HDACs, which results in deacetylation of core histones and other transcription factors, and in turn creates a transcriptional repressive chromatin environment. It should be noted that HDACs are components of several large multi-subunit repressive complexes (Yang and Seto, 2003). Although recent data supports the view that HDACs play an apparently broad role in SUMOylation-mediated transcriptional repression, this family of co-repressors is not likely to account for all of the observed transcriptional repression by SUMO. Other co-repressors that function as effectors of SUMO-dependent transcriptional repression remains to be identified. In addition, HDACs have also been found to enhance the efficiency of SUMO modification of some substrates. Lysine residues of several transcription factors have been shown to be modified by ubiquitin, acetylation and SUMO. Thus, the hypothesis is that deacetylation by HDACs could increase susceptibility of substrate lysines, thereby increase efficiency of SUMOylation. Consistent with this hypothesis, recent studies have shown that a class III HDAC SIRT1 enhances p300-mediated repression depend on its deacetylase activity (Bouras et al., 2005). In addition, two lysine residues in p300 were found to be substrates for deacetylation by SIRT1 which is also modified by SUMO, suggesting that SIRT1 may deacetylate the SUMO acceptor lysine residues and promote SUMOylation of p300 (Bouras et al., 2005). Several HDACs have been reported to be substrates of SUMOylation. SUMO modification of HDAC1 was found to increase both deacetylase activity and transcriptional repression activity (Cheng et al., 2004; David et al., 2002). Taken together, HDACs serve as regulators, effectors and substrates of SUMO modification, indicating that crosstalk between

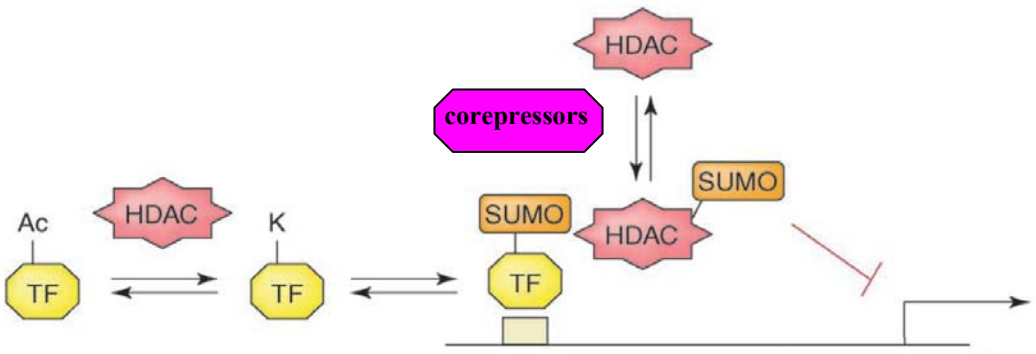

Fig.1.6. Complex interplay between SUMO and HDACs. As depicted here, histone deacetylases (HDACs) might be recruited to SUMO-modified transcription factors (TFs) to mediate repression. In addition, some HDACs are themselves SUMOylated, and SUMO modification of HDACs might alter protein–protein interactions or enzymatic activity that is important for repression. Furthermore, HDACs regulate SUMOylation of transcription factors through enzymatic removal of acetyl groups on SUMO-acceptor lysines. Moreover, SUMO itself can directly bind transcriptional corepressors. Modified after (Gill, 2005).

deacetylation and SUMOylation might be important for regulation of gene expression (Fig.1.6). Second, direct evidence for transcriptional repression by SUMO modification came from the fact that fusion of SUMO-1 to the Gal4 DNA-binding domain represses transcription in reporter gene assay (Holmstrom et al., 2003; Ross et al., 2002; Yang et al., 2003), indicating that SUMO itself is able to directly bind to transcriptional corepressors. Third, SUMO modification redistributes transcription factors to the repressive environment of particular nuclear bodies, such as PML nuclear body. Studies on PML protein revealed that SUMO modification of PML is required for secondary shell-like nuclear body (NB) formation and is necessary for the recruitment of other PML associated components, for example homeodomain interactin protein kinase 2 (HIPK2), Daxx, and Sp100, into the NBs (Duprez et al., 1999; Ishov et al., 1999; Kamitani et al., 1998). In addition, SUMO modified HIPK2 is required for its localization to NBs, and represses transcriptional activity by forming a stable repressor complex with Groucho corepressor and HDAC1 (Choi et al., 1999; Kim et al., 1999). Similarly, SUMO modification of Daxx is also able to recruit HDACs into NBs, and thus mediates transcriptional repression by remodeling chromatin (Lehembre et al., 2001; Li et al., 2000). As to another NB component Sp100, SUMO-modified Sp100 enhances the interaction with heterochromatin protein 1 (HP1), which is well-known for the formation of repressive domain in chromatin (Seeler et al., 2001; Seeler et al., 1998). All these findings supported the view that localization of such proteins to NBs by SUMO modification is to create a local repressive environment within NBs. Another well-characterized example is polycomb group (PcG) protein. SUMO modification of *C. elegans* PcG protein SOP-2 results in its recruitment into subnuclear body, and recruitment SOP-2 into this body is required for transcriptional repression (Zhang et al., 2004). Further research revealed that another polycomb protein, Pc2, recruits the transcriptional corepressor CtBP into polycomb subnuclar domains and mediate SUMO modification of CtBP, which is required for its transcriptional repression (Kagey et al., 2003). Additional mechanisms of SUMOylation-mediated transcriptional repression are possible, but are not yet established.

1.3 Aim of the project

The goal of this project was to further understand the biological functions of hp66 proteins. Previous works have shown that both hp66α and hp66β are transcriptional repressors. However,

the mechanism by which both hp66 protein paralogs mediate transcriptional repression remained unclear. It has been reported that SUMO modification of transcription factors, in most of cases, results in inhibiton of transcription. Thus the first aim of the present study is to address whether both hp66α and hp66β can be SUMOylated, and how SUMO modification regulates hp66 mediated transcriptional repression. Interestingly, several components of Mi-2/NuRD complex have been found in pairs. As decribed above in Table 1.2, these pairwise duplicated subunits form distinct complexes. Since hp66α and hp66β are homologus proteins, the question be answered within this work is whether both hp66 protein paralogs are within the same complex or form distinct complexes, and if so, what is the protein composition of the complexes?

2 MATERIALS AND METHODS

2.1 Materials

2.1.1 Equipment

Agarose electrophoresis system	PEQLAB, Pharmacia, Stratagene
	Biometra software
Blot apparatus	Pharamcia
Centrifuge	Eppendorf microfuge 5417R
	Hettich Microliter
	Heraeus Minifuge RF, GL
	Heraeus Cryofuge 20/30
	Beckman J2-MC
	Beckman Ultracentrifuge L70, XL70
Chromatography equipments	Pharmacia
Cryo 1°C freezing container	Nalgene™
Gel drier	BioRad Geldryer Model 583
Gel electrophoresis system	Pharmacia
	Biorad (PAGE) (MINI PROTEAN II™)
	Hoefer
Microliter Pipettes (10, 20, 200, 1000µl)	Gilson, Eppendorf
Microscope	Leica (Confocal)
	Zeiss (Fluorescence)
Milli Q Ultra pure water system	Millipore
Mono Q HR 5/5	Pharmacia
PCR cycler (Mastercycler gradient)	Eppendorf, Perkin Elmer
	Corbett research
Photometer	Berthold LB1210 B
Rotator	Neolab rotator 2-1175, MAGV
Semi-dry electroblot system	Pharmacia
Sonifier B21	Branson

Spectrophotometer	Pharmacia
Spectrophotometer quartz cuvette	LKB
Superose 6 column HR 10/30	Pharmacia
UV-transilluminator	Bachofer (366nm), UVP (254nm)
Vacuum centrifuge	Bachofer
X-ray film processor	Eastman Kodak

2.1.2 Consumables

Cryotube vials (1.8ml)	NUNC^{TM}
Falcon centrifugation tubes (15ml/50ml)	Sarstedt, Falcon
Filter pipet tips	Greiner
Glassware	Schott
Gloves	Braun, Roth
Microcon YM-30	Millipore
Centricon YM-30/50/100	Millipore
Microplates (6 well, 12 well)	Greiner
Microscope coverslips	Marienfeld, MAGV
Microscope slides	Marienfeld, MAGV
Micro tubes	Eppendorf
Parafilm	American National Can
Pasteur pipette	Brand, Volac
Petri dish	Greiner
PCR soft tubes, 0.2m1	Abgene, Eppendorf
Photometer cuvette	Ratiolab
Pipette tips	Brand, Eppendorf
Polyvinylidene difluoride membrane	Millipore
Quickseal tube (13 × 51mm)	Beckman
Sterile filters (0.45µm/0.2µm)	Millipore, Sartorius
Tissue culture dish	Greiner
Whatman-3MM-paper	Whatman
X-ray film	Kodak

2.1.3 Chemicals and reagents

Acetate	Merck
Acrylamide/Bisacrylamide 30, 30%, 37.5:1	Roth
Acrylamide/Bisacrylamide 40, 40%, 19:1	Roth
Agar	Difco
Agarose ultra pure	Roth
6-Amino-n-caproic acid	Sigma
Ammonium sulfate	Merck
Ammonium persulfate	Roth
Ampicillin	Serva
Adenosine triphosphate	Sigma
Bacto-peptone	Difco
Bacto-tryptone	Difco
Bovine serum albumin	Sigma
Bromophenol blue	Merck
Caesium chloride	Roth
Calcium chloride	Merck
Cetyl trimethyl ammonium bromide	Sigma
Chloroform	Merck
Chloramphenicol (dosage, 170µg/ml)	Roth
Coenzym A	Sigma
Coomassie brilliant blue R250	Serva
DEPC-ddH_2O	MBI Fermentas
Deoxynucleotidetriphosphate	MBI Fermentas
Dulbecco modified Eagle medium	Gibco BRL
Dimethylformamide	Serva
Dithiothreitol	Amersham
Ethanol absolute	Merck
Ethidium bromide solution (10mg/ml)	Roth
Ethylenediamine tetraacetic acid	Serva
Ethylene glycol-bis(beta-aminoethyl-ether)	
-n, n, n',n'-tetraacetic acid	Serva

Fetal calf serum	GIBCO BRL
G-418	GIBCO BRL
Glacial acetic acid	Merck
Glycerol	Roth
Glycine	Merck
Glucose	Merck
L-Glutamine	Gibco BRL
Hoechst 33342	Sigma
Hydrochloric acid	Merck
n-2-Hydroxyethylpiperazine	Roth
Isoamyl alcohol	Merck
Isopropanol	Roth
Kanamycin (dosage, 30µg/ml)	Merck
Lysozyme	Sigma
D-Luciferin	PJK GmbH
Magnesium chloride	Serva
Magnesium sulphate	Merck
Manganese chloride	Merck
β-Mercaptoethanol	Sigma
Methanol	Merck
Non-fat dry milk	Roth
Nonidet P-40	Merck
N-ethylmaleimide	Sigma
ortho-Nitrophenyl β-D-galactopyranoside	Sigma
Oligonucleotide	Eurogentec, Invitroge
Paraformaldehyde	Sigma
Penicillin/streptomycin solution	GIBCO BRL
Phenol (Roti-Phenol)	Roth
Phenylmethylsulfonyl fluoride	Sigma
Piperazine-n, n'-bis (2-ethane sulfonic acid	Sigma
Potassium chloride	Merck
Potassium dihydrogen phosphate	Merck

di-Potassium hydrogenphosphate	Merck
Potassium hydroxide	Merck
Propidium iodide	Sigma
Roti-Load	Roth
Sodium acetate	Merck
Sodium azide	Sigma
Sodium chloride	Merck
Sodium dihydrogen phosphate dehydrate	Merck
di-Sodium hydrogen phosphate	Merck
Sodium hydroxide	Merck
Sodium dodecyl sulphate	Serva
Sodium hydroxide	Merck
Protein A agarose/ salmon sperm DNA	Biomol
Sucrose	Serva
n,n,n',n'-Tetramethylethylenediamine	Merck
Tris base	Merck
Triton-X-100	Merck
Trichostatin A (TSA)	Biomol
Trypsin	Gibco BRL
Tween® 20	Roth
Urea	Pharmacia
Zinc chloride	Merck

Note: All chemicals are of analytical grade. All buffers were prepared with double distilled water (ddH_2O) or Milli Q water. Glassware, pipette tips and Eppendorf tubes were autoclaved.

2.1.4 Enzymes, reaction buffers and enzyme inhibitors

Calf intestine alkaline phosphatase (CIAP)	MBI Fermentas
Complete protease inhibitor cocktail	Roche Applied Science
DNaseI (RNase-free)	Promega
DpnI	MBI Fermentas
Klenow fragment	MBI Fermentas
Lysozyme	Boehringer

Mung bean nuclease	New England Biolabs
Pfu DNA polymerase	MBI fermentas
Protease K	MBI fermentas
Restriction endonucleases	MBI Fermentas, New England Biolabs
10× restriction enzymes buffer Y, R, B, G,O	MBI fermentas
10× restriction enzymes buffer 1, 2,3, 4	New England Biolabs
RNase A (DNase-free)	MBI fermentas
T_4 DNA ligase	MBI fermentas
T_4 DNA polymerase	MBI fermentas
Taq DNA polymerase	Invitrogen

2.1.5 Molecular weight markers

Prestained SDS-7B protein marker	Sigma
Prestained protein marker (broad range)	New England Biolabs
PageRuler^{TM} prestained protein marker	MBI Fermentas
λ DNA/EcoRI+HindIII marker 3	MBI Fermentas
pUC19 DNA/MspI marker 23	MBI Fermentas
Lamda DNA/Eco130I marker 16	MBI Fermentas

2.1.6 Antibodies

Anti-FLAG antibody:	Rabbit polyclonal, AbCAM 1:3000 in PBST for Western blotting
Anti-Gal antibody:	Rabbit polyclonal, Covance 1:2000 in PBST for Western blotting
Anti-GST antibody:	Mouse polyclonal, Santa Cruz 1:1000 in PBST for Western blotting
Anti-HDAC1 antibody:	Goat polyclonal, Santa Cruz 1:1000 in PBST for Western blotting

Anti-HDAC2 antibody:	Mouse monoclonal, Santa Cruz 1:1000 in PBST for Western blotting
Anti-MBD2 antibody:	Sheep polyclonal, Upstate 1:1000 in PBST for Western blotting
Anti-MBD2 antibody:	Goat polyclonal, Santa Cruz 1:1000 in PBST for Western blotting
Anti-MBD3 antibody:	Rabbit polyclonal, AbCAM 1:1000 in PBST for Western blotting
Anti-MBD3 antibody:	Goat polyclonal, Santa Cruz 1:1000 in PBST for Western blotting
Anti-Mi-2 antibody:	Goat polyclonal, Santa Cruz 1:1000 in PBST for Western blotting
Anti-mSin3a antibody:	Mouse monoclonal, Santa Cruz 1:1000 in PBST for Western blotting
Anti-p66 antibody:	Rabbit polyclonal, Upstate 1:500 in 10% skim milk in PBST for Western blotting
Anti-p66α antibody:	Rabbit polyclonal, AbCAM 1:1000 in PBST for Western blotting
Anti-p66β antibody:	Rabbit polyclonal, AbCAM 1:1000 in PBST for Western blotting
Anti-PRMT5 antibody:	Rabbit polyclonal (Dr.Uta Bauer)

	1:2000 in PBST for Western blotting
Anti-RbAp46 antibody:	Goat polyclonal, Santa Cruz 1:1000 in PBST for Western blotting
Anti-RbAp48 antibody:	Goat polyclonal, Santa Cruz 1:1000 in PBST for Western blotting
Anti-SUMO1 antibody:	Rabbit polyclonal, Zymed laboratories 1:1000 in PBST for Western blotting
Anti-SUMO1 antibody:	Rabbit polyclonal, Alexis biochemicals 1:1000 in PBST for Western blotting
Anti-rabbit, HRP conjugate:	Amersham 1:10,000 in PBST for Western blotting
Anti-goat IgG, HRP conjugate:	Santa cruz 1:10,000 in PBST containing 0.5% milk for Western blotting
Anti-mouse IgG, HRP conjugate:	Santa cruz 1:10,000 in PBST for Western blotting
Anti-sheep IgG, HRP conjugate:	Upstate 1:4000 in PBST containing 0.5% milk for Western blotting
Anti-FLAG M2 gel	Sigma For binding FLAG fusion proteins
FLAG peptide	Sigma

For elution of FLAG fusion proteins

2.1.7 Kits

TriFast™	peqLab
TNT *in vitro* Translation system	Promega
QIAquick® PCR purification kit	QIAGEN
High purity plasmid purification system	Marligen Biosciences
GeneAmp® RNA PCR core kit	Applied Biosystems
Platinum® SYBR Green qPCR SuperMix UDG	Invitrogen
ECL detection system	Amersham/Millipore
GENECLEAN® DNA purification kit	Q-Biogene
Nucleospin® DNA purification kit	Marcherey-Nagel
PlusOne™ Silver staining kit	Amersham Biosciences

2.1.8 E.coli strains

DH5α: genotype: F-, ϕ80d*lacZ*#M15, *endA*1, *recA*1, *hsdR*17 (r_k^-,m_k^+), *supE44, thi-1, gyrA96, relA1, #(lacZYA-argF)U169,* λ-, is a high transformable competent cell, which was generally used in DNA subcloning and production of plasmid DNA.

2.1.9 Eukaryotic Cell lines

CV-1: (ATCC # CCL70), the CV-1 cell line was derived from the kidney of a male adult African green monkey, which was cultured in DMEM with 2 mM L-glutamine, 10% FCS at 37°C, 5% CO_2.

HeLa: (ATCC # CCL2), a human epithelial cell line derived from cervix adenocarcinoma, which was cultured in the same medium as CV-1 cells.

HEK293: (ATCC # CRL1573), adenovirus 5 DNA transformed epithelial cells from human kidney, which was cultured in the same medium as CV-1 cells.

HEK293T: (ATCC # CRL-11268), a highly transfectable derivative of the 293 cell line with integration of the temperature sensitive gene for SV40 T-antigen, which was cultured in the same medium as CV-1 cells.

MCF7: (ATCC # HTB-22), a human epithelial cell line derived from breast carcinoma, which was cultured in the same medium as CV-1 cells.

NIH3T3: (ATCC # CRL-1658), EBV-transformed lymphoblasts with karyotype 48, XXXX, which was cultured in the same medium as CV-1 cells.

2.1.10 Plasmids

pBluescript II SK (Stratagene)

This vector was derived from pUC19 and contains LacZ gene which provides α-complementation for blue/white colour selection of recombination. This vector was used for cloning in cycle sequencing or as carrier DNA in eukaryotic cell transfections.

pAB-Gal$_{94}$. (Dr. Baniahmad)

This vector contains the Gal4 DNA binding domain (DBD), MCS, SV40 polyadenylation site**.**

pAB-Gal$_{94}$-hp66α. (Dr. Brackertz)

This vector was constructed by inserting the *Sal*I/*Nde*I-linker 5'-TCGACCATATGACCGAAG AAGCATG-3' in front of the *Sph*I site of pOTB7-hp66α to generate pOTB7-hp66α and subcloning the *Sal*I/*Xba*I fragment in-frame into the pAB-Gal$_{94}$ linker.

pAB-Gal$_{94}$-hp66β. (Dr. Brackertz)

This vector was generated by amplification of hp66β cDNA via RT-PCR from 293 mRNA using the gene specific 5' *SalI*-primer 5'-CACCGTCGACATGGATAGAATGACAGAAGA-3' and the respective 3' *BamHI*-primer 5'-TCAAGGATCCGGCAGTACAAGTGGAACAG-3'. The RT-PCR product was cut with *Sal*I/*BamH*I and cloned into the *Sal*I/*BamH*I site of pAB-Gal$_{94}$ linker.

pAB-Gal$_{94}$-MBD2b. (Dr. Böke)

This vector was created by excision of the corresponding MBD2b sequences out of pGEX-2T-MBD2b and in-frame insertion into pAB-Gal$_{94}$ linker.

pCMX-Gal-NCoR. (Dr. Baniahmad)

This vector was constructed by in-frame insertion of the corresponding NCoR sequences into

pCMX vector, a plasmid containing the GAL4 DNA binding domain (DBD)**.**

pEGFPC2. (Clontech)

This vector encodes a red-shift variant of the *Aequorea Victoria* green fluorescence protein (GFP) which has been optimized for brighter fluorescence and higher expression in mammalian cells. Genes cloned into the MCS are expressed as fusions to the C terminus of EGFP. The vector contains a kanamycin resistance gene and a neomycin-resistance cassette (Neo^r) which allows stably transfected eukaryotic cells to be selected using G418.

pEGFPC1-hp66α. (Dr. Brackertz)

This vector was cloned by ligating the *Sal*I/*BamH*I fragment from pAB-Gal_{94}-hp66α into pEGFP-C1 digested with *Sal*I/*BamH*I .

pEGFPC2-hp66β. (Dr. Brackertz)

This vector was created by insertion of the *EcoR*I/*BamH*I-fragment from pAB-Gal_{94}-hp66β into pEGFP-C2 cut with *EcoR*I/*BamH*I.

pSG5-hp66α. (Dr. Brackertz)

This vector was generated by subcloning the *EcoR*I/*Xba*I fragment from pOTB7-hp66α into pSG5 opened with *EcoR*I/*BamH*I.

pSG5-hp66β. (Dr. Brackertz)

This vector was cloned by ligating the *EcoR*I/*BamH*I fragment of pAB-Gal_{94}-hp66β into pSG5 cut with *EcoR*I/*BamH*I.

pcDNA3-FLAG-hp66α. (Dr. Brackertz)

This vector was generated via PCR with the sense primer :5'-AGGGGATCCATATGACC GAAGAAGCA-3' and the antisense primer : 5'- CCTGTCTAGAACTATTTCCACGTGGC TG- 3' from vector pGBKT7-hp66α. The PCR product was digested with *BamH*I/*Xba*I, and ligated into vector pcDNA3-FLAG-Alien α cut with *BamH*I/*Xba*I.

pcDNA3-FLAG-hp66β. (Dr. Brackertz)

This vector was constructed by subcloning the *Cfr9*I/*Xba*I fragment from pSG5-hp66β followed in-frame insertion into pcDNA3-FLAG-Alien α opened with *BamH*I/*Xba*I.

pBS1479. (Euroscarf)

A plasmid for TAP-tagging at the C-terminus, which also contains the *Kluyveromyces lactis* TRP1 gene.

pSilencer negative. (Ambion)

The plasmid is a circular plasmid encoding a hairpin siRNA whose sequence is not found in the mouse, human, or rat genome database.

pN3-FLAG-SUMO1. (Dr. Suske)

This vector was created by excision of the corresponding SUMO1 sequences out of pHM976 and in-frame insertion into pN3 vector digestion with *Xba*I/*Hind*III.

pcDNA3-HA-Ubc9. (Dr. Suske)

This vector was created by in-frame insertion of the corresponding hUbc9 sequences into pCDNA3-HA vector**.**

pCMV-tag-2B-PIAS1. (Dr. Suske)

This vector was constructed by in-frame ligation of the corresponding PIAS1 sequences into pCMV-tag-2B vector containing a FLAG tag**.**

pCMV-GST. (Dr. Baniahmad)

This eukaryotic expressing plasmid contains a CMV promoter, GST coding region, MCS, SV40 polyadenylation site, a thrombin cleavage sequence, and a PKA phosphorylation site.

pCMV-GST-MBD2b. (Dr. Böke)

This eukaryotic expression vectors was created by excision of the *BamH*I/*EcoR*I fragment out of pGEX-2T-MBD2b and in frame insertion into pCMV-GST opened with *BamH*I/*Cfr9*I.

pCMV-Myc-MBD3. (Dr. Pfeifer)

This vector was constructed by insertion of the corresponding MBD3 sequence into pCMV-Tag1 vector digested with *BamH*I/*Hind*III.

RbAp46 (pPK44). (Dr. Stillman)

This vector was created by in-frame ligation of the corresponding RbAp46 sequence into pET-19b vector cut with *Nco*I/*BamH*IIII.

RbAp48 (pPK40). (Dr. Stillman)
This vector was cloned by in-frame insertion of the corresponding RbAp48 sequence into pET-19b vector opened with *Nco*I/*Xho*I.

pcDNA3-HDAC1. (Dr. Baniahmad)
This vector was cloned by in-frame ligation of the corresponding HDAC1 sequences into pCDNA3 vector**.**

4×UAS-TK-Luciferase. (Dr. Baniahmad)
This vector contains four Gal binding sites upstream of the thymidine kinase promoter that drives the luciferase reporter gene.

pCMV-LacZ. (Dr. Baniahmad)
This expression plasmid encodes β-galactosidase.

2.2 Methods

2.2.1 Working with Escherichia coli (E.coli)

2.2.1.1 Preparation of competent bacterial cells: classical $CaCl_2$ method

Preparation of DH5α competent cells was carried out as described previously (Hanahan, 1983) with modification. A single colony of *E.coli* was inoculated into 3ml of antibiotic-free LB medium and cultured 8 hours at 37°C. This bacterial culture was then diluted into fresh 500ml TB medium and cultured until an OD_{600nm} of 0.5 was reached. Bacteria were pelleted at 3200rpm for 10 minutes at 4°C. All the following steps were performed at 4°C. The pellet was carefully resuspended in 40ml of TB buffer using a pre-chilled glass pipet, and incubated for 10 minutes, then transferred to 50ml Falcon. The suspension was then pelleted at 3200rpm at 4°C for 3 minutes. The pellet was resuspended and incubated with 9.3ml TB buffer and 0.7ml DMSO for 10 minutes. The suspension of bacteria was then dispensed as 220µl aliquots into pre-chilled tubes. The aliquots were frozen immediately in liquid nitrogen and stored at -80°C.

TB buffer: 10mM PIPES
15mM $CaCl_2$

250mM KCl
adjust pH to 6.7 with KOH, autoclaved.
55mM $MnCl_2$ (sterile filtration)

LB medium: 10 g/l Bacto-tryptone
5 g/l yeast extract
10 g/l NaCl
pH 7.5, autoclaved

TB-Medium 12 g/l Bactotrypton
24 g/l Yeast extract
4 ml/l Glycerol
autoclave

10x Phosphat-Puffer 170 mM KH_2PO_4
720 mM K_2HPO_4
autoclave

LB-agar plate: 10 g/l Bacto-tryptone
5 g/l yeast extract
5 g/l NaCl
15 g/l Agar
pH 7.5, autoclaved and cooled to about 50°C in a waterbath. After adding antibiotics, medium was poured into Petri dishes and allowed to solidify. Plates were then stored at 4°C in darkness for up to 4 weeks.

Antibiotic plates: contain 100µg/ml Ampicillin or 33µg/ml Kanamycin in LB-agar plates.

2.2.1.2 Transformation of competent cells

Frozen ompetent cells were thawed by placing on ice just before use. Plasmid DNA (100-500ng) or 15µl of ligation mixture was mixed with 100µl of competent bacteria by stirring gently with a pipet tip, and then incubated on ice for 30 minutes. Competent cells were heat shocked at 42°C for 90 seconds, and then placed on ice for 2 minutes. For each transformation, 900µl LB medium without antibiotics was added. After 1 hour incubation at 37°C, the mixture was centrifuged at 3000rpm for 3 minutes. After discarding off supernatant, the rest about 80µl transformation mixture was spread onto pre-warmed selective LB-agar plates. The plates were incubated overnight at 37°C. The colonies were then analysed for positive clones using restriction enzymes and further confirmed by DNA sequencing.

2.2.2 Working with DNA

2.2.2.1 Storage of DNA

Basically, DNA was dissolved in TE buffer and stored at -20°C.

TE buffer: 10mM Tris-HCl, pH 7.5
1mM EDTA,
sterilfilter/autoclave

2.2.2.2 Small-scale preparation of plasmid DNA (Mini-prep)

A Mini-prep of plasmid DNA was performed as described by Holmes and Del Sal. (Del Sal et al., 1989; Holmes and Quigley, 1981). A single bacterial colony from the antibiotics containing plates was inoculate 3ml sterile LB medium with appropriate antibiotics, then grown in incubator overnight at 37°C. An overnight 1.5ml LB culture was spun at maximum speed in a microfuge for 20 seconds. The cell pellet was completely resuspended in 300µl STET buffer by vigorous vortexing. Then 10µl lysozyme (10mg/ml) was added to the suspension and the mixture was immediately placed in a boiling water bath (100°C) for 1 minute. Afterwards, the mixture was centrifuged at 14000rpm for 10 minutes. After taking off the bacterial pellet, 15µl CTAB solution was added to the supernatant and mixed by inversion. The mixture was further centrifuged at full speed in a microfuge for 10 minutes. After discarding off the supernatant, the pellet was dissolved in 500µl 1.2M NaCl on a multitube vortexer for 5-30 minutes until pellet dissolved. Afterwards, 1ml 100% (v/v) ethanol was added and the mixture was further incubated at room temperature (RT) for 10 minutes. The mixture was centrifuged at full speed in a microfuge for 15min and the DNA pellet was retrieved. The pellet was washed once with 70% (v/v) ethanol, dried by placing under a vacuum for 3-5 minutes, and finally dissolved in 30µl TE buffer.

STET-Puffer 50 mM Tris-HCl (pH 7,5)
50 mM EDTA
0.5% (v/v) Triton X-100
8%(v/v) Saccharose
sterilfilter

5% CTAB) (W/V) 5g CTAB in 100ml ddH_2O

2.2.2.3 Large-scale preparation of plasmid DNA (Maxi-prep)

Large-scale preparation of plasmid DNA (Maxi-prep) was performed as described previously (Birnboim and Doly, 1979). A single transformed bacterial colony was inoculated into 3ml LB medium supplemented with appropriate antibiotics and incubated overnight at 37°C. The overnight culture was diluted in fresh medium containing 360ml TB medium and 40ml 10× Phosphate buffer and the appropriate antibiotics. The bacteria were grown at 37°C with vigorous agitation for 8 hours and 2ml chloramphenicol solution (34mg/ml in ethanol) was added to enhance the amplification of plasmid in *E.coli* (in particular for low-copy plasmids). After overnight incubation (12-16 hours), cells were collected by centrifugation at 4000 rpm (rotor JA-10, Beckman) for 15 minutes at 4°C. The cell pellet was resuspended in 10ml Sol I and incubated at RT for 5 minutes. Sol II (20ml) was added and the suspension was well mixed by gently shaking. The mixture was kept on ice for 10min and 15ml Sol III was added. The mixture was gently mixed, and incubated on ice for 10 minutes. The mixture was clarified by centrifugation at 7000 rpm (rotor JA-10, Beckman) for 20 minutes at 4°C. The supernatant was poured into 2×50ml Falcons through 3 layers of gauze, then mixed with 0.6 vol of isopropanol by inversion and placed at RT for 15 minutes. Centrifugation was then performed at 6000 rpm (Heraeus) for 20 minutes at RT to recover nucleic acids. After gently discarding the supernatant, the pellet was dried at 37°C and was then dissolved in 2ml TE at 37°C with agitation. The samples in two Falcons were combined. CsCl (4.5g) and 500µl ethidium bromide (10mg/ml) were added to the mixture. Then the mixture was agitated at 37°C until the salt was dissolved. Centrifugation was performed at 6000rpm (Heraeus) for 10 minutes at RT. The supernatant was transferred into a Quickseal tube and the tube was filled up with 50% (w/w) CsCl and TE buffer to a final weight of 9.5-9.8g. Ultracentrifugation was carried out at either 70000rpm for 3 hours or at 55000rpm for ≥14 hours at 20°C (rotor VTi-90, Beckman). Afterwards, the tube was carefully removed from the ultracentrifuge. The plasmid band (the lower of the two bands) was recovered by inserting a 2ml syringe attached with a 20-G needle into the side of the tube 0.5cm below the plasmid band. The recovered plasmids were transferred into another Quickseal tube and the tube was balanced again with a final weight of 9.5-9.8g. The second centrifugation either 55000rpm for ≥14 hours or 70000rpm for 3 hours was performed at 20°C (rotor VTi-90, Beckman). After recovering the plasmid band, 2ml of isopropanol / saturated CsCl solutions was added. The mixture was vortexed and the red upper phase containing ethidium bromide was removed. This step was repeated at least 6 times until no red colour was left. After last

wash, the upper phase was all discared, and 2 vol of water were added to the lower phase. The solution was then well mixed with 0.6 vol isopropanol and incubated on ice for 15 minutes. The plasmid DNA was recovered by centrifuging at 6000rpm (Heraeus) for 30 minutes at 4°C and was then washed once in 70% ethanol. The pellet was dried and then dissolved overnight in 300-500µl TE at 4°C. After measuring plasmid DNA concentration, the dissolved plasmid DNA was stored at –20°C. Alternatively, High purity plasmid purification systems (Marligen Biosciences), which is a unique anion exchange resin, was available to purify plasmid DNA according to manufacturer's instructions.

Sol I:	50mM glucose 25mM Tris-HCl, pH 8.0 10mM EDTA autoclaved 4g/l Lysozyme (freshly added)
Sol II:	0.2N NaOH 1% SDS (w/v) prepared freshly and kept at RT
Sol III:	24.5g potassium acetate 35ml glacial acetic acid pH 4.8, adjusted with glacial acetic acid fill up to 100ml with ddH_2O, sterilized by filtration
50% (w/w) CsCl:	50g CsCl in 50g ddH2O
TB-Medium	12 g/l Bactotrypton 24 g/l Yeast extract 4 ml/l Glycerol autoclave
10× Phosphat-Puffer	170 mM KH_2PO_4 720 mM K_2HPO_4 autoclave

2.2.2.4 Measurement of DNA concentration

The concentration of DNA in a given sample was calculated based on the OD_{260nm} and OD_{280nm} measured with a spectrophotometer. Pure DNA should have an OD_{260nm}/OD_{280nm} ratio of

1.8~2.0. An OD_{260nm}/OD_{280nm} lower than 1.8 indicates that the DNA sample is contaminated with proteins and aromatic substances, whereas an OD_{260nm}/OD_{280nm} higher than 2.0 means a possible contamination with RNA. The concentration of dsDNA was calculated with the following formula: DNA concentration (µg/ml) = OD_{260nm} × 50 × dilution factor.

2.2.2.5 Molecular cloning

2.2.2.5.1 Restriction endonuclease digestion

Digestion with restriction endonucleases was carried out according to manufacturer's instruction. Briefly, plasmid DNA or PCR product, optimal 10× reaction buffer, restriction endonucleases and ddH_2O were mixed in an eppendorf tube in a total volume of 15-20µl. The reaction mixture was incubated at different temperature as recommended by the manufacturer. Restriction endonucleases were inactivated by either heating at 65°C or 80°C or the digestion was terminated by phenol/chloroform extraction.

2.2.2.5.2 Filling-in of recessed 3'-termini of DNA with Klenow Fragment

The Klenow Fragment is the Large Fragment of DNA polymerase 1, *E.coli*, which exhibits a 5'-3' polymerase activity, and is used to fill-in of recessed 3'-termini ends with deoxynucleotides(dNTPs) (Tabor and Richardson, 1987). The reaction mixture was prepared mixing digested DNA (0.1-4µg), 2µl of 10× Reaction buffer, 0.5µl 2mM dNTPs (50µM final concentration) and Klenow Fragment (1-5U) with ddH_2O up to final volume of 20µl. The reaction was performed at 37°C for 10 minutes and was terminated by heating at 75°C for 10 minutes.

2.2.2.5.3 Removing of 3' and 5' protruding ends with Mung Bean Nuclease

The properties of Mung Bean Nuclease (McCutchan et al., 1984) is removal of 3' and 5' protruding ends of DNA creating ligatable blunt ends. Standard assay was prepared by mixing digested DNA, Mung Bean Nuclease, 10× Reaction buffer and ddH_2O and was incubated at 30°C for half an hour. The reaction was stopped by phenol/chloroform extraction.

2.2.2.5.4 Dephosphorylation of DNA ends

To avoid re-circulization and self-ligation of the linearized vector DNA during subcloning, calf intestinal alkaline phosphatase (CIAP) was employed to dephosphorylate the terminal 5'-

phosphate of the vector DNA (Ausubel, 1989). The reaction mixture was prepared by mixing DNA, CIAP, 10× Reaction buffer and ddH_2O and was incubated at 37°C for half an hour. Alternatively, CIAP was added directly to the restriction endonuclease mixture after DNA cleavage when the reaction buffer is compatible to CIAP. CIAP was inactivated either by heating at 85°C for 15 minutes or phenol/chloroform extraction.

2.2.2.5.5 Phenol/chloroform extraction and ethanol precipitation of DNA

Phenol/chloroform extraction was routinely employed to purify and concentrate the DNA preparation. The volume of DNA mixture was adjusted to ≥ 200µl. An equal volume of phenol and chloroform were added to the DNA containing solution followed by vortexing vigorously. After centrifugation at maximum speed for 5 minutes at RT, the upper aqueous phase was transferred to a new tube and precipitated with 1/10 vol 3M NaAc (pH 5.2) and 2.5 vol of ice-cold 100% ethanol. After incubation for 20 minutes at -20°C, DNA was recovered by centrifugation at 14000rpm for 15 minutes at 4°C. Pellet was washed once with 70% ethanol, air-dried and then dissolved in an appropriate volume of ddH_2O or TE buffer.

2.2.2.5.6 PCR cloning

This strategy was used to amplify DNA of interest with desired restriction enzyme by polymerase chain reaction (PCR) for subcloning. For PCR cloning, the high-fidelity Pfu polymerase was used. PCR primers were designed with 1-5 extra nucleotide at their 5'-end adjacent to the recognition site for the desired restriction enzyme. The standard PCR reaction was prepared (Table 2.1).

Table 2.1 standard PCR reaction composition

dsDNA template (50ng/µl)	**1.0µl**
sense primer (10µM)	**1.0µl**
antisense primer (10µM)	**1.0µl**
dNTP mix (10mM)	**1.0µl**
10×Pfu polymerase reaction buffer	**5.0µl**
Pfu polymerase (2.5U/µl)	**1.0µl**
ddH_2O	**40.0µl**
Total volume	**50.0µl**

The reaction mixture was prepared in a thin-wall tube, and placed in a thermal cycler. The

mixture was first denatured for 2 minutes at 95°C followed by cycles as shown in Table 2.2.

Table 2.2 standard protocol for PCR

denaturation	**30 second**	**95°C**
annealing	**30 second**	**60-65°C**
extension	**2 minutes/kb**	**68°C**
cycles	**30**	
final extension	**10 minutes**	**68°C**

The PCR product was loaded on an agarose gel and the DNA band was excised and purifed by GENECLEAN® or Nucleospin® DNA purification Kit. Then the PCR product was digested with specific restriction enzyme, and ligated into corresponding linear vector DNA. Then transformation was carried out with competent cells, and the correct clones were confirmed by digestion and further DNA sequencing.

2.2.2.5.7 Agarose gel electrophoresis

Agarose powder was melted in 1×TAE buffer using a microwave oven and the solution was cooled to about 55°C, and 0.5μg/ml ethidium bromide was added. The solution was then poured into a casting platform and allowed to solidify. 0.8-2% agarose gels were routinely employed for analyzing DNA. DNA samples were mixed with a final volume of 1× loading buffer before loading into the slots. The voltage of electrophoresis was set to ~10V/cm gel length. DNA was visualized by illuminating the gel with a UV light source and was photographed directly. For subcloning, the desired bands were excised with a clean scalpel.

50× TAE: 2M Tris-HCl, pH7.8
150mM NaAc
50mM EDTA

6× loading buffer: 0.025% (w/v) bromophenol blue
30% (v/v) glycerol

2.2.2.5.8 Extraction of DNA fragments from agarose gel

The desired DNA bands were cut from ethidium bromide stained agarose gel under the UV light. DNA fragments were extracted from agarose gel slices with a Nucleospin DNA purification kit (Marcherey-Nagel) or GENECLEAN® II KIT (Q- Biogene) according to the manufacturer's instructions.

2.2.2.5.9 Ligation

The T4 DNA ligase catalyzes the formation of phosphodiester bonds between adjacent 3'-hydroxyl and 5'-phosphate termini in duplex DNA with blunt or sticky end termini (Ausubel, 1989). A ligation reaction mixture was mixed with 1µl T_4 DNA ligase, 1.5µl of 10× Ligation buffer, an appropriate molar ratio of linearized vector DNA and purified insert DNA fragment (1:5 for blunt ends and 1:3 for sticky ends) in a total volume of 15µl. The reaction was incubated at 22°C overnight for blunt-end ligation or for 4-6 hours for sticky-end ligation. Ligated DNA was transformed into competent cells after the ligation reaction.

2.2.2.6 Site-directed mutagenesis

This protocol is based on Quickchange® Site-Directed Mutagenesis Kit (Stratagene) with modifications. The strategy is used to make point mutations, switch amino acids, and delete or insert single or multiple amino acids. The general procedure utilizes a supercoiled double-stranded DNA vector with insert of interest and two synthetic primers containing the desired mutation. The mutagenic oligonucleotide primers were designed according to recommended instructions. The mutagenesis PCR reaction was prepared as indicated above (see section 2.2.2.5.6). The cycling parameters for the mutagenesis PCR was shown in Table 2.3. The cycle number was adjusted based on the type of desired mutation (Table 2.4). To each amplification reaction 1µl of *Dpn*I restriction enzyme (10U/µl) was added, which is used to disgest the parental DNA template, and then incubate overnight at 37°C. For each sample, an aliquot of 100µl DH5α competent cells was added to a prechilled tube with 1µl of the *Dpn*I treated DNA.

Table 2.3 The cycling parameters for the mutagenesis PCR

Segment	Cycles	Temperature	Time
1	**1**	**95**	**30 sec**
2	**12-18**	**95**	**30 sec**
		55	**1 min**
		68	**1 min/kb of plamid length**

Table 2.4 The cycle number was adjusted based on the type of desired mutation

Type of mutation desired	Number of cycles
Point mutations	**12**
Single amino acid changes	**16**
Multiple amino acid deletions or inserions	**18**

The transformation reaction was carried out (see section 2.2.1.2). The colonies were further confirmed by nucleic acid sequencing.

2.2.3 Working with RNA

2.2.3.1 Isolation of total RNA from mammalian cells

To prevent contamination of RNase, gloves were worn and RNase-free tubes, filter pipette tips, glassware and solutions were used. Eukaryotic HEK293 cells with or without transfection were washed twice with PBS. Cells from one $10cm^2$ dish were directly lysed in 1ml TriFast^{TM} solution for 5 minutes by gently pipetting up and down. The lysate was transferred to a new tube, and kept at RT for 5 minutes. The lysate was shaken by hand vigorously after addition of 0.2ml of chloroform for 15 seconds and kept at RT for 5-10 minutes. Then the samples were clarified at 11,000rpm for 5 minutes at RT. The colorless upper aqueous phase was transferred to a new tube. The RNA was precipitated with 0.5ml isopropanol and kept on ice for 10 minutes. The RNA pellet was formed by centrifugation at 11,000rpm for 10 minutes at 4°C. The pellet was then washed twice with 1ml 75% ethanol by centrifugation at 9,000rpm for 8 minutes at 4°C and air-dried about 10-15 minutes in a clean space. The dried pellet was dissolved in 40µl DEPC-H_2O.

2.2.3.2 Measurement of RNA concentration

The concentration of RNA of a given sample was calculated depending on the ratio of OD_{260nm}/OD_{280nm} measured with a spectrophotometer. Pure RNA should have an OD_{260nm}/OD_{280nm} ratio of approximately 2.0. An OD_{260nm}/OD_{280nm} smaller than 2.0 indicated that the samples is contaminated with proteins and aromatic substances. The concentration of RNA was calculated based on the OD_{260nm} with the following formula: RNA concentration (µg/ml) = $OD_{260nm} \times 40 \times$dilution factor

2.2.3.3 cDNA synthesis from total RNA by reverse transcription

Reverse transcription was employed to convert mRNAs into cDNAs by using reverse transcriptase and random hexamers. The components of reverse transcription reaction were

mixed (Table 2.5). The mixture was first incubated at RT for 10 minutes for extension of the hexameric primers by reverse transcriptase, and then incubated at 42°C for 15 minutes and the reaction was terminated by incubation at 99°C for 5 minutes. Finally, the mixture was kept at 5°C.

Table 2.5 standard reverse transcription reaction mixture

10× Reaction buffer	**2.0µl**
$MgCl_2$ (25mM)	**4.0µl**
dNTPs (25mM)	**2.0µl each**
Random Hexamers (50µM)	**1.0µl**
RNase Inhibitor (20U/µl)	**1.0µl**
DEPC-ddH_2O	**2.0µl**
Total RNA (1µg/µl)	**1.0µl**
MuLV reverse transcriptase (50U/µl)	**1.0µl**
Total volume	**20µl**

2.2.3.4 PCR amplification

PCR was used to amplify a segment of DNA of a known sequence with gene-specific primers. A repetitive series of cycles involving template denaturation, primer annealing, and extension of the annealed primers by the polymerase leads to exponential accumulation of a specific DNA fragment. The ends of the fragment are defined by the 5' ends of the primers. Basically, PCR reaction mixture contains 1.0µl cDNA from reverse transcription, dNTPs, two appropriate synthesized primers, Taq polymerase (instead of Pfu polymerase), and reaction buffer (see 2.2.2.5.6). The mixture was first denatured for 2 minutes at 95°C followed by cycles (Table 2.6). The PCR reaction was loaded on an agarose gel, and visualized under the UV light resourse.

Table 2.6 standard protocol for PCR reaction

denaturation	**30 second**	**95°C**
annealing	**20 second**	**55-65°C**
extension	**30 second**	**72°C**
cycles	**25-35**	
final extension	**10 minutes**	**72°C**
cool to 4°C		

2.2.4 Working with eukaryotic cells

2.2.4.1 Cell culture

Cells were cultured in the complete culture medium containing Dulbecco modified Eagle medium (DMEM) supplemented with 10% FCS, penicillin (100U/ml), and streptomycin (100µg/ml) at 37°C, 5% CO_2. Adherent cells were passaged by trypsinization. The medium in culture dishes was aspirated and discarded. Cells were washed twice with PBS by pipetting onto the side of the plate. Afterwards, 1-2ml Trypsin/EDTA solution was added and swirled to cover the whole dish. Cells were incubated at 37°C until they were fully trypsinized. Cells were detached from the bottom of dishes by flicking the plate. DMEM culture medium was then added and cell clumps were dispersed into single cells by gently pipetting. The cell number was counted using a blood cell counting chamber. Afterwards, cells were diluted to a desired density and split into new dishes.

10× PBS:
100mM $Na_2HPO_4 \cdot 2H_2O$
17mM KH_2PO_4
1.37M NaCl
27mM KCl
pH 7.4, autoclaved

Trypsin/EDTA:

A
6mM $Na_2HPO_4 \cdot 2H_2O$
1mM KH_2PO_4
137mM NaCl
2.7mM KCl
3mM EDTA
0.125% (w/v) trypsin (Bovine Pancreas)
pH 7.0, prepared in 3/4 of the final volume

B
0.6mM $CaCl_2$
0.4mM $MgSO_4$
prepared in 1/5 of the final volume

mix A and B and fill up to the final volume with ddH_2O, sterilized by filtration and stored at -20°C

2.2.4.2. Freezing, thawing and storage of eukaryotic cells

Cells grow at least to 80% confluence for freezing preservation. Adherent cells were suspended by trypsinization and were collected by centrifugation at 500-1000g for 5 minutes. The cell pellet was resuspended in 2ml fresh DMEM medium and dispensed as 0.8ml aliquots into Cryotube vials. To each tube, 0.8ml DMSO frozen medium was slowly added. The cell suspension was gently mixed by inversion of tubes. The cell aliquots were then placed into a Cryo 1°C freezing container and were placed in -80°C overnight. The next day, the cells were stored in liquid nitrogen. For thawing cells, frozen aliquots were removed from liquid nitrogen and thawed immediately at 37°C water bath. The cell suspension was then transferred into tissue culture dishes containing 20ml of fresh complete DMEM medium at an appropriate cell density. The next day, the medium had to be refreshed with pre-warmed DMEM medium.

Frozen medium: 15% DMSO
40% FCS
45% DMEM medium

2.2.4.3. Transfection of DNA into mammalian cells

2.2.4.3.1 Calcium phosphate transfection

Cells were seeded out in 6-well or 10cm tissue culture dishes at a density such that 50-70% confluence could be reached for transfection. Calcium phosphate precipitation of plasmid DNA (Wigler et al., 1978) was prepared in Eppendorf tubes (Table 2.7).

Table 2.7 standard transfection reaction mixture

Components	6-well	10 cm
DNA (1μg/μl)	**5.4μl**	**20-30μl**
10×HEBS	**21.6μl**	**125μl**
ddH_2O	**178.2μl**	**1042.5/1032.5μl**
2M $CaCl_2$	**10.8μl**	**62.5μl**
Total volume	**216μl**	**1250μl**

DNA was well mixed with 10× HEBS and ddH_2O. 2M $CaCl_2$ was then added and the whole mixture was immediately vortexed for 10secs and incubated at RT for 10-15 minutes. Finally,

the mixture was dropped onto the cells. 24 hours after transfection, cells were washed twice with PBS and fresh culture medium was added.

10× HEBS:
1.37M NaCl
0.06M glucose
0.05M KCl
0.007M Na_2HPO_4
0.2M HEPES
pH 7.2 adjusted with NaOH, sterilized by filtration and aliquots were stored at -20°C

2.2.4.3.2 jetPEI transfection

jetPEI™ (Polyplus) is a cationic polymer transfection reagent that ensures effective and reproducible transfection with low toxicity. jetPEI™ was employed according to manufacturer's instructions.

2.2.4.3.3 Luciferase reporter assay

For luciferase reporter assay, about 2×10^5 cells were seeded into each well of a 6-well plates 24 hours prior to transfection and then transfected using the $CaPO_4$ method as described above. Each transfection contained 5.4µg of total plasmid DNA, includuing 0.25µg of 4×UAS-TK-luciferase reporter plasmid, 0.05µg of pCMV-lacZ encoding β-galactosidase and varying amounts of expression plasmids Gal, Gal-hp66α, Gal-hp66β. Cells were harvested 48 hours after transfection by addition of 200µl lysis buffer after removal of old medium and washing with 1×PBS buffer twice in each well. The reaction was incubated at RT for 15 minutes. The cell lysate was then transferred to a new tube, and kept on ice. 5-20µl of cell lysate was taken together with 100µl luciferin buffer for assay on luminometer. The luciferase activity was expressed as relative light units per second (RLU/s). In addition, transfection efficiency was normalized to β–galactosidase activity. 5-10µl of cell lysate was taken together with 0.8ml Z-buffer and 0.2ml ONPG solution (4mg/ml in Z-buffer) and the mixture was incubated at 30°C until the color of mixture turned out light yellow. The β–galactosidase activity was measured on spectrophotometer with absorbance at 420nm. The results are the average of at least two independent transfection experiments.

Lysis buffer: 50mM Tris/Ac, pH 7.8

10mM MgAc
0.1mM EDTA
10% Triton X-100
15% glycerol
sotered at -20°C, freshly added 0.1mM PMSF and 1mM DTT

Luciferin buffer:
360µM Luciferin (5mg)
1mM ATP
50mM Tris/Ac, pH 7.8
400µM Coenzyme A
fill up to 50ml, stored at -20°C

Z-buffer:
60mM $Na_2HPO_4 \cdot 2H_2O$
40mM $NaH_2PO_4 \cdot H_2O$
10mM KCl
1mM $MgSO_4 \cdot 7H_2O$
pH 7.0 adjust with HCl, autoclaved, stored at -20°C

2.2.4.4. Establishment of stably transfected HEK293 cell lines

Basically, the stable cell lines is that the transfected DNA is integrated into chromosomal DNA, and can be distinguished by using selectable markers (usually an eukaryotic antibiotic-resistance gene). Several expression plasmids were created for generation of stable cell lines, such as pcDNA3-FLAG-hp66α/β-CBP which contain FLAG tag, CBP tag and neomycin-resistance gene. In addition, pcDNA3-FLAG-CBP was used to generate control stable cell lines. Prior to selection with G418, it is important to titrate with selection antibiotics, for example G418, to determine the optimal concentration for selection with particular cell line being tested. For selecting the optimal concentration of antibiotics, it is recommended to use the minimum concentration that starts to give maximum cell death in 5 days and kills all the cells within two weeks. In this study, we found that the optimal concentration of G418 is 1.5mg/ml in HEK293 cells. HEK293 cells were grown in 6-well plates, and transfected with 1.0µg pcDNA3-FLAG-CBP, pcDNA3-FLAG-hp66α-CBP or pcDNA3-FLAG-hp66β-CBP constructs by using calcium phosphate transfection. Cells were transferred to DMEM medium containing 1.5mg/ml G418 48 hours after transfection. The DMEM medium containing 1.5mg/ml G418 was refreshed every 3 days until individual colonies appeared. Cell colonies were then picked and expanded individually. The stable cell colonies were identified by RT-PCR using specific primers (see section 2.2.3) and by Western

blotting using FLAG antibody (see section 2.2.5.2), and were prepared frozen aliquots to be a reusable source of cells.

2.2.4.5. Cellular fractionations

2.2.4.5.1 Preparation of whole cell extract

Whole cell extract was prepared by lysing cells in lysis buffer. Cells were washed twice with PBS. Lysis buffer (10^6-10^7 cells/ml) was then added, and the cells were incubated at 4°C for 15-30 minutes on a shaker. The cells were scraped and collected. The cell suspension was centrifuged at 12,000rpm for 15 minutes at 4°C. The supernatant was transferred to a prechilled tube. 10% glycerol was added and aliquots of the whole cell extract were stored at -70°C, if the supernatant was not to be used immediately. For immediate use, the whole cell extract was kept on ice, and Roti-Load 1 solution (Roth) was added. The samples were then boiled for 5 minutes to denature proteins and were ready for Western blotting analysis.

Lysis buffer: 50mM Tris HCl, pH 7.4
150mM NaCl
1mM EDTA
1% Triton X-100

2.2.4.5.2 Nuclear protein extraction

Nuclear extracts were prepared as described previously with modification (Standke et al., 1994). Briefly, the cells with or without transfection were washed twice with PBS, and trypsinized with trypsin. The cells were then harvested after adding DMEM medium, and centrifuged at 3000rpm for 3 minutes at 4°C. Afterwards, the cell pellet was resuspended in 3 volumes of buffer A, and incubated on ice for 7 minutes. After centrifugation at 5600rpm for 10 minutes at 4°C, the supernatant (cytoplasmic fraction) was transferred into a new tube for later use. The remaining nuclear pellet were resuspended in 2 volumes buffer B, followed by incubation for 40 minutes at 4°C on a rotator. The lysate was centrifuged at 14000rpm for 10 minutes at 4°C and the supernatant that is nuclear extract was transferred into a new tube. The nuclear extract was diluted with 2 volumes of Buffer C, and kept at -20 °C.

Buffer A: 20mM HEPES, pH 7.9
10% glycerol

1mM EDTA
10mM KCl
0.2% Nonidet P-40
freshly added 0.1mM PMSF and 1mM DTT

Buffer B: 20mM HEPES, pH 7.9
420mM NaCl
1mM EDTA
10mM KCl
freshly added 0.1mM PMSF

Buffer C: 20mM HEPES, pH 7.9
10mM KCl
1mM EDTA

2.2.4.5.3 Measurement of protein concentrantion

Bradford Assay (Bradford, 1976) is a rapid and accurate method commonly used to determine the total protein concentration of a sample. The method is based on the observation that the absorbance maximum for an acidic solution of Coomassie Brilliant Blue G-250 shifts from 465nm to 595 nm when binding to protein occurs. Within the linear range of the assay (~5-25 mg/ml), the more protein present, the more Coomassie bind. The concentration of given samples were measured by mixing 1-5 µl proteins extract with 800 µl 0.25 M Tris/HCl (pH 7.8) and 200 µl Roti-Quant (Roth). Then the mixture was incubated for 5 minutes at RT. The absorbance was read in the photometer at 595nm, and the concentration was caculated with the following formula: protein concentration (µg/µl) = OD_{595nm} × 19.89 (µg) / volume of protein extract (µl).

2.2.5 Preparation and analysis of proteins

2.2.5.1. Protein precipitation with TCA

The whole procedure was carried out at 4°C. 100µg samples were diluted to 300µl volume with water, and 100µl ice-cold 80% TCA was added. The mixture was vortexed briefly, and incubated on ice for 20 minutes. The mixture was spun at 14000 rpm for 5 minutes in a microfuge and the protein pellet at the bottom was generally visible. The supernatant was carefully removed without disturbing the pellet. Afterwards, 500µl ice-cold aceton was added

and the protein pellet was recovered by centrifugation at 14000rpm for 5 minutes. This step was repeated two times. The pellet was air-dried for 10-15 minutes and dissolved in the appropriate buffer. If the color of sample turns into yellow, add 1-5 drops of 1M NaOH until the color of sample turns into blue again.

2.2.5.2. SDS polyacrylamide gel electrophoresis and Western blotting analysis

SDS polyacrylamide gel electrophoresis (SDS-PAGE) was carried out as described from Laemmli (Laemmli, 1970)on acrylamide slab gels. The glass plate sandwich mold were assembled according to the manufacturer's instruction using 1mm thick spacers. Acrylamide gels was prepared (Table 2.8).

Table 2.8 compositions of separating gel and stacking gel

Separating gel	7.5%	10%	12%
ddH_2O	5.0ml	4.1ml	3.5ml
1.5M Tris-HCl, pH 8.8	2.5ml	2.5ml	2.5ml
Acrylamide/Bis (30/0.8, 37.5:1)	2.5ml	3.4ml	4.0ml
10% (w/v) SDS		100µl	
40% (w/v) APS		30µl	
TEMED		20µl	

Stacking gel	5%
ddH_2O	6.2ml
0.5 M Tris-HCl, pH 6.8	2.5ml
Acrylamide/Bis (30/0.8, 37.5:1)	1.3ml
10% (w/v) SDS	100µl
40% (w/v) APS	30µl
TEMED	20µl

Ingredients were mixed gently, and APS and TEMED were added just before pouring the gels. The separating gel was poured to an appropriate level and the top of gel was slowly covered with a layer of ethanol to ensure a flat surface and to exclude air. After the gel was polymerized, the ethanol was poured off. The stacking gel was then poured above the separating gel with a comb inserted. After the stacking gel was polymerized, the comb was carefully removed and the gel slots were rinsed with ddH_2O and excessive gel debris were removed. The gel slabs

were assembled into the electrophoresis chamber and the chamber was filled with Laemmli buffer. Protein samlpes were denatured by boiling in SDS-loading buffer or Roti-Load 1 (Roth) for 5 minutes. Samples and prestained protein molecular mass markers were loaded and empty slots were filled with equal volume loading buffer to prevent spreading of adjoining lanes. For electrophoresis, a constant current of 20-25mA/gel was used for stacking gels and 30-35mA/gel for separating gels.

After SDS-PAGE, proteins on the gel were transferred to PVDF membrane using a semi-dry blotting system. The transfer sandwich was assembled on the bottom of anode electrode by laying, one after the other, 6 pieces of whatman paper (soaked in anode buffer I), 3 pieces of whatman paper (soaked in anode buffer II), a piece of PVDF membrane, the gel and 6 pieces of whatman paper (soaked in cathode buffer III). Air bubbles were extruded by gentle rolling with a glass pipet. Finally, the cathode electrode was placed on top of the transfer sandwich. The transfer was performed at a constant current of 1mA/cm^2 for 1-2 hours.

After transfering, membranes were blocked in PBST containing 5-10% non-fat milk at RT for at least 2 hours or at 4°C overnight with regular shaking and then incubated with the corresponding primary antibodies overnight at 4°C or at RT for 1.5 hour. After 3×10 minutes washing with PBST, membranes were incubated with secondary antibodies at RT for 1 hour. All the secondary antibodies are coupled to horseradish peroxidase and can be visualized by enhanced chemoluminescence (ECL). Membranes were washed 3×10 minutes with PBST after the incubation with the secondary antibodies, and ECL solution (Amersham/Millipore) was added to membranes according to manufacturer's instructions. The membranes were then sealed in plastic bags. X-ray films were laid over the membrane and different exposure time was chosen. Films were finally developed in an X-ray film processor.

Membranes were stripped in a stripping buffer I at 65°C for 40 minutes or a stripping buffer II for 30 minutes at RT with frequently shaking. This strips the bound antibodies from the membrane so that it can be re-immunoblotted with different antibodies. After stripping, membranes were washed 3× 10 minutes with PBST and were blocked and immunoblotted as described above.

SDS-loading buffer:
62.5 mM Tris, pH 6.8
3% SDS
2% 2-mercaptoethanol
0.01% bromophenol blue
15% glycerol

Laemmli buffer: 192mM glycine
25mM Tris-base
0.1% (w/v) SDS
Do not adjust the pH with acid or base

Anode buffer I: 0.3M Tris, pH 10.4
10% methanol

Anode buffer II: 25mM Tris, pH 10.4
10% methanol

Cathode buffer: 40mM 6-amino-n-caproic acid
pH is not adjusted

PBST: 1× PBS
0.1% (v/v) Tween® 20

Stripping buffer I: 62.5mM Tris-HCl, pH 6.7
2% (w/v) SDS
100mM 2-mercaptoethanol

Stripping buffer II: 25mM glycine, pH 2.0
1% (w/v) SDS

2.2.5.3. Detection of proteins on the PVDF membrane by Coomassie blue staining

The membranes were incubated in Coomassie staining buffer for 2 minutes and were then destained in destaining buffer I for 10 minutes. Afterwards, the membranes were washed in destaining buffer II until no background was left. The membranes were then kept in ddH_2O or air-dried between two pieces of Whatman paper.

Coomassie staining buffer: 0.1% Coomassie brilliant blue R250
50% methanol
7% acetic acid

Destaining buffer I: 50% methanol
7% acetic acid

Destaining buffer II: 90% methanol
10% acetic acid

2.2.5.4 Mammalian pulldown

HEK293 cells were transiently cotransfected with mammalian expression vectors pCMV-GST, pCMV-GST-MBD2/MBD3, pCMV-GST-HDAC1 or pCMV-GST-RbAp46/RbAp48 with Gal, Gal-hp66α, four single mutant forms of Gal-hp66α (K30R, K149R, K451R, K487R), Gal-hp66β or two single mutant forms of Gal-hp66β (K33R, K454R). Cells were collected 48 hours after transfection and nuclear extracts were prepared as described above. 400µg of nuclear extract was incubated with 40µl glutathione-Sepharose 4B beads (Amersham Biosciences) for 30 minutes at room temperature. The beads were washed six times with washing buffer NTEN-100. Bound proteins were eluted with SDS sample buffer, fractionated together with the corresponding input fractions on SDS-PAGE and subsequently detected by Western blotting using the anti-Gal4 polyclonal IgG antibody. The membranes were stripped as described above. Blots were subsequently reprobed with mouse anti-GST polyclonal IgG at a dilution of 1:3000 and subsequently with horseradish peroxidase-conjugated goat anti-mouse IgG at a dilution of 1:10000. The ECL™ kit was used to visualize the proteins on the membrane following the manufacturer's protocol.

NTEN-100:
20mM Tris, pH 8.0
100mM NaCl
1mM EDTA
0.5% Nonidet P-40
freshly added 1mM DTT

2.2.6 Fluorescence microscopy analysis

2.2.6.1 Cleaning of coverslips

For cleaning, coverslips were immerged in 40% HCl in a glass beaker and were agitated at RT for 1 hour. Afterwards, coverslips were washed 15-20 times with distilled water followed by acetone. After air-drying on Whatman paper, coverslips were used immediately or stored at RT in a sterile tissue culture dish.

2.2.6.2 Fluorescence assay

Fluorescence assay was carried out on cells growing on coverslips or microscope slides. NIH3T3 cells were cultured to subconfluency on coverslips and transfected with pEGFP-C2, pEGFP-hp66α, pEGFP-hp66αK30R, pEGFP-hp66αK487R, pEGFP-hp66β or pEGFP-hp66βK33R. Transfection of NIH 3T3 cells was performed using jetPEI (Polyplus) according to manufacturer's protocol. Cells (80-90% confluence) were washed with PBS twice 24-48 hours after transfection. DNA was counter stained with Hoechst 33342 for 10min at 37°C. Coverlips were mounted on slides and sealed with nail polish. Images were taken by fluorescence microscopy using a 1000-fold magnification.

Hoechst 33342 stock:	5mg/ml Hoechst 33342 in PBS
	0.2µm filter filtration and stored at -20°C
	use 1-5µg/ml as the final concentration.

2.2.6.3 Fluorescence microscopy and image-editing

Fluorescence microscopy was performed with a Zeiss Axiophot fluorescence microscope. Filters were selected according to the excitation/emission of the fluorescence dyes used which are listed below. Images were edited with Adobe Photoshop software.

GFP	488nm/507nm
Hoechst 33342	352nm/461nm

2.2.7 Purification of the hp66 proteins complexes

2.2.7.1 Preparation of whole cell extract

The whole cell extract was prepared as described above (see section 2.2.4.5.1), thawn on ice, and was ultracentrifuged at 50,000rpm for 2 hours at 4°C. The supernatant was filtered through 0.22µm filter, and concentrated using Centricon® Ultracel YM-30 membrane (Millipore). The total amount of protein is about 20-50mg. The samples were ready for ion-exchange chromatography.

2.2.7.2 Ion-exchange chromatography (Mono Q column)

Ion-exchange chromatography separates molecules on the basis of their net charge. Mono Q column purification was used during this study. Mono Q is a strong anion exchanger based on a beaded hydrophilic resin with a particle size of 10μm. Practical protein loading capacity is around 20-50mg/column. Large volumes of sample can be applied by a Superloop. A gradient volume of 20ml is basically sufficient. A Mono Q HR5/5 (1ml) column was equilibrated with anion-exchange solution A and then allowed for the proteins to bind to resin. Non-specifically bound proteins were washed with equilibrated solution A (100mM KCl) and the resin bound proteins were eluted using salt gradient (from 100mM KCl to 1M KCl)with Buffer B which was similar to Buffer A but had 1M KCl. SDS-PAGE analysis of Mono Q eluted fractions was detected with FLAG antibody.

Briefly, a typical conditions for a separation on a Mono Q HR 5/5 column are as follows:

Column: Mono Q HR 5/5
Sample volume: 10ml (Superloop)
Buffer A: anion-exchange solution Acontaining 100mM KCl
Buffer B: anion-exchange solution A containing 1.0M KCl
Flow rate: 0.5ml/min
Gradient: 0-100%B in 20ml
Detector: UV-M, 280nm
Chart speed: 0.5cm/min

The method should contain the following steps: a. The extract was filled in Superloop. b. The column was equilibrated with 5 column volumes buffer A. c. The valve was changed to

Table 2.9 standard program of ion-exchange chromatography

Volume (ml)	Function	Value
0	%B	0
0	ml/min	1.0
0	cm/min	0.5
0	valve position	1.1
5	port set	6.1
5	%B	0
25	%B	100
30	%B	100
30	port set	6.0

"INJECT" position and sample was applied to column with 5ml buffer A. d. The valve was changed to "LOAD" position. e. The linear gradient was run from buffer A to 100% buffer B in 20ml. f. The column was washed with 5ml buffer B. The general program can be composed (Table 2.9).

Anion-exchange solution A: 100mM KCl
20mM Tris/HCl, pH 7.9
0.2mM EDTA
10mM 2-mercaptoethanol
0.2mM PMSF
10% glycerol
Filtered and degas, store at 4°C

Anion-exchange solution B: 1M KCl
20mM Tris/HCl, pH 7.9
0.2mM EDTA
10mM 2-mercaptoethanol
0.2mM PMSF
10% glycerol
Filtered and degas, store at 4°C

2.2.7.3 Gel filtration chromatography (superpose 6)

Further purification was carried out with gel filtration chromatography, which separates molecules according to their size. In gel filtration chromatography, fractionation is based on the diffusion of molecules into the pores of the resin. Large proteins do not enter the pores of the resin as readily, but pass through the fluid volume of a column faster than smaller proteins. Proteins that are small enough can fit inside all the pores in the beads and therefore elute last in a gel filtration separation. Molecular weight determination of unknown proteins is made by comparing the ratio of V_e/V_o for the protein to the V_e/V_o of protein standards of known molecular weight (V_e is the elution volume and V_o is the void volume). The V_o of a given column is based on the volume of effluent required for the elution of a large molecule such as blue dextran. The standard curve was made by separation of a mixture of alcohol dehydrogenase (150KDa), apoferritin (443KDa), thyroglobulin (669KDa) on a gel filtration column (Superose 6 HR10/30). The Void was determined according to manufactures's guidelines (1/3 of column volume or 7ml). Estimation of the relative molecular weight of

protein complexes was based on the elution profile of the standard curve. The running buffer was used in this study as follows:

Running buffer: 200mM KCl
10mM Hepes, pH 7.5
1.5mM $MgCl_2$
10μM $ZnCl_2$
10% glycerol
Filtered and degas, store at 4°C

2.2.7.4 Affinity purification with anti-FLAG M2 affinity gel

The anti-FLAG M2 affinity gel was thoroughly suspended in the vial to make a uniform suspension of the resin, and 40-60μl of suspension was transferred to a new tube immediately using a clean, cut pipette tip. The resin was centrifuged at 6900rpm for 30 seconds at 4°C. The supernatant was removed with a narrow-end pipette tip. The packed gel was washed twice with 0.5-0.8ml TBS buffer, and most of the wash buffer was removed. Then 200-400μl fractions from gel filtration was added to the washed resin. If necessary, the final volume was filled up to 1ml by adding running buffer of gel filtration. The mixture was incubated for 2 hours or extended overnight on a roller shaker at 4°C. The next day, the mixture was centrifuged at 6900rpm for 30 seconds at 4°C and the supernatant was removed. The resin was incubated with 1ml buffer A for 30 minutes at 4°C on a roller shaker, and then centrifuged at 6900rpm for 30 seconds. This step was repeated 3 times. Afterwards, the resin was incubated with 1ml buffer B for 30 minutes at 4°C on a roller shaker and then centrifuged at 6900rpm for 30 seconds. This step was repeated 3 times. Finally, the resin was incubated with 100μl buffer B containing 200μg/ml 3×FLAG peptide for 3hours at 4°C on a roller shaker and then centrifuged at 6900rpm for 30 seconds. The supernatant is the eluted fraction, and transferred to a fresh tube. Then the eluted fraction was pooled and precipitated with TCA as described above (see section 2.2.5.1). Finally, these fractions were ready to load on 10% SDS-PAGE.

TBS Buffer: 50mM Tris/HCl, pH 7.4
150mM NaCl

Buffer A: 400mM NaCl
20mM Hepes, pH 7.9

0.2mM EDTA
0.3% NP-40
20% glycerol
freshly added 0.4mM PMSF and protease inhibitor complex

Buffer B: 500mM NaCl
20mM Tris/HCl, pH 7.4
0.1% NP-40
5% glycerol
freshly added protease inhibitor complex

FLAG peptide stock solution: 150mM NaCl
10mM Tris/HCl, pH 7.4
FLAG peptide was dissolved in stock solution
to a final concentration of 5mg/ml

2.2.8 Mammalian GST purification

HEK293 cells were transiently transfected with mammalian expression vectors pCMV-GST, pCMV-GST-hp66α, pCMV-GST-hp66β, respectively. Cells were collected 48 hours after transfection and nuclear extract was prepared as described above. 400µg of nuclear extract was incubated with 60µl glutathione-Sepharose 4B beads, which had been equilibrated with NTEN-200 buffer, for 2 hours at 4°C. The beads were washed six times with washing buffer NTEN-200. Bound proteins were eluted with Roti Load 1 sample buffer, fractionated together with the corresponding input fractions on SDS-PAGE and subsequently analysed by Western blotting using the anti-Mi2 antibody. The membranes were stripped as described above. Blots were subsequently reprobed with anti-HDAC1/HDAC2, RbAp46/RbAp48, MBD2/MBD3, PRMT5 antibodies. The ECL™ kit was used to visualize the proteins on the membrane following the manufacturer's protocol.

NTEN-200: 20mM Tris, pH 8.0
200mM NaCl
1mM EDTA
0.5% Nonidet P-40
freshly added 1mM DTT

3 RESULTS

3.1 hp66 mediates repression and interacts with HDAC and MBD2

3.1.1 The transcriptional repression activity of hp66α is stronger than that of hp66β

Previously, two proteins termed hp66α and hp66β were detected as interaction partners of MBD2 in a yeast two-hybrid screen and it was shown that hp66β is the p66 components of the MeCP1 complex. In addition, both hp66 proteins were identified as transcriptional repressors (Brackertz et al., 2002; Feng et al., 2002). The high homology in the amino acid sequences of hp66α and hp66β (Brackertz et al., 2002) rises the question whether the transcriptional repression activity mediated by hp66α or hp66β proteins is similar as well. In order to asses this, the reporter plasmid 4×UAS-TK-Luc, which contains four Gal binding sites upstream of the thymidine kinase promoter that drives the luciferase reporter gene, was used in transient transfection assay. Cotransfection with the Gal-DNA binding domain fusion constructs Gal-hp66α and Gal-hp66β resulted in a strong transcriptional repression of the reporter gene in a dose dependent manner (Fig.3.1A). More importantly, the transcriptional repression activity of

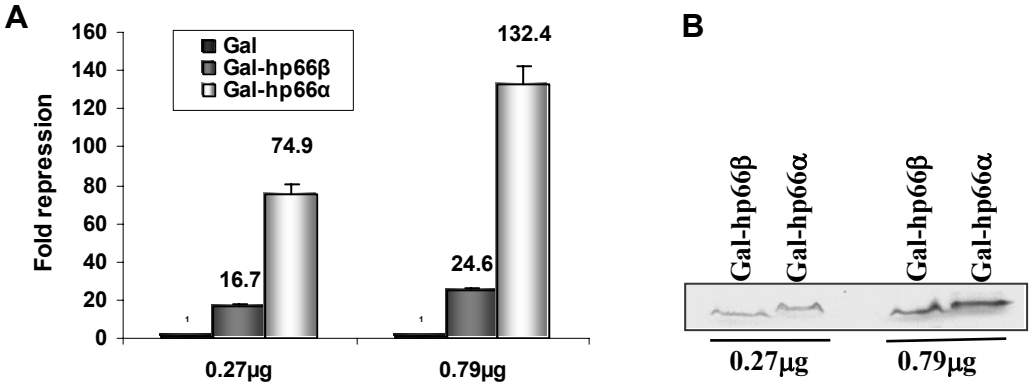

Fig.3.1 The transcriptional repression activity of hp66α is stronger than that of hp66β. HEK293 cells were cotransfected with a 4×UAS-TK-luciferase reporter together with constructs coding for the Gal-DNA binding domain or the indicated Gal fusions hp66α and hp66β. (A) Cell extracts were analyzed for reporter gene activity and protein expression 48 hours after transfection. Transfection efficiency was normalized with the β–galactosidase assay. Fold repression was determined relative to the Gal-DNA binding domain alone. Error bars represent variations within duplicate transfections. (B) The relative expression levels of each of the constructs were detected by Western blotting using anti-Gal4 antibodies.

Gal-hp66β is significantly lower than that of Gal-hp66α. Analysis of the protein expression of hp66 proteins was analyzed with anti-Gal antibody by Western blotting demonstrated a relative expression similar for both fusion proteins (Fig.3.1B) confirming, that indeed the transcriptional repression activity of hp66α is much stronger than that of hp66β.

3.1.2 Identification of potent repression domains in hp66α

Based on the protein aligment, deletion constructs representing corresponding domains in both hp66 proteins were generated in order to identify possible domains responsible for the difference in transcriptional repression activity of hp66α and hp66β. Fusions of these deletion constructs to the Gal-DBD and transfection into HEK293 cells together with the Gal-dependent luciferase reporter gene identified several domains that mediate gene repression (Fig.3.2A and 3.2B). The protein expression of both hp66α and hp66β derived proteins was analyzed by Western blotting using an anti-Gal antibody, demonstrating that similar amounts of the fusionproteins are expressed in all of the transfections (Fig.3.2C). Four domains were distinguished in both proteins, the N-terminal region including CR1, a central region between CR1 and CR2, the CR2 region, and the C-terminal domain outside of CR2. In general, each corresponding domain contributes to the transcriptional repression activity of the full length protein. Comparison of hp66α with hp66β revealed that the N-terminal domain including CR1 as well as the central region mediate similar repression activity. In contrast, the CR2 region as well as the C-terminal region differ in repression, with the hp66α domains being about 5-fold stronger than the corresponding hp66β domains. For p66α in details, the central region between CR1 and CR2 has only little effect on transcriptional repression activity of hp66α, whereas the N-terminal region, the CR2 domain and the C-terminal part outside of CR2 contributed to about 20%, 35%, 30% transcriptional repression activity of full length hp66α, respectively. Further results showed that the transcriptional repression activity of C-terminal region including CR2 possesses about half of the transcriptional repression activity of full length hp66α. In the case of hp66β, the N-terminal region including CR1 domain contributes to 70% transcriptional repression activity of full length hp66β. In summary, the major repression domains of hp66α are within the C-terminus including CR2, and within the N-terminus including CR1, which together mediate the full transcriptional repression activity of hp66α. In

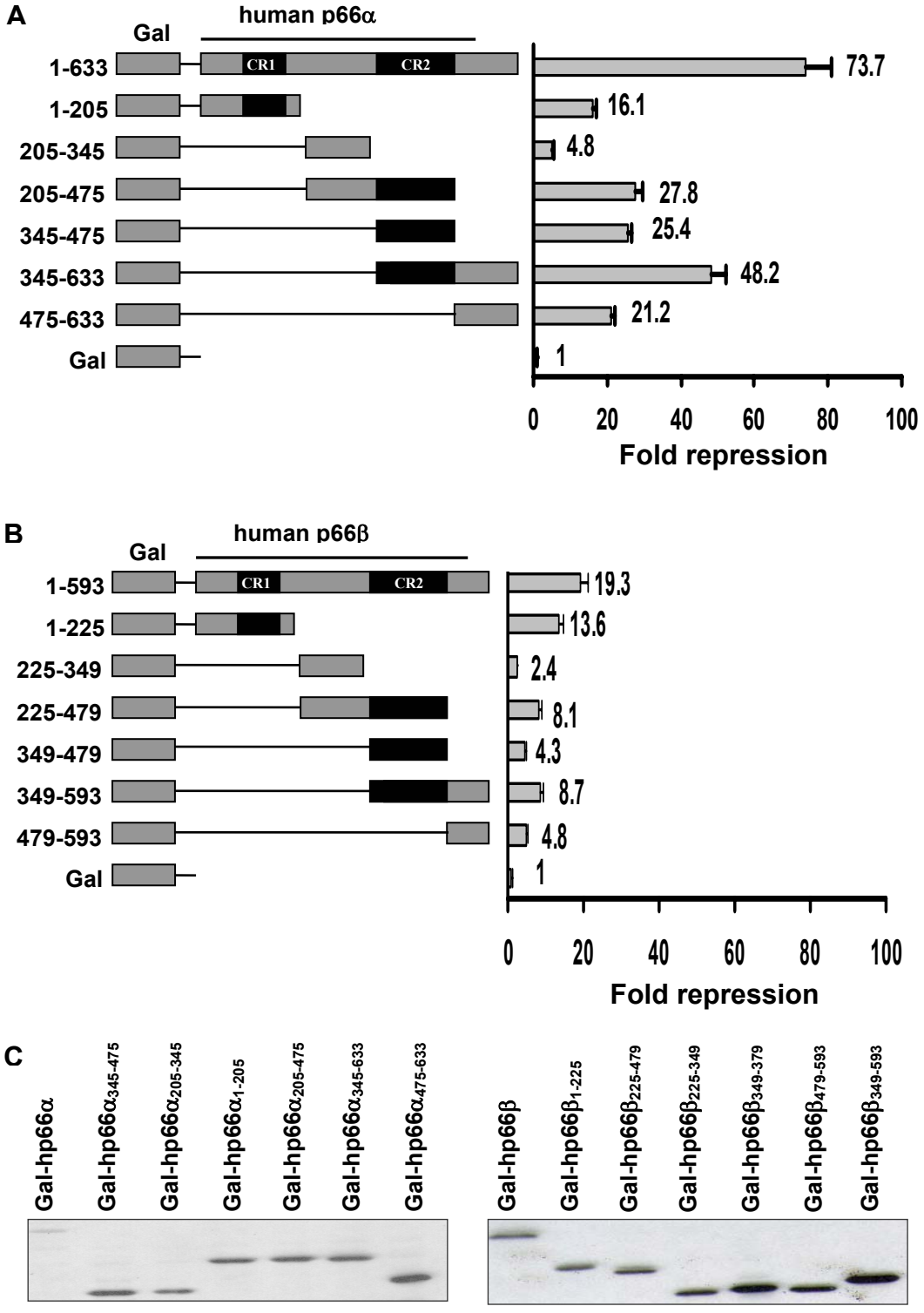

Fig.3.2 Identification of potent repression domains in hp66 proteins. HEK293 cells were cotransfected with a 4×UAS-TK-luciferase reporter together with vectors coding for the Gal-DNA binding domain or the indicated Gal-hp66α/Gal-hp66β fusion constructs. Cell extracts were analyzed for reporter gene activity and protein expression. (A and B) Schematic overview of the Gal-hp66α/Gal-p66β deletion constructs and reporter gene activity expressed as fold repression as in Fig.1. (C) The relative expression levels of each of the constructs were detected by Western blotting using anti-Gal4 antibodies.

contrast, only the N-terminus in hp66β shows a comparable activity to the corresponding region of hp66α, whereas the C-terminus of hp66β is about 5-fold less active as compared to this region of hp66α. The data indicated that the N-terminal part is major repression domain of hp66β, which is consistent with previous data (Feng et al., 2002) and shows, that the region responsible for the increased repression by hp66α is located in the C-terminus of the protein.

3.1.3 The transcriptional repression activity of hp66α is partially dependent on histone deacetylase activity

It has previously been shown that p66β-mediated transcriptional repression is partially dependent on histone deacetylation (Feng et al., 2002). Therefore, possibly the transcriptional repression mediated by hp66α involves histone deacetylase activity as well. To test this assumption the transcriptional activity of wild type Gal-hp66α and Gal-hp66β as well as comparable deletion constructs of both Gal-hp66α and Gal-hp66β was analyzed in the presence and absence of the histone deacetylase inhibitor TSA. Gal-NCoR and Gal-hp66β was used as a positive control (Feng et al., 2002; Polly et al., 2000). As shown in Fig.3.3, the transcriptional repression of both Gal-NCoR and Gal-hp66β is partially released by TSA, especially, N-terminal part of Gal-hp66β shows strong TSA sensitiviy. More importantly, the strong transcriptional repression mediated by Gal-hp66α is sensitive to TSA as well, in particular, the transcriptional repression of C-terminal part of hp66α is partially released in the presence of TSA. This results indicated that histone deacetylase activity contributes to the repressive function of the hp66α C-terminus.

3.1.4 Enhancement of MBD2-mediated transcriptional repression is dependent on interaction between MBD2 and hp66α

Recent results clearly demonstrated that both hp66α and hp66β are able to enhance MBD2-mediated transcriptional repression, with the enhancement by hp66α being stronger than that by hp66β (Brackertz et al., 2006). Therefore it showed be tested whether this effect is directly mediated by the interaction of the both hp66 proteins with MBD2. Previously, a critical amino acid sequence (minimal overlapping region) was identified within conserved region 1 (CR1) by

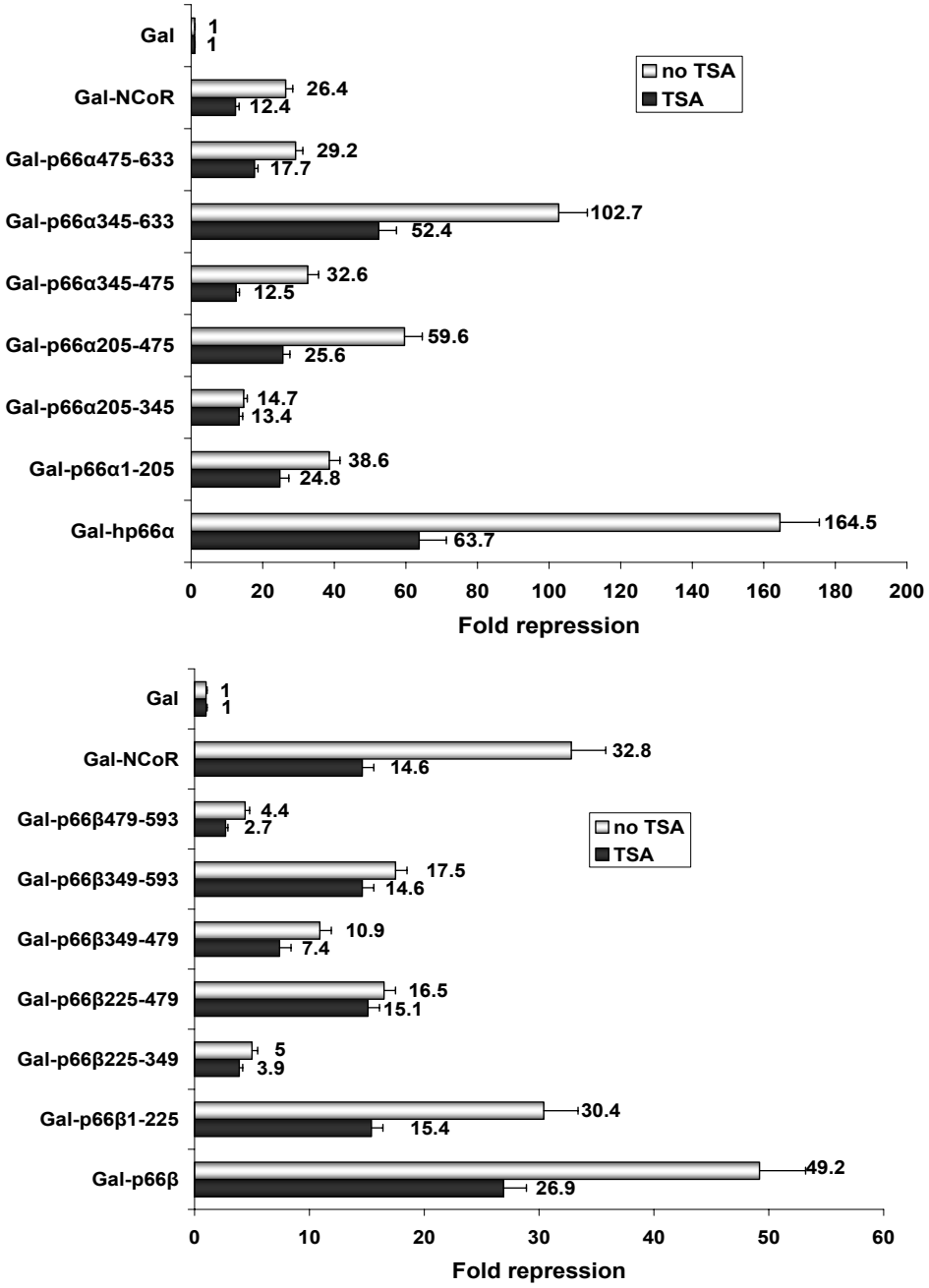

Fig.3.3 The transcriptional repression activity of hp66α is partially dependent on histone deacetylase activity. HEK293T cells were cotransfected with a 4×UAS-TK-luciferase reporter together with constructs coding for the Gal-DNA binding domain or the indicated Gal fusions in the presence or absence of TSA. Cell extracts were analyzed for reporter gene activity. Gal-NCoR is a positive control for TSA sensitive repression (Polly et al., 2000). Fold repression was determined relative to the Gal-DNA binding domain alone. Error bars represent variations within duplicate transfections.

GST pulldwon, which is required for the interaction between hp66α protein and MBD2 (Brackertz et al., 2002). SUMO (small ubiquitin-like modifiers) has been shown to affect many biological processes such as transcription regulation (Hay, 2005). hp66α and hp66β were first

examined for the SUMOylation consensus sequence ψKXE, where ψ represents a large hydrophobic amino acid, most frequently isoleucine or valine, K (lysine) is the SUMO acceptor site, and X represents any amino acid (Rodriguez et al., 2001). Inspection of the amino acid sequence of hp66α and hp66β revealed four potential SUMO modification sites at Lys-30, Lys-149, Lys-451 and Lys-487 in case of hp66α, and two potential SUMO modification sites at Lys-33 and Lys-454 in case of hp66β (Table 3.1).

Table 3.1 Potential SUMOylation sites of both hp66 proteins

hp66α SUMOylation prediction sites

No.	Pos.	Group	Score
1	K30	VESKK IKME RGLLA	0.94
2	K149	RMIKQ LKEE LRLEE	0.91
3	K451	NQKKA LKVE HTSRL	0.91
4	K487	TAPAQ AKAE PTAAP	0.80
5	K367	LEIPP PKPP APEMN	0.50

hp66β SUMOylation prediction sites

No.	Pos.	Group	Score
1	K33	VLAKR LKME GHEAM	0.94
2	K454	NQKKA LKAE HTNRL	0.91
3	K432	DFTPH WKQE KNGKIL	0.64

Red value indicates motifs with high probability for SUMOylation
(SUMOplot™ Prediction program)

The SUMOylation consensus site Lys-149 (K149) can not be SUMOylated in hp66α (see section 3.2.1), and K149 is not present in hp66β. To further investigate the interation of hp66α and MBD2, the eukaryotic expression vector pCMV-GST or pCMV-GST-MBD2 was cotransfected with Gal, Gal-hp66α, Gal-hp66β or their respective mutants (lysine mutated into arginine) (Fig.3.4A and 3.4B) into HEK293 cells and nuclear extract was bound to glutathione-Sepharose beads. Coprecipitated proteins were detected via western blotting using an antibody directed against Gal-DBD. The results clearly revealed that GST-MBD2 retains wild type Gal-hp66α and most of the mutant forms with one exception: Gal-hp66αK149R. Since all mutant forms as well as wild type Gal-hp66α are similarly expressed in these cells, this indicates that the interaction of MBD2 with hp66α requires an intact site K149 within hp66α. In addition, the GST-MBD2 containing sample retains Gal-hp66β and all single mutant forms (Fig.3.4B), which indicated that mutation of the SUMO modification sites (see section 3.2.1) does not influence MBD2 binding to hp66β. Since hp66α is able to enhance MBD2-meidiated transcription repression, the consequence of point mutant hp66αK149R (lysine mutated into arginine) in MBD2-mediated transcriptional repression was further investigated. Hela cells

were cotransfected with the Gal-DNA binding domain, or Gal-MBD2b and increasing amounts of hp66α or hp66αK149R and an appropriate luciferase reporter. The mutant hp66αK149R

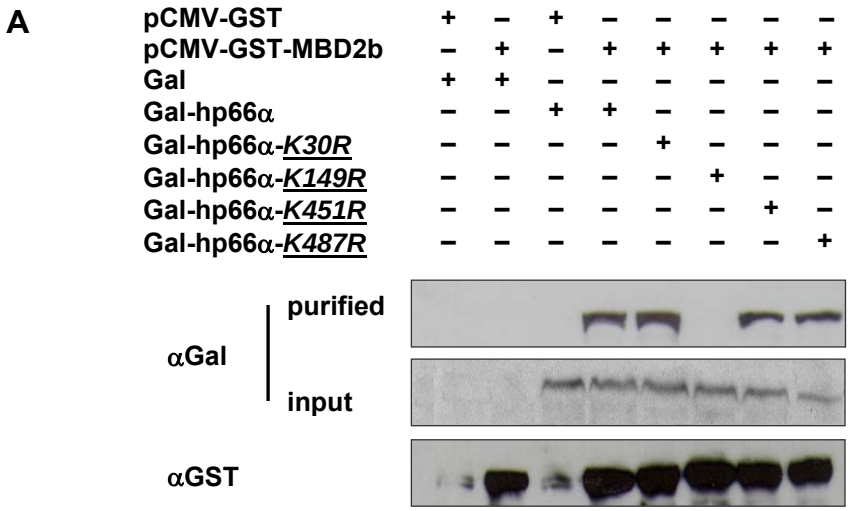

Fig.3.4A K149 of hp66α is required for the MBD2 interaction. HEK293 cells were harvested 48hours after transfection with various combinations of DNA constructs, as indicated above the figure. Nuclear protein extract was prepared (input) and purified with glutathione-Sepharose beads. The bound protein together with the input fractions were analyzed by western blotting using the anti-Gal antibody compared to input, which was analyzed with the anti-GST antibody as well.

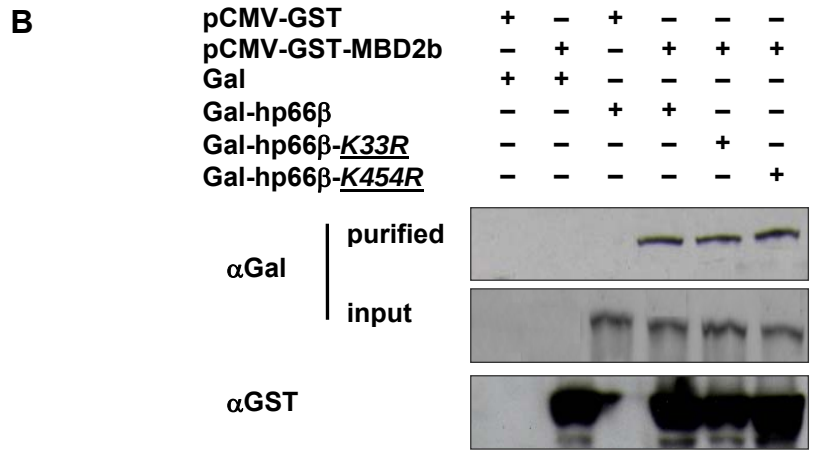

Fig.3.4B SUMO modification sites does not influence hp66β binding to MBD2. HEK293 cells were harvested 48hours after transfection with various combinations of DNA constructs, as indicated above the figure. Nuclear protein fraction was prepared and purified with glutathione-Sepharose beads. Bound protein (purified) together with the input fractions were analyzed via western blotting using the anti-Gal antibody compared to input, which was analyzed with the anti-GST antibody as well.

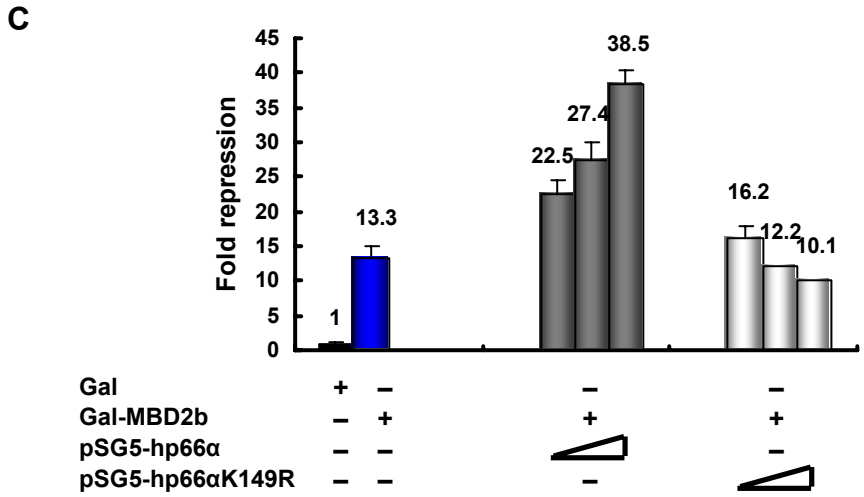

Fig.3.4C K149R mutant of hp66α decreases MBD2-mediated repression. Hela cells were cotransfected with a 4×UAS tk luciferase reporter together with vectors expressing the Gal-DNA binding domain, or Gal-MBD2b and increasing amount of pSG5-hp66α or pSG5-hp66αK149R. Fold repression was determined relative to the Gal-DNA binding domain.

protein is not able to enhance MBD2-mediated transcriptional repression as observed by the the wild type site (Fig.3.4C). Thus the interaction of MBD2 and hp66α, in particular via K149, is essential for the functional enhancement of MBD2-mediated transcriptional repression.

However, by using wild type $MBD2^{+/+}$ mouse fibroblast cells or $MBD2^{-/-}$ mouse fibroblast cells which MBD2 has been knocked out, both hp66 proteins still maintain their ability to repress transcription, even in an $MBD2^{-/-}$ environment (Brackertz et al., 2006). To further investigate the influence of MBD2 on hp66 paralogs-mediated transcriptional repression, endogenous MBD2 was knocked down by using RNAi, and the effect on hp66 paralogs-mediated transcriptional repression was subsequently analyzed. pSilencer vector such as pSil-MBD2X was generated, which can drive shRNA procedure with targeting sequences identified in target genes in this study. Hela cells were either transfected with pSil-MBD2X or a non-targeting control (pSil-neg) and MBD2 protein expression was analyzed by Western blotting using MBD2 antibody. As shown in Fig.3.4D, the expression of MBD2 protein was significantly reduced 96hours after RNAi treatment. Since suitable condition for MBD2 knockdown was established, Hela cells were cotransfected with vectors expressing the Gal-DNA binding domain, Gal fusions of hp66 proteins, and pSil-MBD2X, pSil-neg. Fig.3.4E demonstrated that both Gal-hp66β and Gal-hp66α are still able to repress transcription after knockdown of MBD2, with hp66β-mediated transcriptional repression also being about 2-fold lower as compared with hp66α-mediated transcriptional repression. MBD2 is therefore not essential for the repression

by either Gal-hp66α or Gal-hp66β, and thus does not function as a downstream factor for hp66 paralogs-mediated transcriptional repression. Rather, in case of wildtype hp66, MBD2 may act to target p66 to DNA.

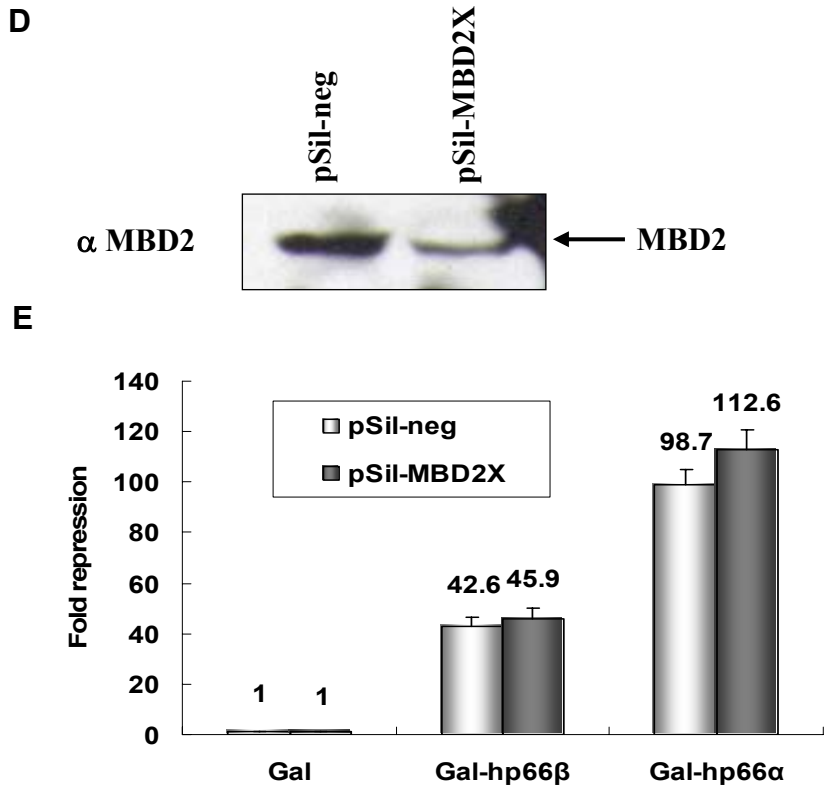

Fig.3.4 Knockdown of endogenous MBD2 does not affect hp66α or hp66β-mediated transcriptional repression. (D) Endogenous expression of MBD2 is reduced 96hours after RNAi treatment. Hela cells were transfected with either pSil-MBD2X or a non-targeting control (pSil-neg). Nuclear extract was prepared and detected by Western blotting using the MBD2 antibody. (E) Both hp66 paralogs-mediated transcriptional repression are independent of MBD2. Hela cells were transfected with the pSilencer constructs together with the Gal or Gal-hp66 paralogs constructs with a 4×UAS-TK-luciferase reporter. Cell extracts were analyzed for reporter gene activity. Transfection efficiency was normalized with the β–galactosidase assay. Fold repression was determined relative to the Gal-DBD alone. Error bars represent variations within duplicate transfections.

3.1.5 Nuclear distribution of hp66α depends on MBD2

Previously, hp66α and hp66β were identified as interaction partners with MBD2, which is thought to recruit the Mi-2/NuRD complex to methylated DNA (Brackertz et al., 2002). Further results revealed that nuclear distribution of both hp66 proteins is dependent on MBD2 and conserved region 2 (CR2) (Brackertz et al., 2006). The CR1 domain of hp66α and hp66β have already been shown to interact with MBD2 and a point mutation within the CR1 domain of

hp66α (hp66α K149R) disrupts MBD2-binding (see above). Therefore, the mutant hp66αK149R fused to EGFP was used to analyze the MBD2-dependent nuclear distribution of the protein. The nuclear localization of EGFP-hp66α and EGFP-hp66αK149R was tested in NIH 3T3 cells. EGFP-hp66α shows a speckled distribution in the nucleus, whereas EGFP-hp66αK149R leads to overall loss of the speckled pattern and displays a diffuse nuclear localization (Fig.3.5). Taken together, the results suggest that the interaction with MBD2 via the K149 site of the CR1 domain determins the nuclear distribution of hp66α.

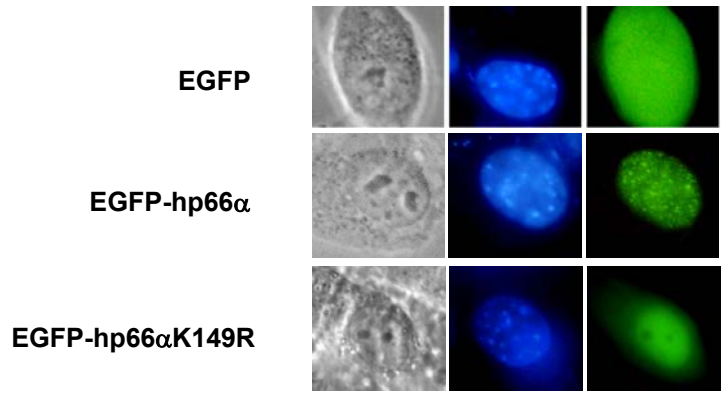

Fig.3.5 Nuclear distribution of hp66α depends on K149 site of CR1 domain. NIH3T3 cells were transfected with the indicated EGFP-fused hp66 proteins. Phase contrast (left column) and fluorescent images were taken 24-48 hours post transfection after incubation with "Hoechst DNA stain" (center column). pEGFP-hp66α revealed similar nuclear speckle patterns, whereas pEGFP-hp66αK149R lead to diffuse pattern(right column). EGFP control expression resulted in a diffuse whole cell distribution.

3.2 SUMO modification enhances hp66-mediated transcriptional repression of the Mi-2/NuRD complex

3.2.1 hp66α and hp66β can be SUMOylated in vivo

SUMO (small ubiquitin like modifier) has been shown to modify the function of target proteins upon covalent binding. Here, I tested whether both hp66 proteins could be SUMOylated. As described in Table 3.1, there are four potential SUMO modification sites at K30, K149, K451 and K487 within hp66α, and two potential SUMO modification sites at K33 and K454 within hp66β.

To examine whether hp66α and hp66β can be SUMOylated *in vivo*, HEK293T cells were cotransfected with Gal-hp66α or Gal-hp66β in the presence or absence of pcDNA3-FLAG-SUMO1 and pcDNA3-HA-Ubc9 (expressing the E2 conjugating enzyme). Expression of either

or both proteins has been used in several cases to detect SUMOylated proteins *in vivo*. Gal fused hp66 was used in order to to generate mutants which can be distinguished functionally from endogenous wild type hp66. SDS-PAGE separation and Western blotting using anti-Gal antibody detected SUMOylation of hp66α and hp66β. Various bands of presumably SUMOylated proteins in whole cell extract are seen (Fig.3.6A, arrow). Therefore, all future experiments were performed with nuclear extract. Again, Western blotting using anti-Gal antibody detected Gal-hp66 proteins as well as a higher band presumably corresponding to SUMO-modified hp66α or hp66β when FLAG-SUMO1 and HA-Ubc9 were overexpressed (Fig.3.6B and 3.6C, arrow).

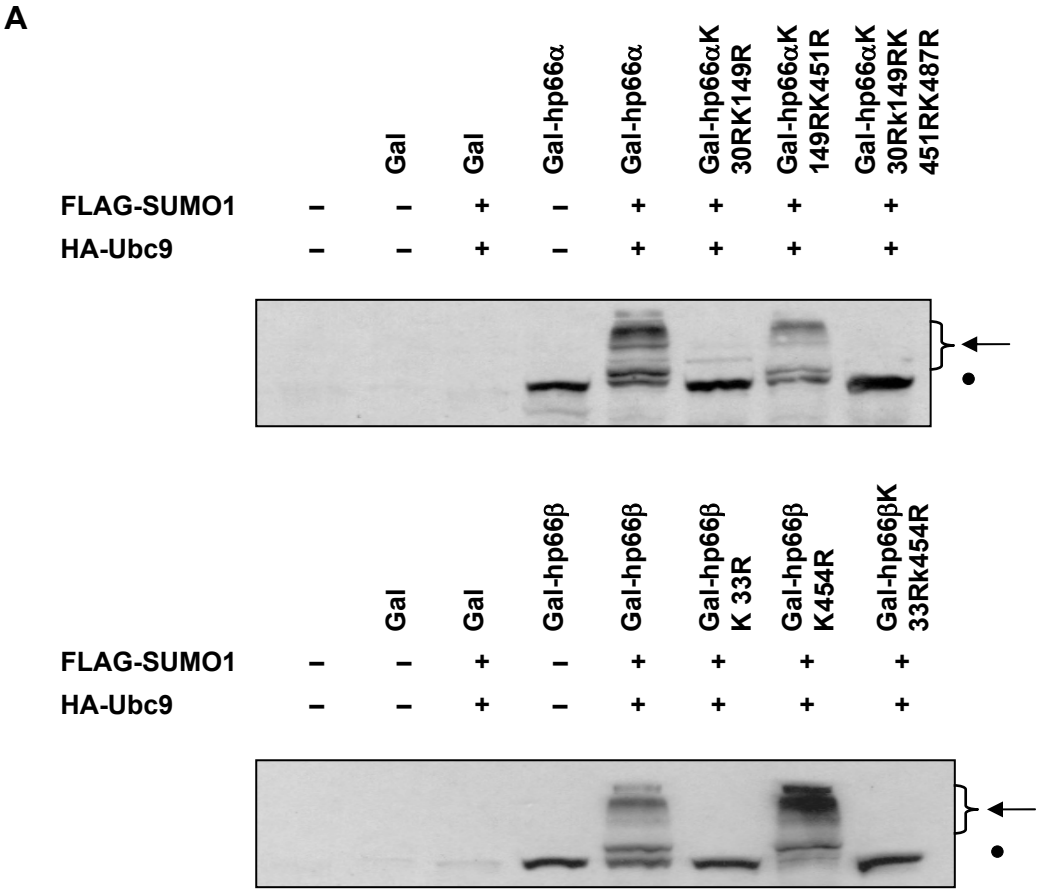

Fig.3.6 hp66α and hp66β can be SUMOylated *in vivo*. HEK293T cells were cotransfected with vectors expressing the indicated Gal fusions together with vectors for FLAG-SUMO1, HA-Ubc9. After 48h, equal amounts of whole cell extracts were separated by SDS-PAGE and analyzed by Western blotting using an anti-Gal antibody. The position of the non-SUMOylated (dot) and of the SUMOylated form (arrow) of hp66α or hp66β is indicated.

To verify the involvement of SUMO1 Gly-97, the essential amino acid of SUMO1 required to

conjugate to substrates (Kim et al., 2000; Schwienhorst et al., 2000), was mutated to alanine (A) via mutagenesis PCR. HEK293T cells were cotransfected with FLAG-SUMO1G97A and Gal-hp66α or Gal-hp66β in the presence of HA-Ubc9. As expected, no higher band was detected(Fig.3.6B and 3.6E), confirming that hp66α and hp66β are specifically conjugated by SUMO-1. To further confirm the SUMOylation pathway, I generated a dominant negative-Ubc9 (DN-Ubc9) by mutating Cys-93 of Ubc9, that has previously been shown to efficiently inhibit SUMO1 conjugation (Bernier-Villamor et al., 2002; Lin et al., 2002). Cotransfection of DN-Ubc9 with Gal-hp66α or Gal-hp66β in the presence of FLAG-SUMO1 resulted in the loss of the higher band (Fig. 3.6B and 3.6C). To identify one or several target sites for SUMOylation I mutated all SUMO consensus sites individually or in combination. In case of hp66α, the mutant form K30R or K487R or any combination including one of these two sites reduces SUMOylation to below detectable levels (Fig.3.6D). Thus K30 and K487 are the major SUMOylation target sites within hp66α. Apparently both sites synergize in SUMOylation since mutation of a single site alone reduces SUMOylation dramatically. Analysis of the two consensus sites of hp66β by testing the K33R or K451R mutants individually clearly showed that a single SUMOylation site at Lys-33 could be detected (Fig.3.6E). Despite the presence of two SUMOylation sites in hp66α and a single site in hp66β, migration of the SUMOylated wild type forms seems to be similar, suggesting that only a single site is modified at a time.

To test SUMOylation in the absence of overexpressed components one has to purify hp66 to visualize any small SUMOylated fraction. It has been shown in many cases that only a fraction of the substrate is modified although the bulk of the substrate is functionally changed (Hay, 2005)**.** Since there was no commercially hp66 antibodies for immunoprecipitation, I generated stable cell lines which stably express low amounts of FLAG tagged hp66 proteins. Several colonies such as clone 54 (pcDNA3-FLAG-CBP), clone 29 (pcDNA3-FLAG-hp66α-CBP), or clone 87 (pcDNA3-FLAG-hp66β-CBP), were identified by RT-PCR and Western blotting (see section 3.3.2). There is no significant difference in the amount of hp66 proteins (Fig.3.6F, input) as compared to endogenous hp66 proteins (Ctrl). Despite the fact that clones C29 and C87 clearly express FLAG-hp66α or FLAG- hp66β. Nuclear extracts were immunoprecipitated with the FLAG M2 agarose gel, and the resulting elution fractions were subjected to Western blotting with anti-FLAG anitibody and anti-SUMO1 antibody (Fig.3.6F, IP). As shown in Figure 3F, the FLAG antibody detected in addition to the major FLAG-hp66 protein a small

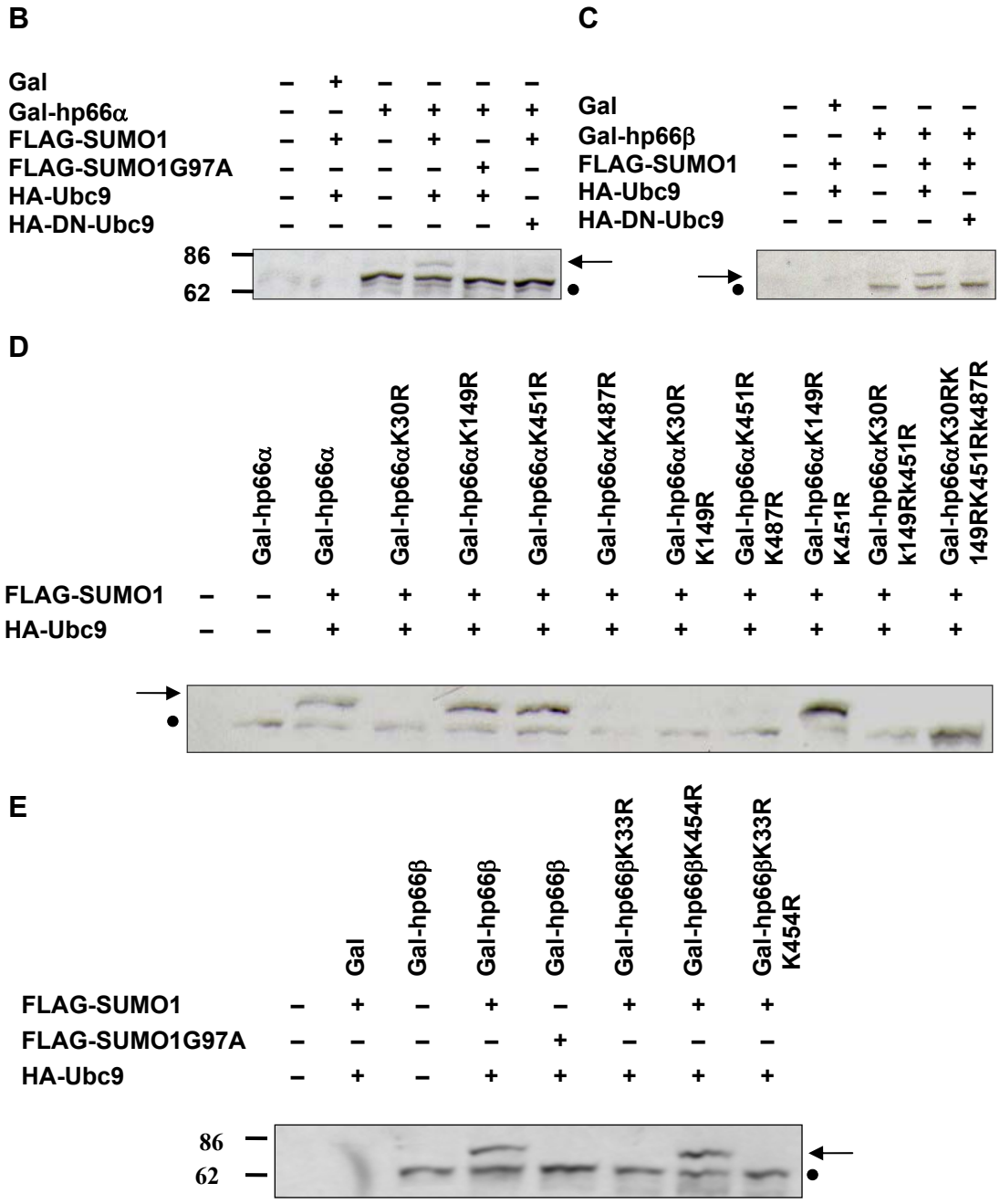

Fig.3.6 hp66α and hp66β can be SUMOylated *in vivo*. (B-E) HEK293T cells were cotransfected with vectors expressing the indicated Gal fusions together with vectors for FLAG-SUMO1, FLAG-SUMO1G97A, HA-Ubc9 or HA-DN-Ubc9. After 48h, equal amounts of nuclear extracts were separated by SDS-PAGE and analyzed by Western blotting using an anti-Gal antibody. The position of the non-SUMOylated (dot) and of the SUMOylated form (arrow) of hp66α or hp66β is indicated.

fraction with a higher molecular weight in case of the C29 and C87 clones. Using the SUMO1 antibody the higher molecular weight band was identified to represent the SUMOylated form. These results indicated that endogenous hp66α and hp66β are modified by SUMO1 *in vivo*.

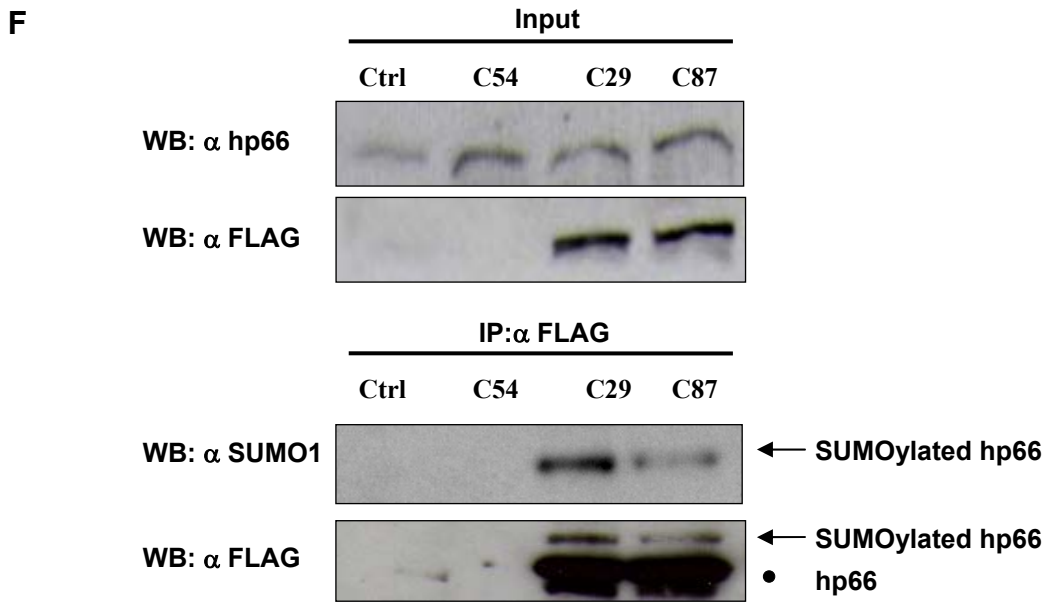

Fig.3.6 hp66α and hp66β can be SUMOylated *in vivo*. Nuclear extract was prepared from 293 cells (Ctrl) and stable cell clones C54 (expressing pcDNA3-FLAG-CBP), C29 (expressing pcDNA3-FLAG-hp66α-CBP), and C87 (expressing pcDNA3-FLAG-hp66β-CBP). Extracts (input) were analyzed by Western blotting with an antibody against both hp66 paralogous (α hp66) showing no major changes in overall p66 amounts even upon expression of the FLAG tagged hp66 as detected with an antibody against FLAG (α FLAG). After purification with FLAG M2 gel and elution with FLAG peptide (IP: α FLAG), the eluted fractions were analyzed by Western blotting using the antibody against FLAG and against SUMO1. The position of the non-SUMOylated (dot) and of the SUMOylated form (arrow) of hp66α or hp66β is indicated.

It is generally known that a E3 ligase, for example PIAS1 protein, is able to enhance the efficiency of SUMO conjugation to target substrates *in vivo* (Johnson and Gupta, 2001; Kahyo et al., 2001). Therefore I tested Whether SUMO modification of both hp66α and hp66β could be enhanced by co-expressing PIAS1 protein. PIAS1 was co-expressed with Gal-hp66α and Gal-hp66β constructs in the presence of FLAG-SUMO1 and HA-Ubc9. The results revealed that, in the case of hp66α, there are two extra bands in the presence of PIAS1 protein, referred to as mono-SUMOylated form and bi-SUMOylated form of hp66α. The data further confirmed two major SUMO modification sites within hp66α. However, in the case of hp66β, there is still one extra band by co-expressing PIAS1 protein, indicating one major SUMO modification site within hp66β (Fig.3.6G and 3.6H).

3.2.2 SUMO modification sites of hp66 proteins are required for maximal repression

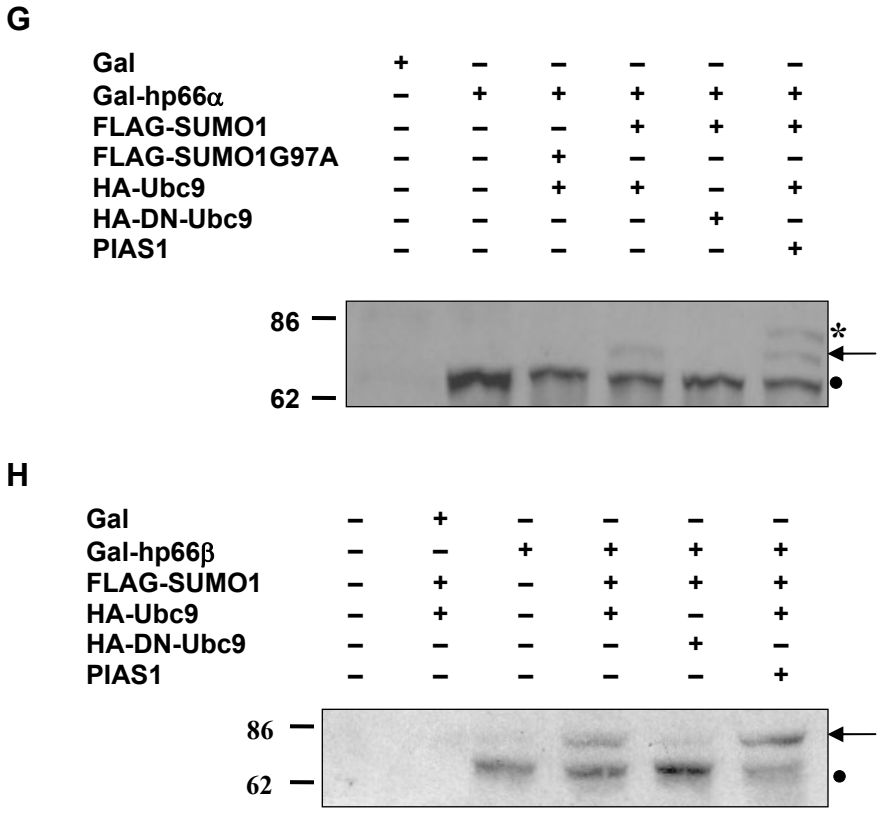

Fig.3.6 E3 ligase PIAS1 enhances the SUMOylation efficiency of hp66 proteins *in vivo*. (G-H) Human 293T cells were cotransfected with indicated Gal fusions together with FLAG-SUMO1, FLAG-SUMO1G97A, HA-Ubc9, HA-DN-Ubc9 or PIAS. After 48h, equal amounts of nuclear extracts were separated by SDS-PAGE and analyzed by Western blotting using an anti-Gal antibody. The position of the non-SUMOylated (dot), of the mono-SUMOylated form (arrow) and of the bi-SUMOylated form (star) of hp66α or hp66β is indicated.

Next, Gal-hp66 paralogs fusions were employed in reporter gene repression assays in order to test for possible functional differences of hp66 mutants which cannot be SUMOylated. The transcriptional repression activity of wild-type Gal-hp66α and Gal-hp66β and various SUMOylation-deficient mutants were compared. HEK293 cells were cotransfected with the reporter plasmid4×UAS-TK-Luc together with Gal-hp66 fusion constructs. Expression levels of wild type and mutant Gal-hp66α and Gal-hp66β proteins were normalized using Western blotting analysis with anti-Gal antibody. The results demonstrated the relative expression of Gal-fusion proteins to be similar (Fig.3.7A and 3.7B). In addition, the results show that all SUMOylation deficient mutants, Gal-hp66αK30R, Gal-hp66αK487R or Gal-hp66βK33R, are severely impaired in their transcriptional repression activity. Moreover, Gal-hp66αK149R, which has no effect on SUMOylation (see section 3.1.4), but rather abolishes binding to MBD2 (see section 3.1.6), reduces transcriptional repression as well. Furthermore, double mutants,

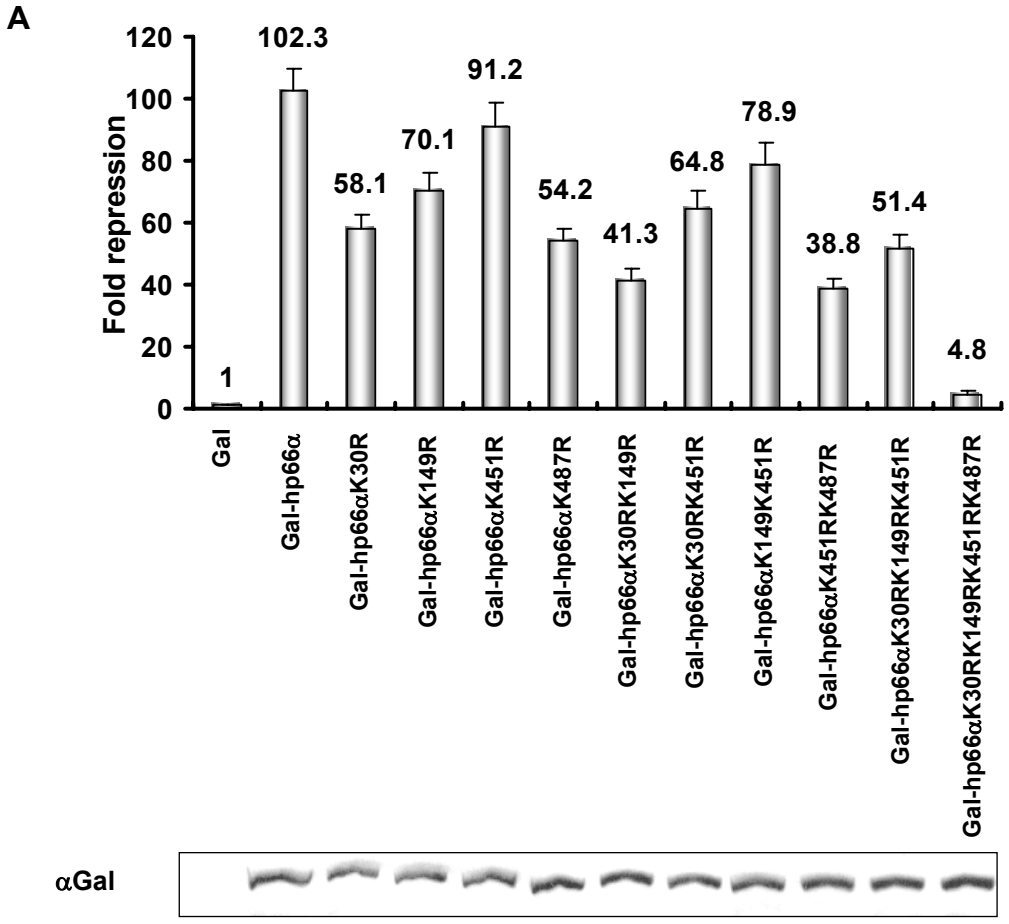

Fig.3.7. Loss of SUMO modification impairs hp66α mediated repression. 293 cells were cotransfected with a 4×UAS-TK-luciferase reporter together with vectors coding for Gal-constructs. Shown is the transcriptional repression of the indicated Gal-hp66α variants. Fold repression was determined relative to the Gal-DNA binding domain. Error bars represent variations within duplicate transfections. Anti-Gal4 Western blotting shows expression levels of wild type Gal-hp66α or mutant forms.

triple mutants as well the quadruple mutants of Gal-hp66 fusions were also examined. In general, any combination of individual mutations that impair SUMOylation also show a strong reduction of transcriptional repression. This is dramatically demonstrated by the quadruple mutation of hp66α that results in a 20-fold reduction of transcriptional repression as compared to wild type hp66α (Fig. 3.7A). This mutant can not be SUMOylated (sites K30 and K487 are mutated, see section 3.1.4). In contrast, there is almost no difference in transcriptional repression activity in the case of Gal-hp66αK451R or Gal-hp66βK454R, the wild-type sites of which are not SUMOylated (see section 3.1.4). These results indicate that SUMOylation influences transcriptional repression of hp66α and hp66β.

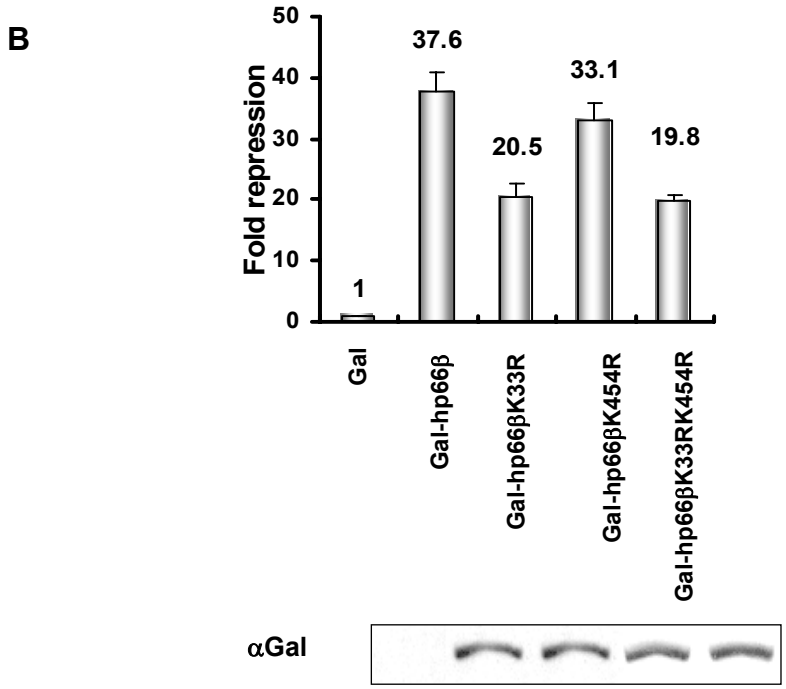

Fig.3.7 Loss of SUMO modification impairs hp66β mediated repression. 293 cells were cotransfected with a 4×UAS-TK-luciferase reporter together with vectors coding for Gal-constructs. Shown is the transcriptional repression of the indicated Gal-hp66β variants. Fold repression was determined relative to the Gal-DNA binding domain. Error bars represent variations within duplicate transfections. Anti-Gal4 Western blotting shows expression levels of wild type Gal-hp66β or mutant forms.

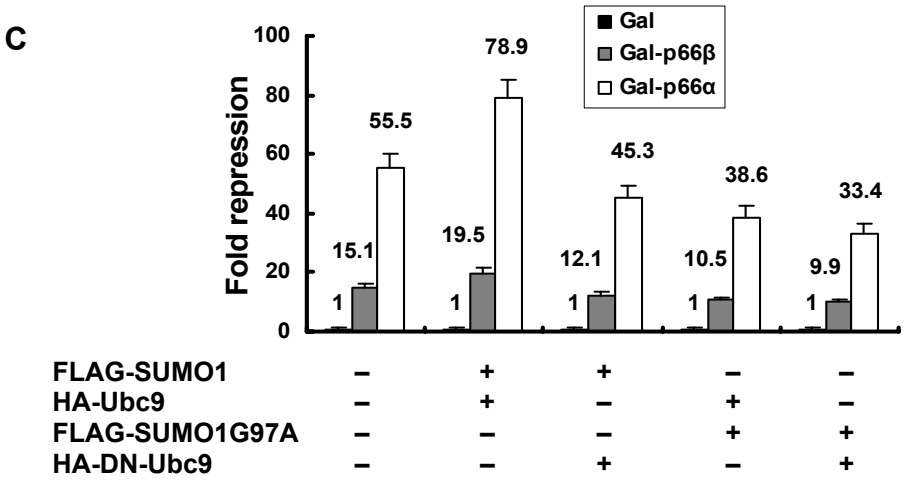

Fig.3.7 Blocking SUMO conjugation pathway impairs hp66 mediated repression. 293 cells were cotransfected with a 4×UAS-TK-luciferase reporter together with vectors coding for Gal-constructs in the presence of FLAG-SUMO1, FLAG-SUMO1G97A, HA-Ubc9, or HA-DN-Ubc9. Shown is the transcriptional repression of the Gal fusion hp66 paralogs. Fold repression was determined relative to the Gal-DNA binding domain. Error bars represent variations within duplicate transfections.

To further confirm the effect of SUMOylation on transcriptional repression, the SUMO mutant FLAG-SUMO1G97A as well as the dominant negative mutation of the E2 ligase HA-DN-Ubc9 were utilized in the transcriptional repression assay (Fig.3.7C). Both transcriptional repression mediated by hp66α or by hp66β can be increased by the wild type FLAG-SUMO1 and Ubc9, and this repression can be relieved by about two fold by the FLAG-SUMO1 mutant and the Ubc9 mutant. Thus, mutation of the two SUMOylation sites of hp66α and the single site of hp66β, and expression of defective SUMO1 and Ubc9 impair the transcriptional repression activity of both hp66 factors.

3.2.3 SUMO modification does not affect hp66α and hp66β nuclear localization

It has been shown that SUMO modification can regulate the subcellular localization of target proteins. To test whether SUMO modification affects nuclear localization of hp66α and hp66β, the subcellular localization of wild-type pEGFP-hp66α and pEGFP-hp66β was compared to the localization of the corresponding SUMOylation defective forms pEGFP-hp66αK30R, pEGFP-

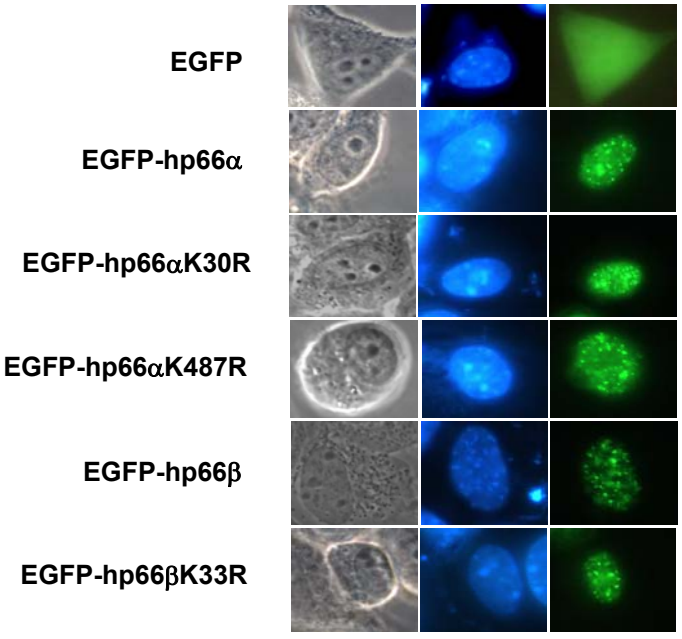

Fig.3.8 Subnuclear distribution of EGFP-hp66α and EGFP-hp66β is not changed in the SUMOylation mutants. NIH3T3 cells were transfected with the indicated EGFP-fused hp66 proteins. Phase contrast (left column) and fluorescent images were taken 24-48 hours post transfection after incubation with "Hoechst DNA stain" (center column). Mutant forms of pEGFP-hp66α and pEGFP-hp66β revealed similar nuclear speckle patterns as observed with wild type pEGFP-hp66α and pEGFP-hp66β (right column). EGFP control expression resulted in a diffuse whole cell distribution.

hp66αK487R and pEGFP-hp66βK33R by fluorescence microscopy. All mutant forms of pEGFP-hp66α and pEGFP-hp66β show a similar speckled nuclear pattern as is observed with wild-type pEGFP-hp66α or pEGFP-hp66β (Fig.3.8). These results suggested that SUMO modification or loss of modification of hp66α and hp66β does not lead to a change in the subcellular or subnuclear localization. Another mechanistic role for SUMO modification of hp66 proteins might be in the protein/protein interaction within the Mi-2/NuRD complex. Therefore, four of the known components of the Mi-2/NuRD complex were tested in their binding to hp66α or hp66β and for a possible effect of the SUMO-defective hp66 mutants.

3.2.4 HDAC1 is recruited to the N-terminal SUMO modification site of hp66α, but not hp66β in vivo

Previous study showed that HDAC1 is the component of the Mi-2/NuRD complex (Le Guezennec et al., 2006; Zhang et al., 1999). As showed in above results, hp66 mediated transcriptional repression is at least partially due to histone deacetylation. Furthermore, most of the mutant forms of Gal-hp66α and Gal-hp66β retain a TSA sensitivity except for Gal-

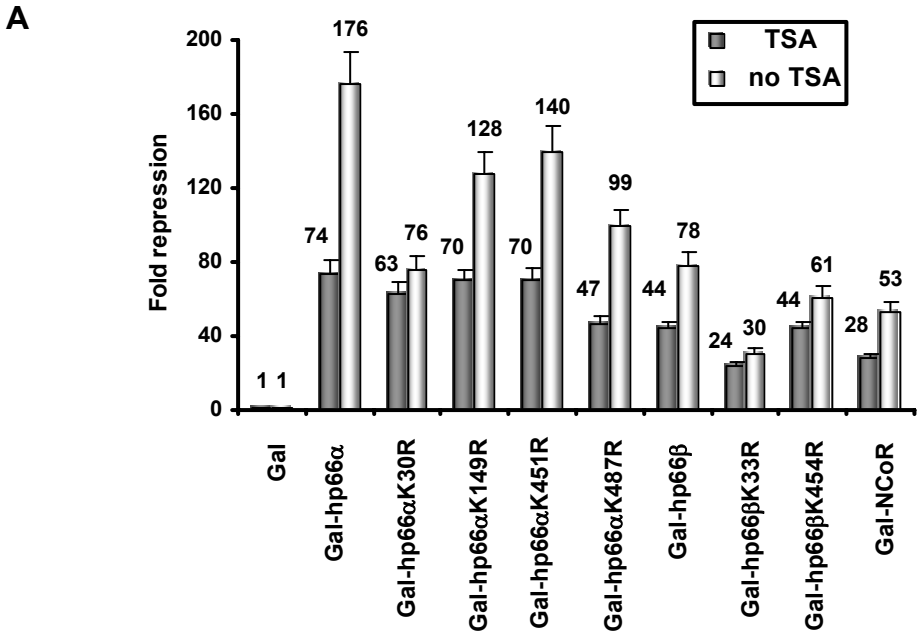

Fig.3.9 The transcriptional repression activity of hp66α is partially released upon TSA treatment. HEK293T cells were cotransfected with a 4×UAS-TK-luciferase reporter together with constructs coding for the Gal-DNA binding domain or the indicated Gal fusions in the presence or absence of TSA. Cell extracts were analyzed for reporter gene activity. Gal-NCoR is a positive control for TSA sensitive repression (Polly et al., 2000). Fold repression was determined relative to the Gal-DNA binding domain alone. Error bars represent variations within duplicate transfections.

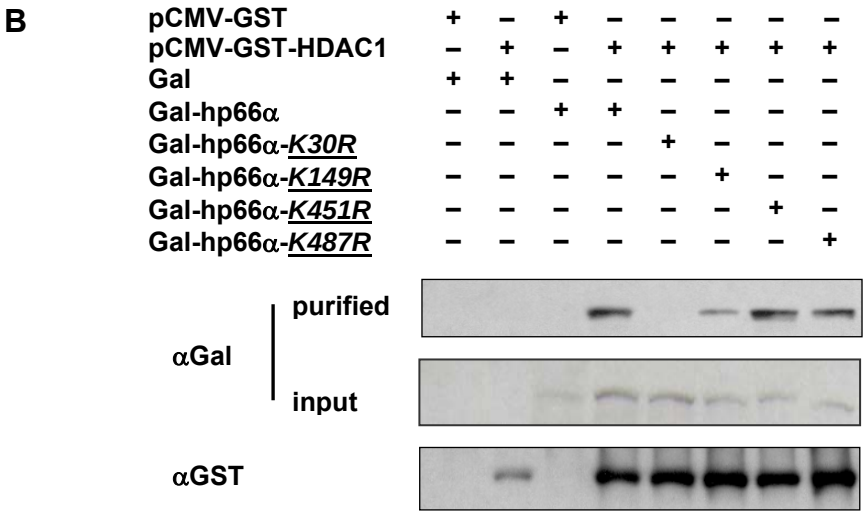

Fig.3.9 Mutation of the N-terminal SUMO modification site inhibits HDAC1 binding to hp66α *in vivo*. HEK293 cells were harvested 48h after transfection with various combinations of DNA constructs as indicated above the figure. Nuclear protein fractions were prepared and purified using glutathione Sepharose beads. Bound proteins (purified) were analyzed by Western blotting using an anti-Gal antibody as compared to input, which was analyzed with the anti-GST antibody as well.

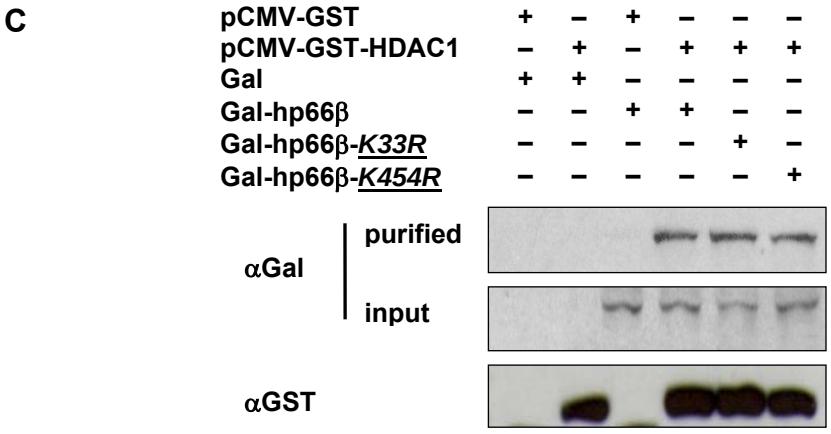

Fig.3.9 Mutation of the N-terminal SUMO modification site does not influence HDAC1 binding to hp66β *in vivo*. HEK293 cells were harvested 48h after transfection with various combinations of DNA constructs as indicated above the figure. Nuclear protein fractions were prepared and purified using glutathione Sepharose beads. Bound proteins (purified) were analyzed by Western blotting using an anti-Gal antibody as compared to input, which was analyzed with the anti-GST antibody as well.

p66αK30R and Gal-p66βK33R (Fig.3.9A). Both sites might be required for interaction with HDAC1 or other NuRD components. To test this assumption, HEK293 cells were cotransfected with mammalian vector pCMV-GST or pCMV-GST-HDAC1 together with Gal, Gal-hp66α, Gal-hp66β or corresponding four single mutant forms of Gal-hp66α and two single mutant forms of Gal-hp66β. After purification of nuclear extract with glutathione beads, GST-HDAC1

containing sample retains wild type Gal-hp66α, Gal-hp66β, and most of the mutant forms with one exception: Gal-hp66αK30R, which destroys the major SUMO modification site of hp66α and which is insensitive to TSA treatment, is not bound to GST-HDAC1 (Fig.3.9B and 3.9C). The results indicated that HDAC1 binding to hp66α and TSA sensitivity of transcriptional repression require an intact SUMJO modification site at K30 of hp66α. In contrast, mutation of a paralogs site in p66β, K33R, does not interfere with HDAC1 binding (Fig. 3.6D). Nevertheless, this mutant is resistant to TSA, indicating that other components of the HDAC complexes are bound at this site (see below).

3.2.5 Mutation of the SUMO modification sites does not affect MBD3 binding to hp66α and hp66β

MBD3 has previously been shown to be part of the Mi-2/NuRD complex (Feng et al., 2002; Hendrich and Bird, 1998; Le Guezennec et al., 2006) and to interact with hp66α and hp66β *in vitro* (Brackertz et al., 2002). In this work, expressing pCMV-GST or pCMV-GST-MBD3 was cotransfected together with Gal, Gal-hp66α, Gal-hp66β or the corresponding point mutant forms in HEK293 cells. After nuclear extract preparation, the input fraction and purified GST bound proteins were analyzed by Western blotting using an anti-Gal antibody. The data revealed that the GST-MBD3 containing sample retained Gal-hp66α, Gal-hp66β and all single mutant forms (Fig.3.10A and 3.10B). The results indicated that mutation of the SUMO modification sites does not influence MBD3 binding to either hp66α or hp66β.

3.2.6 Mutation of the N-terminal SUMO modification site impaired RbAp46 binding to hp66β, but not hp66α in vivo

Other components of the Mi-2/NuRD complex, the RbAp46 and RbAp48 proteins, have been shown to function as histone escort proteins in various histone-related complexes (Loyola and Almouzni, 2004). The binding of RbAp46 to hp66α or hp66β and to the respective mutant forms were examined. The results demonstrated that GST-RbAp46 containing sample retains wild type Gal-hp66α or Gal-hp66β and most of the mutant forms Gal-hp66α or Gal-hp66β, whereas only partially retains Gal-hp66βK33R, which is major SUMO modification site of hp66β (Fig.3.11A and 3.11B). The results suggested that the interaction of RbAp46 with hp66β

requires an intact SUMOylation site K33 of hp66β.

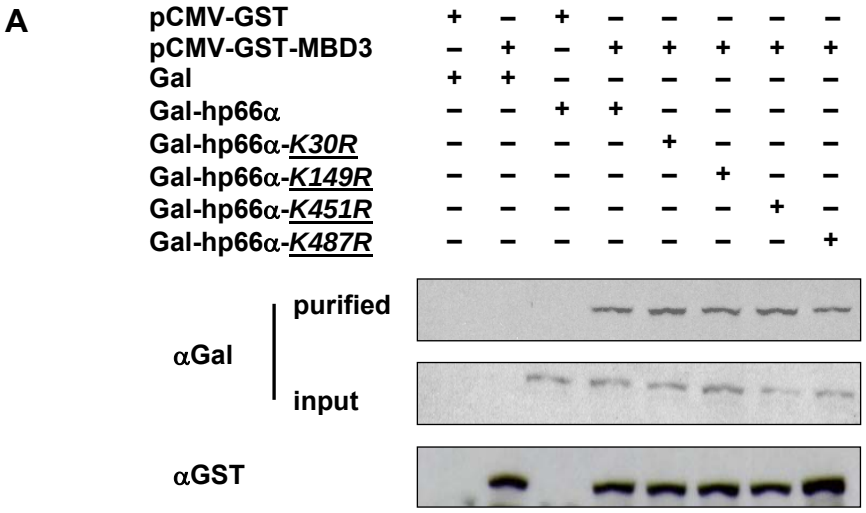

Fig.3.10 Mutation of the SUMO modification sites does not affect MBD3 binding to hp66α *in vivo*. HEK293 cells were harvested 48h after transfection with various combinations of DNA constructs as indicated above the figure. Nuclear protein fractions were prepared and purified using glutathione Sepharose beads. Bound proteins (purified) were analyzed by Western blotting using an anti-Gal antibody as compared to input, which was analyzed with the anti-GST antibody as well.

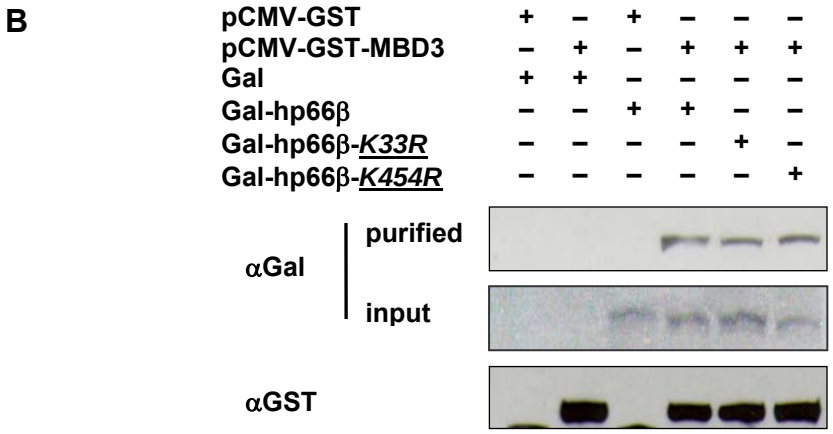

Fig.3.10 Mutation of the SUMO modification site does not inhibit MBD3 binding to hp66β *in vivo*. HEK293 cells were harvested 48h after transfection with various combinations of DNA constructs as indicated above the figure. Nuclear protein fractions were prepared and purified using glutathione Sepharose beads. Bound proteins (purified) were analyzed by Western blot using an anti-Gal antibody as compared to input, which was analyzed with the anti-GST antibody as well.

3.2.7 RbAp48 binding to hp66α and hp66β was independent of the SUMO modification sites

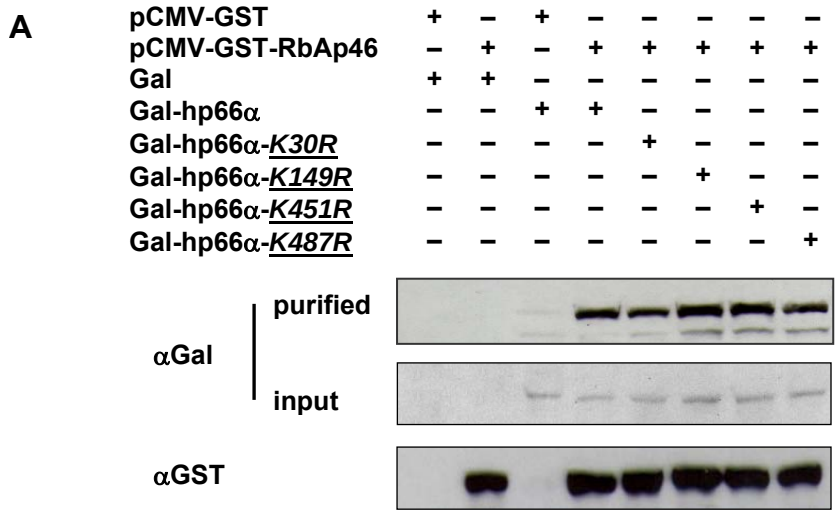

Fig.3.11 Mutation of the SUMO modification site does not affect RbAp46 binding to hp66α *in vivo*. HEK293 cells were harvested 48h after transfection with various combinations of DNA constructs, as indicated above the figure. Nuclear extracts were prepared and GST-RbAp46 were purified using glutathione Sepharose beads. Bound proteins (purified) were analyzed by Western blotting using an anti-Gal antibody as compared to input, which was analyzed with the anti-GST antibody as well.

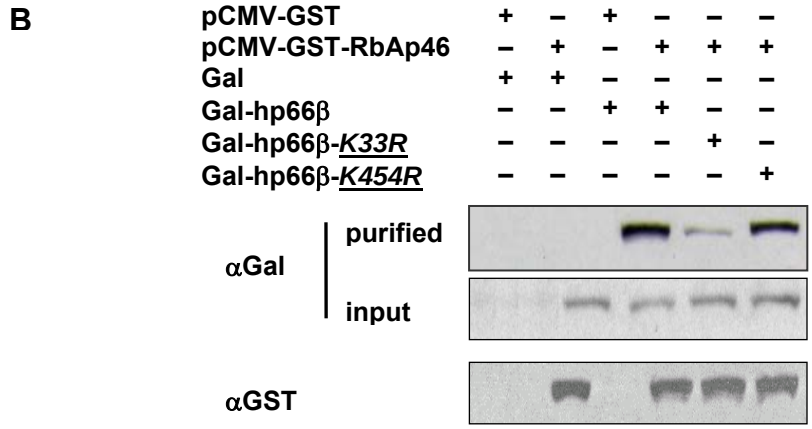

Fig. 3.11 Mutation of the N-terminal SUMO modification site impairs RbAp46 binding to hp66β *in vivo*. HEK293 cells were harvested 48h after transfection with various combinations of DNA constructs, as indicated above the figure. Nuclear extracts were prepared and GST-RbAp46 were purified using glutathione Sepharose beads. Bound proteins (purified) were analyzed by Western blotting using an anti-Gal antibody as compared to input, which was analyzed with the anti-GST antibody as well.

Similar experiment was performed as shown in above work with expressing vector pCMV-GST-RbAp48. All of the hp66α and hp66β mutant forms showed RbAp48 binding similar to the wild type hp66 proteins (Fig.3.12A and 3.12B). Thus the related RbAp46/RbAp48 proteins and the related hp66α/hp66β proteins are highly specific in protein/protein interaction.

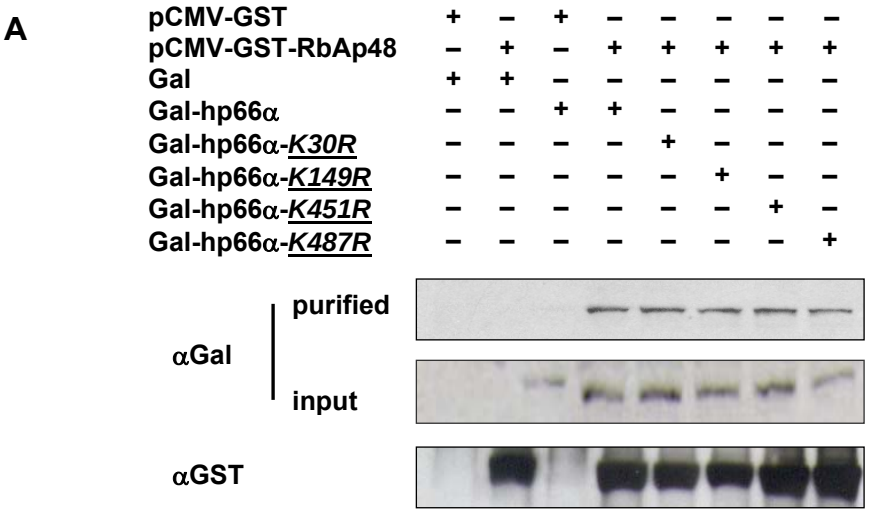

Fig.3.12 Mutation of the SUMO modification site does not influence RbAp48 binding to hp66α *in vivo*. HEK293 cells were harvested 48h after transfection with various combinations of DNA constructs as indicated above the figure. Nuclear protein fractions were prepared and purified using glutathione Sepharose beads. Bound proteins (purified) were analyzed by Western blotting using an anti-Gal antibody as compared to input, which was analyzed with the anti-GST antibody as well.

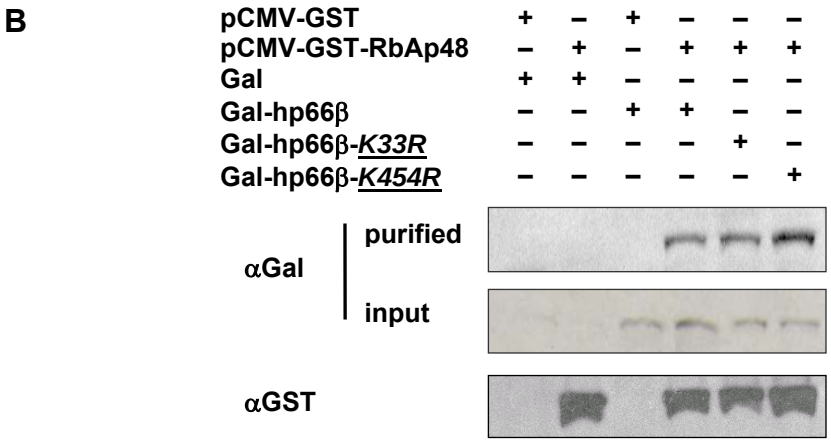

Fig.3.12 Mutation of SUMO modification site does not inhibit RbAp48 binding to hp66β *in vivo*. HEK293 cells were harvested 48h after transfection with various combinations of DNA constructs as indicated above the figure. Nuclear protein fractions were prepared and purified using glutathione Sepharose beads. Bound proteins (purified) were analyzed by Western blotting using an anti-Gal antibody as compared to input, which was analyzed with the anti-GST antibody as well.

3.3 Purification of hp66 protein complexes

3.3.1 Strategies for purification of the hp66 proteins complexes

Several lines of evidence demonstrated that hp66 proteins are components of the MeCP1

complex, the MBD2/NuRD complex, the MBD3/NuRD complex, as well as the MTA1/MTA2 formed complexes (Feng et al., 2002; Feng and Zhang, 2001; Le Guezennec et al., 2006; Yao and Yang, 2003). To gain better insight into the protein composition of the hp66 proteins complexes, further work is required to investigate whether hp66 proteins might be within same complex or different complexes. Since there was no hp66 antibody for immunoprecipitation commercially available, another approach was adopted by establishing stable cell lines expressing hp66 proteins. As a prerequisite step for purification, I established a two-step purification method with epitope-tagged hp66 constructs based on recently developed tandem affinity purification (TAP) method with modifications (Rigaut et al., 1999). This method allows affinity purification with fusion of a tag, usually a peptide, or a small protein, to the target protein. The TAP method has been used successfully to purify protein complexes in yeast and mammalian cells (Gavin et al., 2002; Westermarck et al., 2002). Nevertheless, this method has some potential disadvantages. For example, protein A epitope is rather big and might interfere with protein interaction surfaces in a protein complex. In order to avoid these potential problem, in this study, hp66 paralogs were fused to two tags, one is FLAG tag, the other is calmodulin binding peptide (CBP), which allow

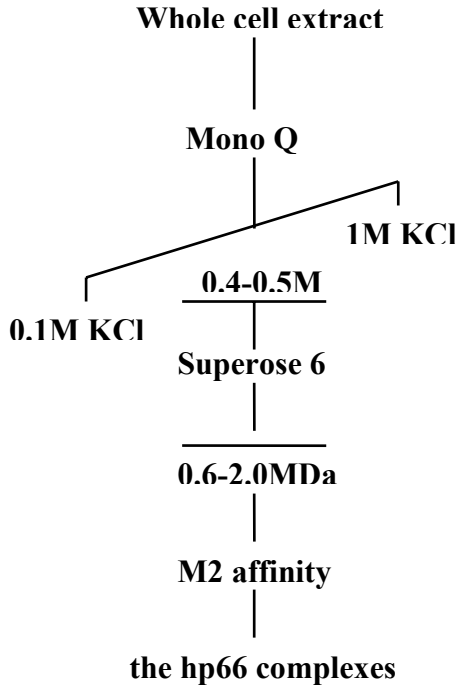

Fig.3.13 Schematic representation of the steps used to purify the hp66 containing complexes. See details in text. The horizontal and diagonal lines indicate stepwise and gradient elution, respectively.

high affinity for both FLAG beads and calmodulin resin. In the prelimary experiment, the calmodulin resin was not able to capture the CBP tagged proteins. Therefore, further approach chosen for purification was ion-exchange chromatography and gel filtration chromatography, which could identified the possible hp66 proteins complexes at certain range of fractions. After each chromatographic separation, I monitored column fractions for the hp66 protein complexes by Western blotting using FLAG antibody. Only the peak fractions containing FLAG-hp66 proteins from each column were used for subsequent chromatographic step. At last, these potential fractions were purified with FLAG M2 antibody directly conjugated to agarose resin, and the beads were eluted with FLAG peptide. The elute fractions were fractionated by SDS-PAGE followed by silver staining or Western blotting using antibodies against the known components of the NuRD complex. The purification step is outlined in Fig.3.13.

3.3.2 Establishment of stable cell lines expressing hp66 proteins

The stable cell lines were established as described above (section 2.2.4.4). Finally, the stable cell colonies were identified by RT-PCR using specific primers and by Western blotting using FLAG antibody. These clones were first identifed on mRNA expression level. Total RNA was isolated from each clone, and was converted into cDNA by using reverse transcription (see section 2.2.3). Then several specific primers were designed for identification of stable cell clones which stably integrate double tagged fusion constructs (Fig.3.14). In the case of control stable cell lines, FLAG-CBP primer was designed, which ranges from FLAG tag to CBP tag. For stable cell lines which stably integrate double tagged hp66 constructs, two pairs of primers were designed, one is FLAG primer which detects N-terminal part of double tagged hp66, the other is CBP primer which is able to amplify C-terminal part of double tagged hp66. To avoid false positive from transfected DNA, total RNA was first digested with DNase, then reverse transcription was performed. During the PCR reaction with specific primers, two templates were utilized, one was total RNA after digestion with DNase, the other was cDNA after reverse transcription. The results showed that one band with expected size was occurred after reverse transcription, whereas no band was observed without reverse transcription and the control HEK293 cells. Based on these findings, several clones were identified such as clone 54 (control stable cell line), cone 29 (stably integrated pcDNA3-FLAG-hp66α-CBP), and clone 87 (stably integrated pcDNA3-FLAG-hp66β-CBP). To further confirm these clones, these clones were detected by Western blotting with FLAG antibody. Moreover, these constructs were overexpressed in HEK293 cells

as positive control. The nuclear extract was prepared from these clones, and separated with SDS-PAGE. Similar band was detected in both stable cell lines clone 29 and clone 87 and HEK293 cells with overexpressed hp66 proteins, but not in control stable cell line clone 54 and in control HEK293 cells by using FLAG antibody. Taken together, several stable cell lines were successfully established for future purification procedure.

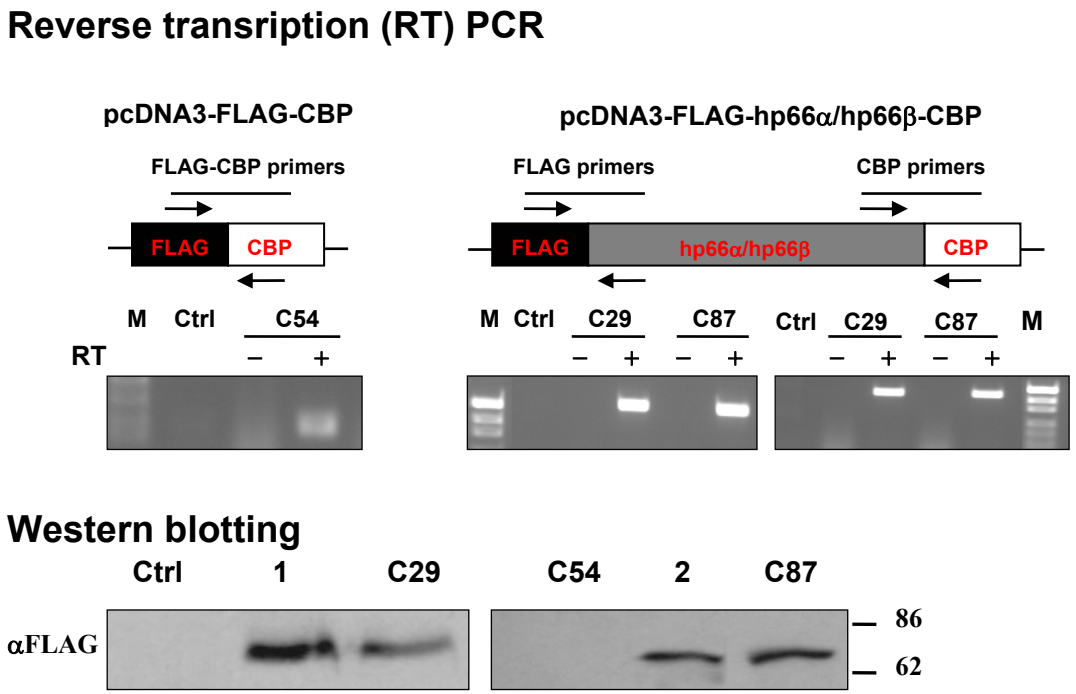

Fig.3.14 Identification of stable cell lines by using RT-PCR and Western blotting. Explanation: see text. Abbreviations: M: Marker; Ctrl: control HEK293 cell; C54: clone 54 (stably integrated pcDNA3-FLAG-CBP); C29: clone 29 (stably integrated pcDNA3-FLAG-hp66α-CBP); C87: clone 87 (stably integrated pcDNA3-FLAG-hp66β-CBP); 1: pcDNA3-FLAG-hp66α-CBP (overexpression); 2: pcDNA3-FLAG-hp66β-CBP (overexpression).

3.3.3 Ion-exchange chromatography

Whole cell extract of stable cell lines was prepared, concentrated, and loaded on Mono Q column, which is a strong anion-exchanger. The typical chromatogram from Mono Q ion-exchange chromatography is shown in Fig.3.15A. The individual fractions were collected with salt gradient from 100mM KCl to 1M KCl. Western blotting analysis of proteins from individual fractions showed that the majority of FLAG-hp66α protein elutes with a broad range from fraction 14 to fraction 26, while the majority of FLAG-hp66β protein elutes with a range from fraction 16 to fraction 30. However, there is no signal detected in the case of control stable cell line clone 54 which stably integrates pcDNA3-FLAG-CBP (Fig.3.15B). These

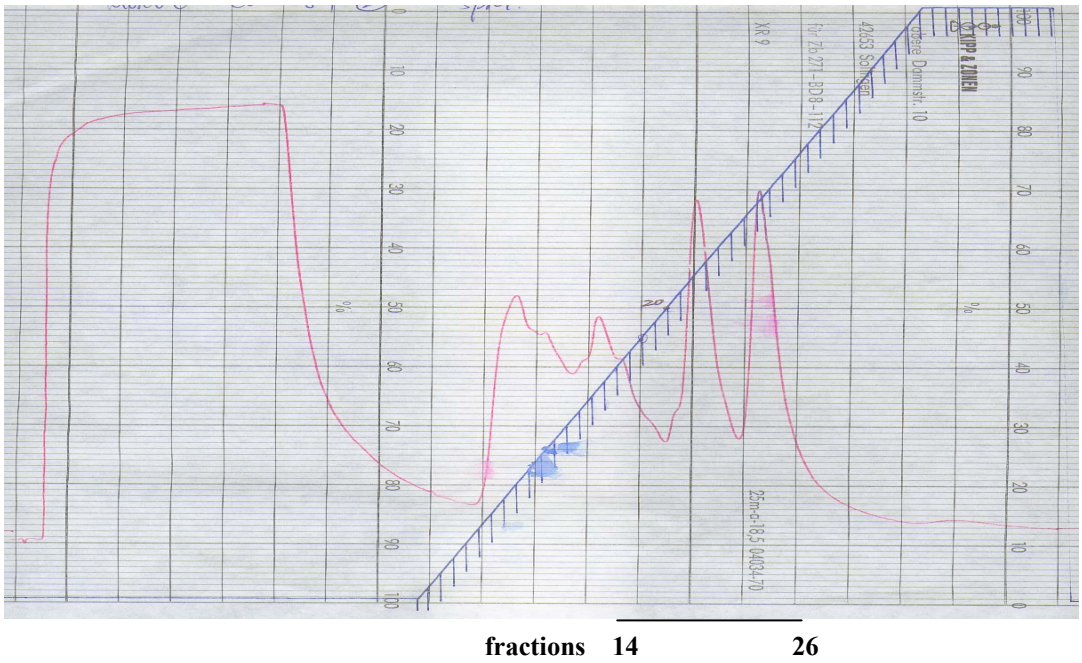

Fig.3.15A The elution profile of Mono Q column ion-exchange chromatography. Absorbance of elute fraction monitored at UV 280nm (red line) and the collected fractions (blue sticks) are shown.

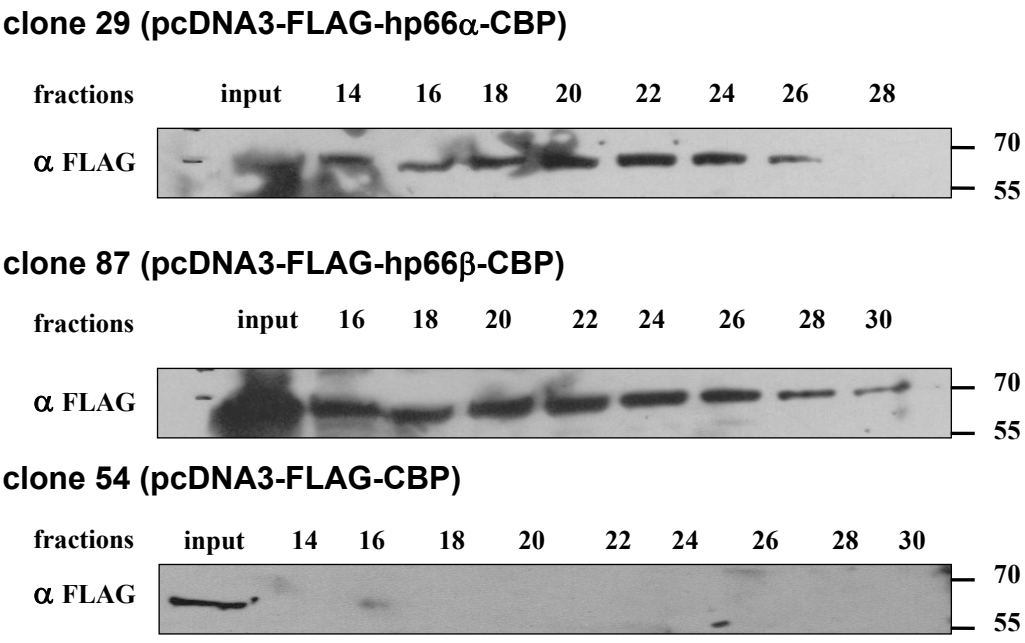

Fig.3.15B Western blotting analysis of the Mono Q fractions using aniti-FLAG antibody. Individual fractions from ion-exchange chromatography were separated by SDS-PAGE and analysed by Western blotting directed against FLAG antibody on the left of the figure. Input denotes the sample used in the ion-exchange purification procedure. Fractions were pooled for analysis on a subsequent gel filtration.

fractions containing FLAG-hp66 protiens elute mainly at estimated 0.4M-0.5M KCl. Finally, those fractions containing FLAG-hp66 proteins from ion-exchange chromatography were pooled, concentrated, and passed through Superose 6 column.

3.3.4 Gel filtration (size exclusion chromatography)

Prior to start gel filtration, I made a standard curve by separation of a mixture of alcohol dehydrogenase (150KDa), apoferritin (443KDa), thyroglobulin (669KDa) on a Superose 6 column (Fig.3.16A). Based on this standard curve, the V_o of this column is 7.0ml, the Ve of alcohol dehydrogenase, apoferritin, thyroglobulin is 14.8ml, 12.8ml, and 11.4ml, separately. Molecular weight of unknown proteins is determined by comparing the ratio of V_e/V_o for the protein to the V_e/V_o of protein standards of known molecular weight.

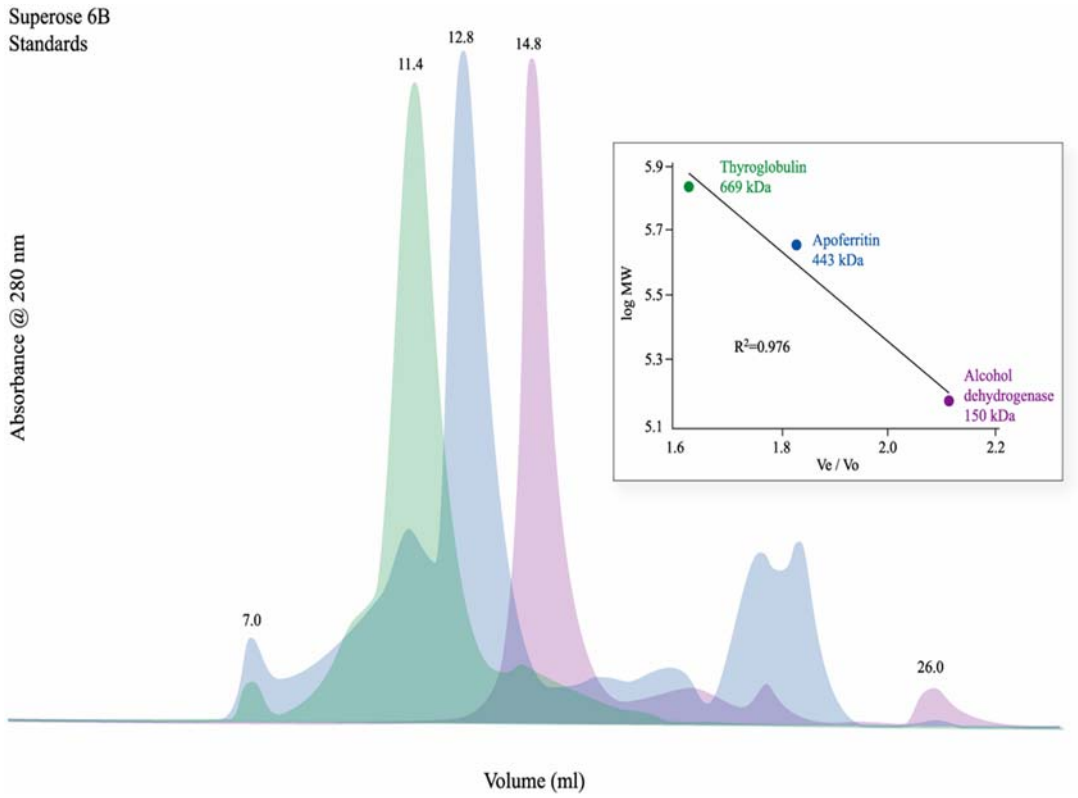

Fig.3.16A Calibration curve obtained with standard proteins on Superose 6 column.

Those fractions containing FLAG-hp66 proteins from ion-exchange chromatography were pooled, concentrated, and applied to a Superose 6 column. The fractions (0.5ml) were collected for further analysis. In case of clone 29 which stably integrates pcDNA3-FLAG-hp66α-CBP,

the elution profile of FLAG-hp66α containing fractions derived from gel filtration was shown in Fig.3.16B. Two major peaks were observed, one peak is appeared at fraction 16 with an estimated size of 1.8MDa, the other peak is occured at fraction 32 which corresponds to a molecular mass of 148KDa.

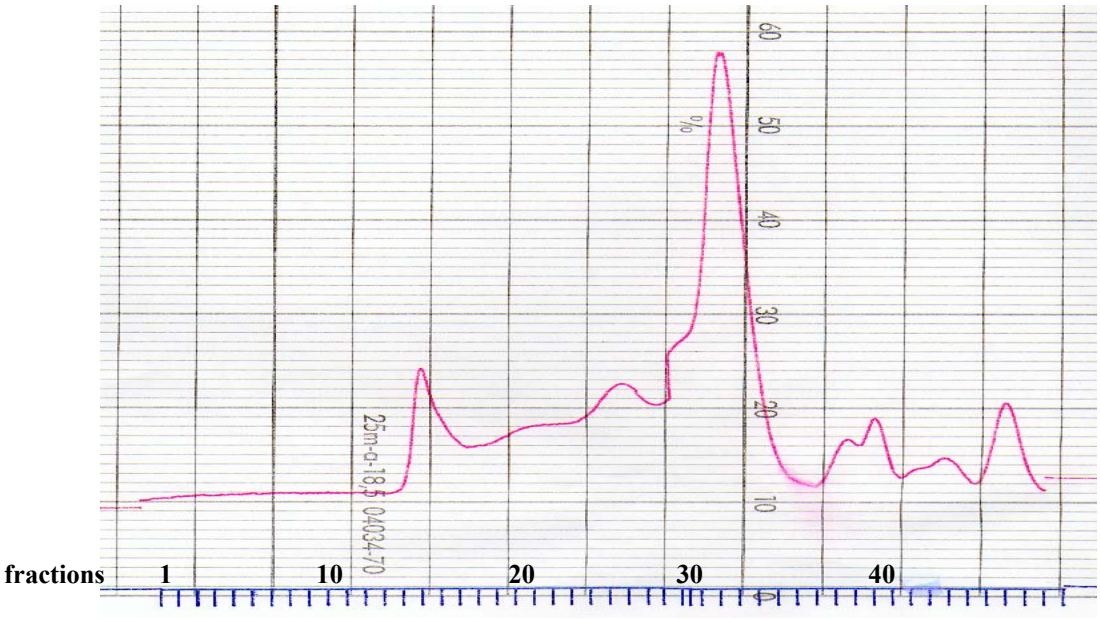

Fig.3.16B The elute profile of fractions dereived from a Superose 6 column in the case of clone 29. Absorbance of elute fraction monitored at UV 280nm (red line) and the collected fractions (blue sticks) are shown.

Western blotting analysis of proteins from individual fractions revealed that the majority of FLAG-hp66α protein elutes with a broad profile encompassing from fraction 16 to fraction 26, and separtates into two peaks, one peak is first detected at fraction 16, very close to the void volume, which could be an indicative of protein aggregation, with an estimated molecular weight of 1.8MDa, and then the other peak was occurred at fraction 22 which corresponds to a molecular weight of 763KDa. The results demonstrated that hp66α protein probably resides in two different size of protein complexes, one is about 1.8MDa, the other is 763KDa. Furthermore, the specific band was observed again at fraction 32which might be hp66α dimers with a theoretical molecular weight of 148KDa (Fig.3.16C).

In another independent experiment, eukaryotic expressing GST-hp66 paralogs were cotransfected with Gal-hp66 proteins into HEK293 cells. Nuclear extract was prepared and incubated with glutathione beads. The bound proteins were detected with Gal antibody. The results obviously showed that GST-hp66α retained Gal-hp66α and Gal-hp66β, and *vice versa*

(Fig.3.16D). The data suggested that both hp66 paralogs interact each other and do not exist as a free form but a dimer *in vivo*.

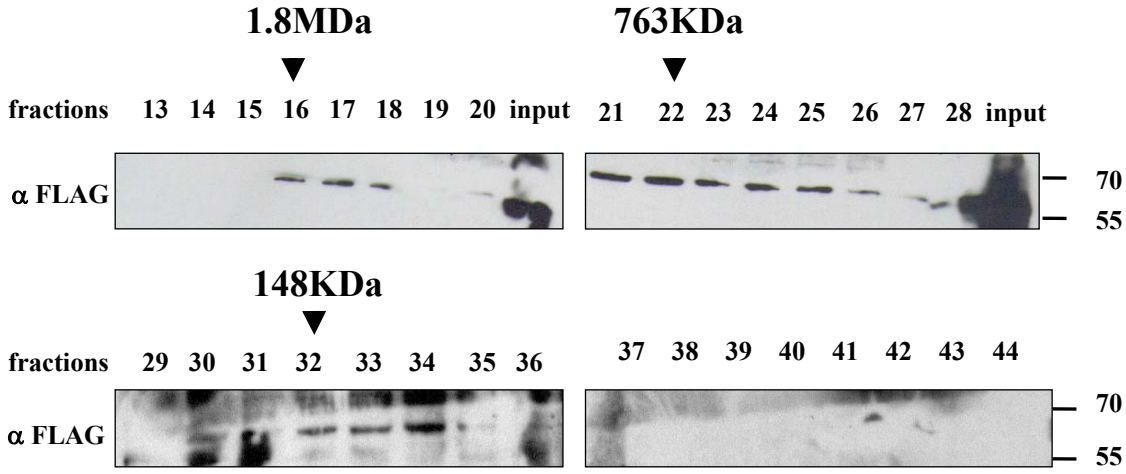

Fig.3.16C Western blotting analysis of the fractions from Superose 6 columm of clone 29 with FLAG antibody. Individual fractions from gel filtration were separated by SDS-PAGE and analysed by Western blotting directed against FLAG antibody shown on the left side of the figure. Input denotes the sample used in the gel filtration purification procedure. The arrows at the top denote the elution positions of calibration proteins of known molecular weights.

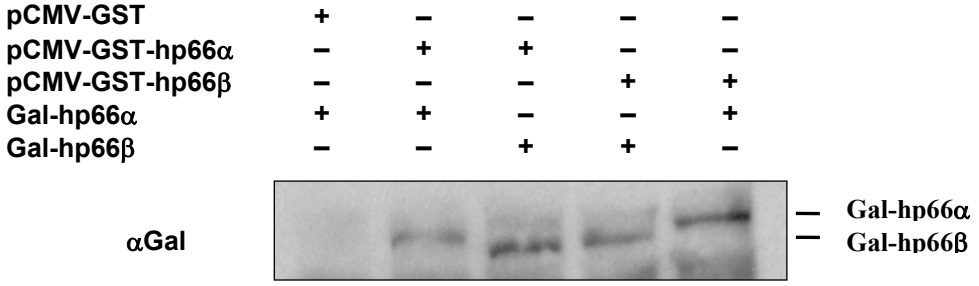

Fig.3.16D Both hp66 paralogs interact each other and form a dimmer. HEK293 cells were harvested 48h after transfection with various combinations of DNA constructs, as indicated above the figure. Nuclear extract was prepared and GST-hp66 proteins were purified using glutathione Sepharose beads. Bound proteins were analyzed by Western blotting using an anti-Gal antibody

It is known that hp66α is a component of the NuRD complex. To determine whether the subunits of the NuRD complex cofractionate with hp66α, individual fractions containing FLAG-hp66α from gel filtration were separated by SDS-PAGE and analyzed by Western blotting using antibodies directed against the known components of the NuRD complex such as HDAC1/HDAC2, RbAp46/RbAp48, MBD2/MBD3, Mi-2, PRMT5, as well as Sin3A

(Fig.3.16E). The results revealed that, as expected, most of the known components cofractionate with FLAG-hp66α in a similar profile of fractions. In detail, these known subunits of the NuRD complex start to occur at fraction 16, then co-elute in an overlapping set of high-molecular weight fractions of FLAG-hp66α, as approximately 1.8MDa complex. furthermore, these known subunits and hp66α are present in fractions of low-molecular weight which forms another possible complex. FLAG-hp66α and members of the NuRD complex

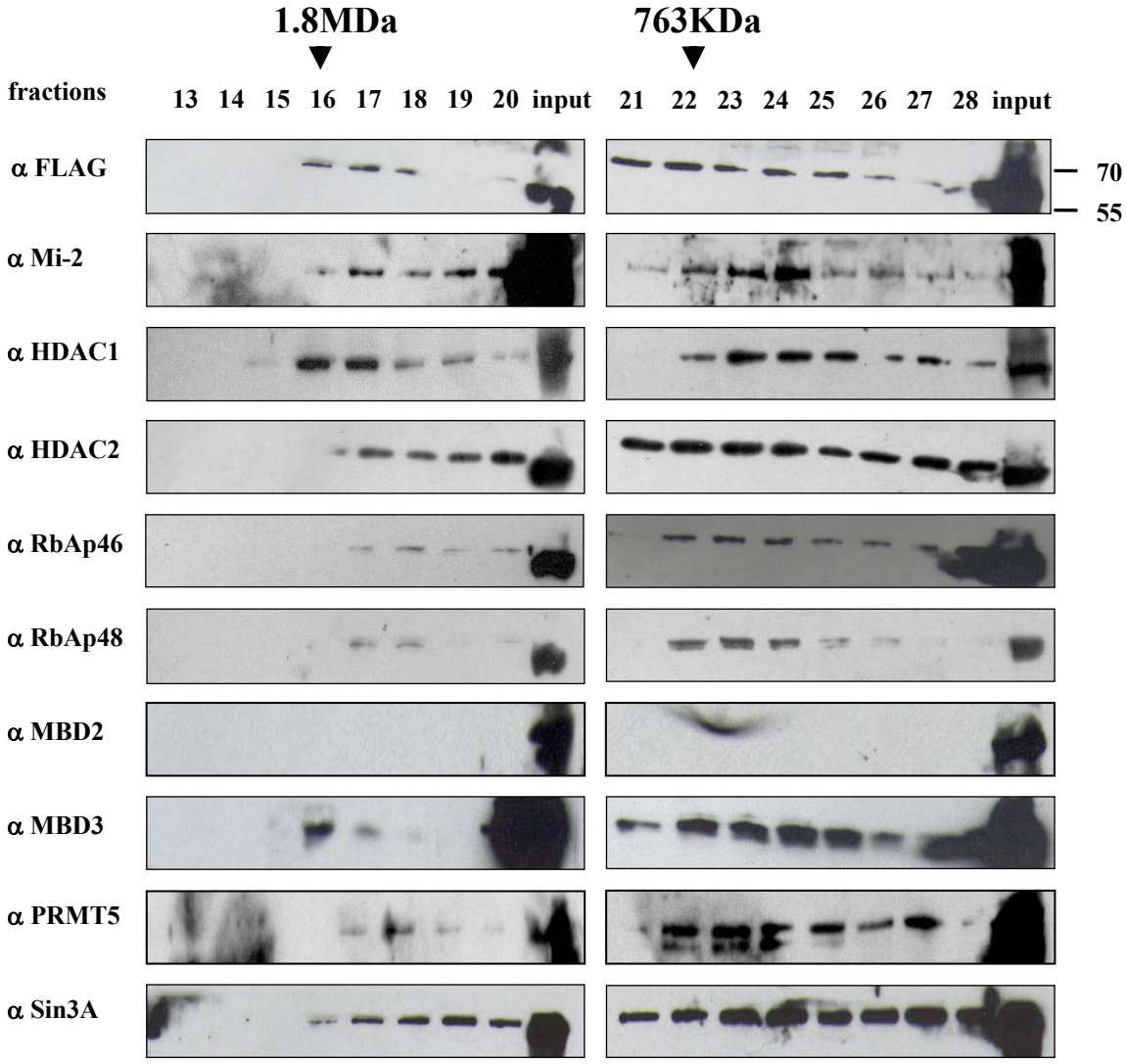

Fig.3.16E Western blotting analysis of the fractions from Superose 6 columm of clone 29 with antibodies against the know components of the NuRD complex and Sin3A. Individual fractions from gel filtration were fractionated by SDS-PAGE and detected by Western blotting using antibodies directed against proteins to the left of the figure. Input denotes the sample used in the gel filtration purification procedure. The arrows at the top denote the elution positions of calibration proteins of known molecular weights.

display similar elution profiles, indicating that the FLAG-hp66α-NuRD association is stable over multiple steps of purification. In particular, all detected proteins are present in fractions 17, 18 of the possible high molecular weight complex and most fractions of the likely low high molecular weight complex. These complexes are likely mixutre of many different complexes. Surprisingly, MBD2, which is the component of the MeCP1 complex or the MBD2/NuRD complex, doesn't cofractionate with FLAG-hp66α. It is assumed that either amout of MBD2 may not be sufficient for detecting by Western blotting, or interaction of MBD2 with hp66α is not stable enough. Interestingly, mSin3A, which is a subuit of the Sin3A/HDAC complex, also coelutes with fractions of two different molecular mass of FLAG-hp66α containing complexes, indicating that mSin3A may be recruited to histone deacetylases core which coexists with the NuRD complex. Taken together, hp66α stably associates with the NuRD complex.

As to another stable cell line clone 87 which stably integrates pcDNA3-FLAG-hp66β-CBP, the elution profile of FLAG-hp66β containing fractions derived from gel filtration showed three main peaks, first peak is located at fraction 14 which is void volume (7ml), the second peak is located at fraction 24 which indicates a molecular mass of 600KDa, and a third peak is loacated at fraction 32 which stands for a molecular mass of 148KDa (Fig.3.16F).

Individual fractions from gel filtration were then fractionated on SDS-PAGE and detected by Western blotting with FLAG antibody. As shown in Fig.3.16G, two different peak fractions containing the majority of FLAG-hp66β protein were detected in a broad range from fraction 16 to fraction 26, one is at fraction 16 which corresponds to molecular weight of 1.8MDa, and the other is at fraction 24 which indicates molecular weight of 600KDa. The results suggested that hp66β appears to form two different sizes of protein complexes, one is about 1.8MDa, the other is 600KDa. Moreover, the specific band again was found at fraction 32 which indicates the molecular weight of 148KDa, which corresponds to theoretical dimers of hp66β protein. Previously, hp66β was identified as a component of the MeCP1 complex or the NuRD complex. To confirm the association of hp66β with the NuRD complex and to get insight into the members of the hp66β-containing complex, individual fractions from gel filtration were further analyzed by Western blotting using antibodies directed against the known components of the NuRD complex same to above experiments (Fig.3.16H). Again, MBD2 doesn't coelute with FLAG-p66β protein after gel filtration, indicating that interation of hp66β with MBD2 might

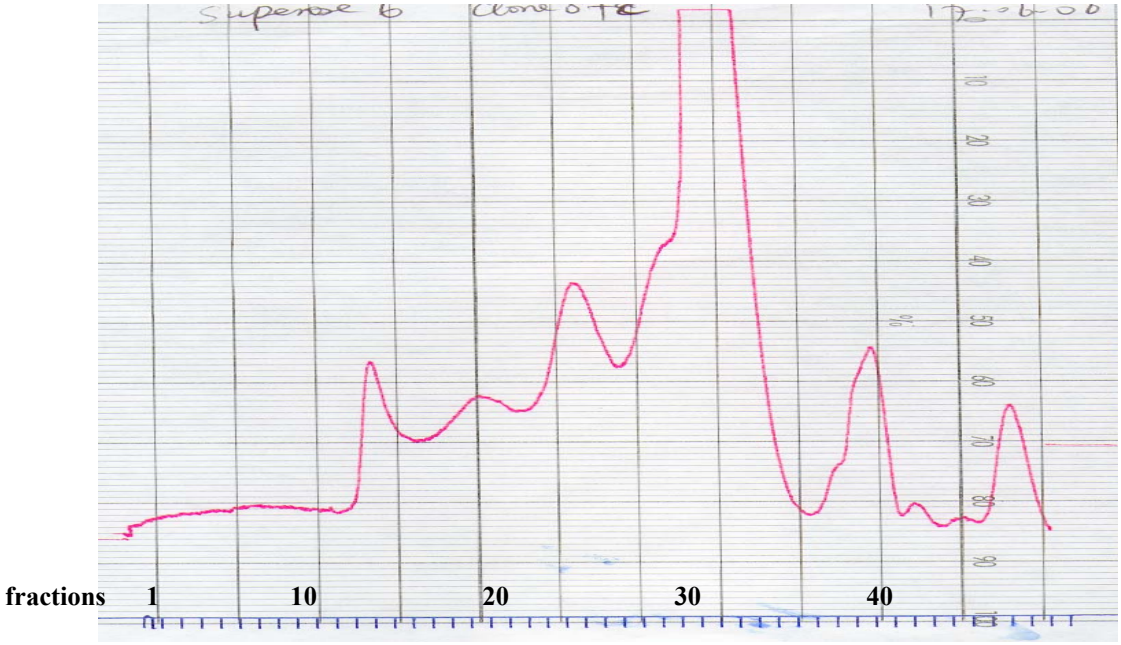

Fig.3.16F The elute profile of fractions dereived from a Superose 6 column in the case of clone 87. Absorbance of elute fraction monitored at UV 280nm (red line) and the collected fractions (blue sticks) are shown.

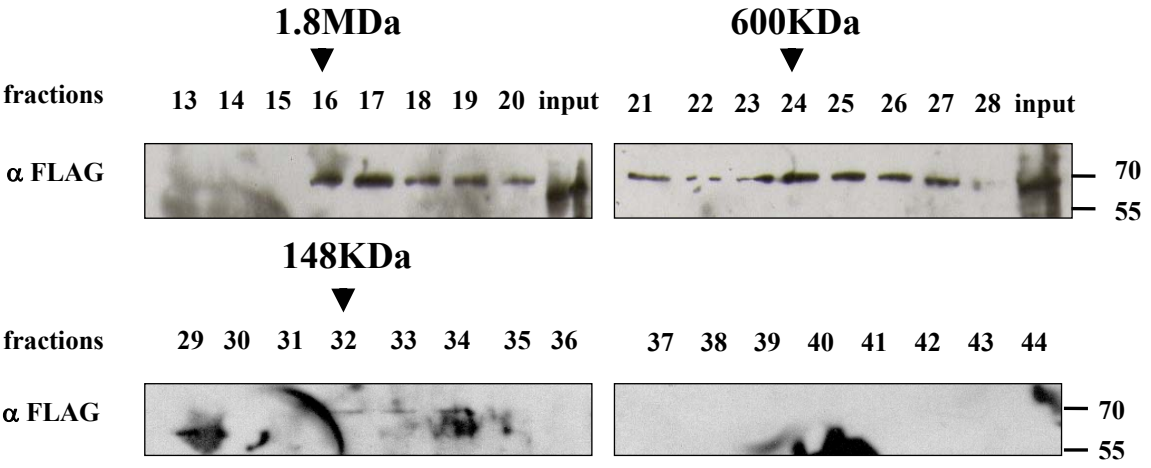

Fig.3.16G Western blotting analysis of the fractions from Superose 6 columm of clone 87 with FLAG antibody. Individual fractions from gel filtration were separated by SDS-PAGE and analyzed by Western blotting directed against FLAG antibody indicated on the left side of the panel. Input denotes the sample used in the gel filtration purification procedure. The arrows at the top denote the elution positions of calibration proteins of known molecular weights.

not be stable after several purification steps, although it was detected in the following purification step and mammalian GST pulldown experiment (see below). Nevertheless, most of the known components such as HDAC1/HDAC2, RbAp46/RbAp48, MBD3, Mi-2, PRMT5 of the NuRD complex cofractionate with FLAG-hp66β at the possible high/low molecular mass

complexes similar to elution profile of FLAG-hp66β. As shown in Fig.16C, these components start to appear at the high molecular weight fractions, then these known subunits and FLAG-hp66β are detected at the low-molecular weight fractions. The data indicated that FLAG-hp66β coexists with the NuRD complex after multiple steps of purification. Again, all detected proteins are present in fractions 19, 20 of the possible high molecular weight complex and most fractions of the likely low high molecular weight complex. Furterhmore, Sin3A, a component of the Sin3A/HDAC complex, also cofracionates with fractions of the possible high/low-moledular weight complexes containing FLAG-hp66β, indicated that Sin3A may be recruited

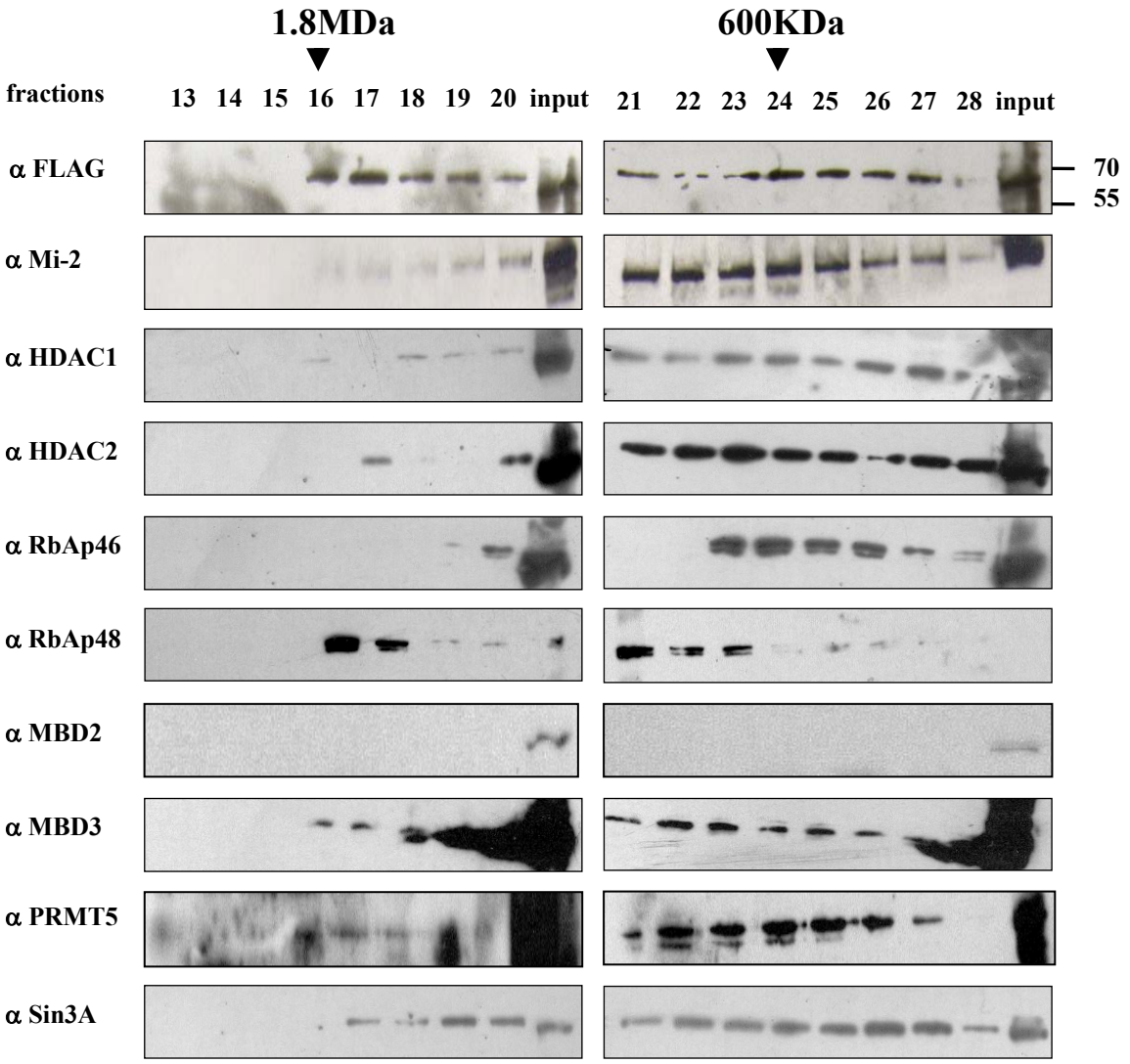

Fig.3.16H Western blotting analysis of the fractions from Superose 6 columm of clone 87 antibodies against Sin3A and the known subunits of the NuRD complex. Individual fractions from gel filtration were fractionated by SDS-PAGE and detected by Western blotting. The antibodies used are indicated the left side of the panel. Input denotes the sample used in the gel filtration purification procedure. The arrows at the top denote the elution positions of calibration proteins of known molecular weights.

to histone deacetylases which share with the NuRD complex.

Next, to examine whether possible hp66 proteins complexes stably bind to FLAG M2 agarose beads, individual fractions such as fraction 8, fraction 16, and fraction 24 from gel filtration were incubated with FLAG M2 beads. After stringent washing of beads, the bound proteins were separated by boiling in SDS sample buffer, and then loaded on 10% SDS-PAGE. Western blotting analysis was used to detect the possible association of several known subunits of the NuRD complex. Most of the known components such as HDAC1/HDAC2, RbAp46/RbAp48, MBD3, Mi-2 of the NuRD complex as well as MBD2 are clearly retained with FLAG-hp66 proteins at the possible high and low molecular mass complexes, suggesting that they are *bona fide* subunits of the NuRD complex (Fig.3.16I). Recently, arginine methyltransferase PRMT5 was identified as specific subunit of the MBD2/NuRD but not the MBD3/NuRD complex (Le Guezennec et al., 2006). In this study, PRMT5 also binds to FLAG hp66 proteins. Furterhmore, mSin3A, a component of the Sin3A/HDAC complex, is not retained with FLAG-hp66 proteins, indicating that mSin3A may not be component of the hp66 proteins containing complexes. The data suggested that the possible hp66 complexes are stably bind to beads after stringent washing, which indicated the further elution step by using FLAG peptide is practical.

After extensive washing, proteins were eluted from the beads with FLAG peptide and were separated on SDS-PAGE followed by Western blotting against with different antibodies or silver staining. The results revealed that the known components of the NuRD complex as well as MBD2 and PRMT5 are associated with hp66 paralogs. In addition, I observed that hp66α and hp66β are not mutually exclusive, which is consistent with above findings. (Fig.3.16J). So far, it seems that hp66 paralogs within same complex containing HDAC1/HDAC2, RbAp46/RbAp48, MBD2/MBD3, Mi-2, PRMT5 as well as hp66α/hp66β, however, the fact is that hp66 paralogs containing distinct complexes remain to be further investigated.

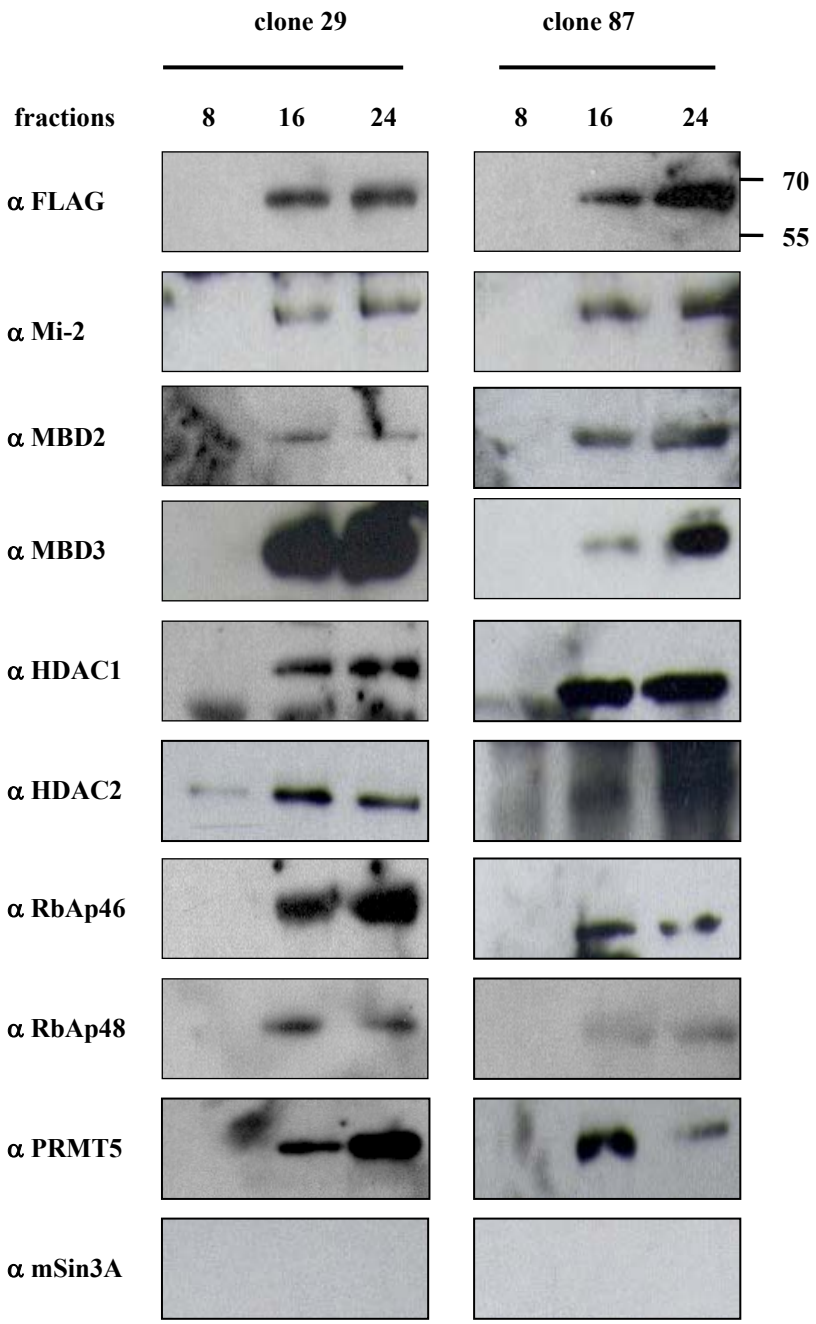

Fig.3.16I hp66 proteins associate with the components of the NuRD complex on FLAG agarose beads. Individual fractions 8, 16, and 24 from gel filtration were incubated with FLAG M2 beads. After washing of the beads, the bound proteins were separated by boiling in SDS sample buffer and loaded on 10% SDS-PAGE. The interacting proteins were analyzed by Western blotting using antibodies against mSin3A, MBD2, PRMT5 and the known components of the NuRD complex.

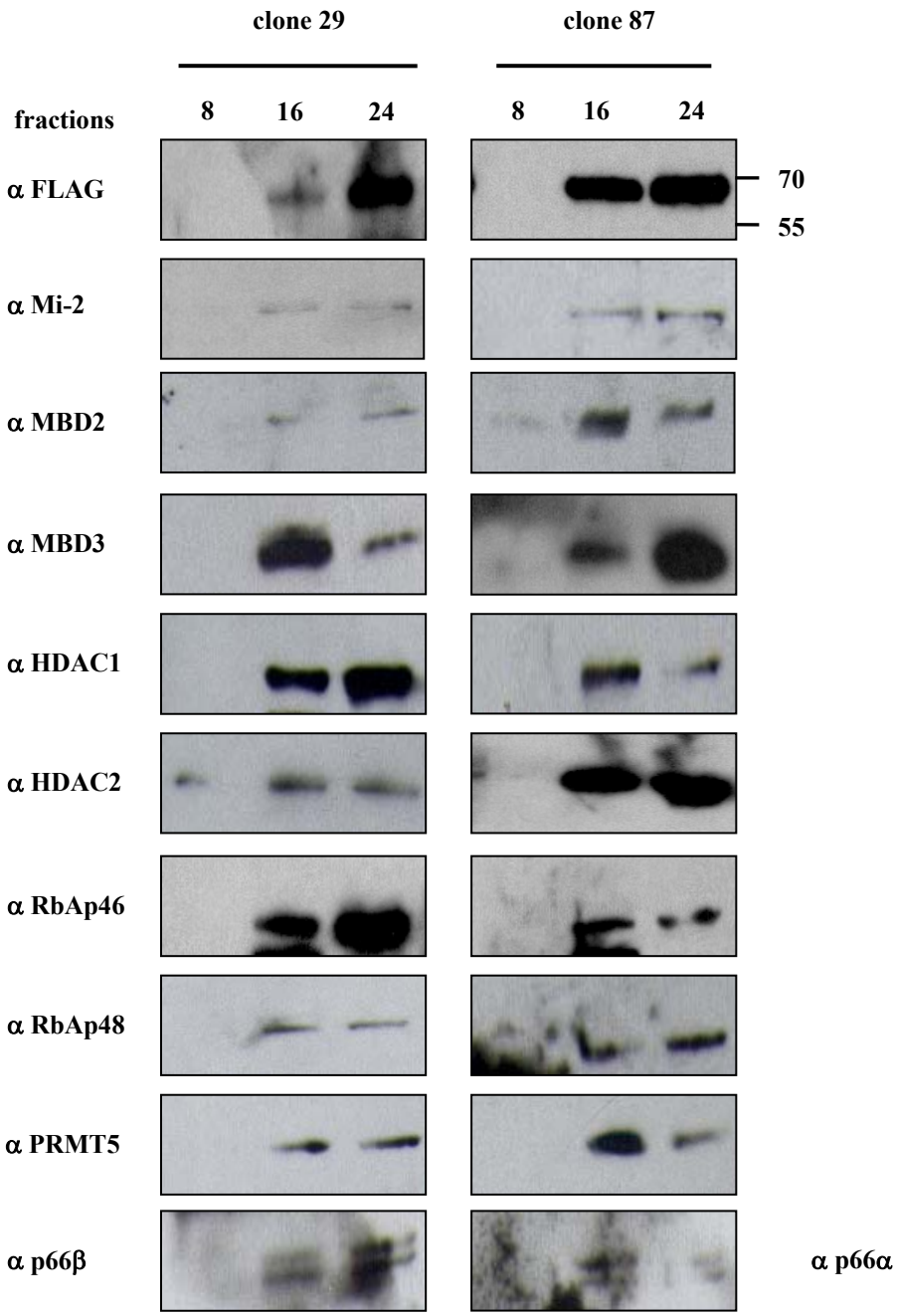

Fig.3.16J hp66 proteins associate with the components of the NuRD complex on elution with FLAG peptide. Individual fractions 8, 16, and 24 from gel filtration were incubated with FLAG M2 beads. After washing of the beads, the bound proteins were eluted with FLAG peptide and fractionated on 10% SDS-PAGE. The interacting proteins were analyzed by Western blotting using antibodies against MBD2, PRMT5 and the known components of the NuRD complex.

3.3.5 hp66 proteins associate with the components of the NuRD complex

The subunits of the NuRD complex binding to hp66 proteins were further determined by conducting mammalian GST pulldown experiments with transfection of mammalian expressing GST proteins or GST fusions of hp66 proteins into HEK293 cells. Western blotting analysis was used to determine the possible association of several endogenous proteins with GST-hp66 proteins. The proteins specifically retained by GST-hp66 resins are Mi-2, HDAC1/HDAC2, MBD2/MBD3, RbAp46/RbAp48, PRMT5 which are the known components of the NuRD complex (Fig.3.17). The interaction of hp66 proteins with MBD2/MBD3, HDAC1/HDAC2, RbAp46/RbAp48, Mi-2 as well as PRMT5 indicated that hp66 proteins are associated with the MBD2/NuRD and the MBD3/NuRD complex. In addition, mSin3A is not retained with GST fusion hp66 paralogs, indicating that mSin3A is not associated with the hp66 proteins containing complexes.

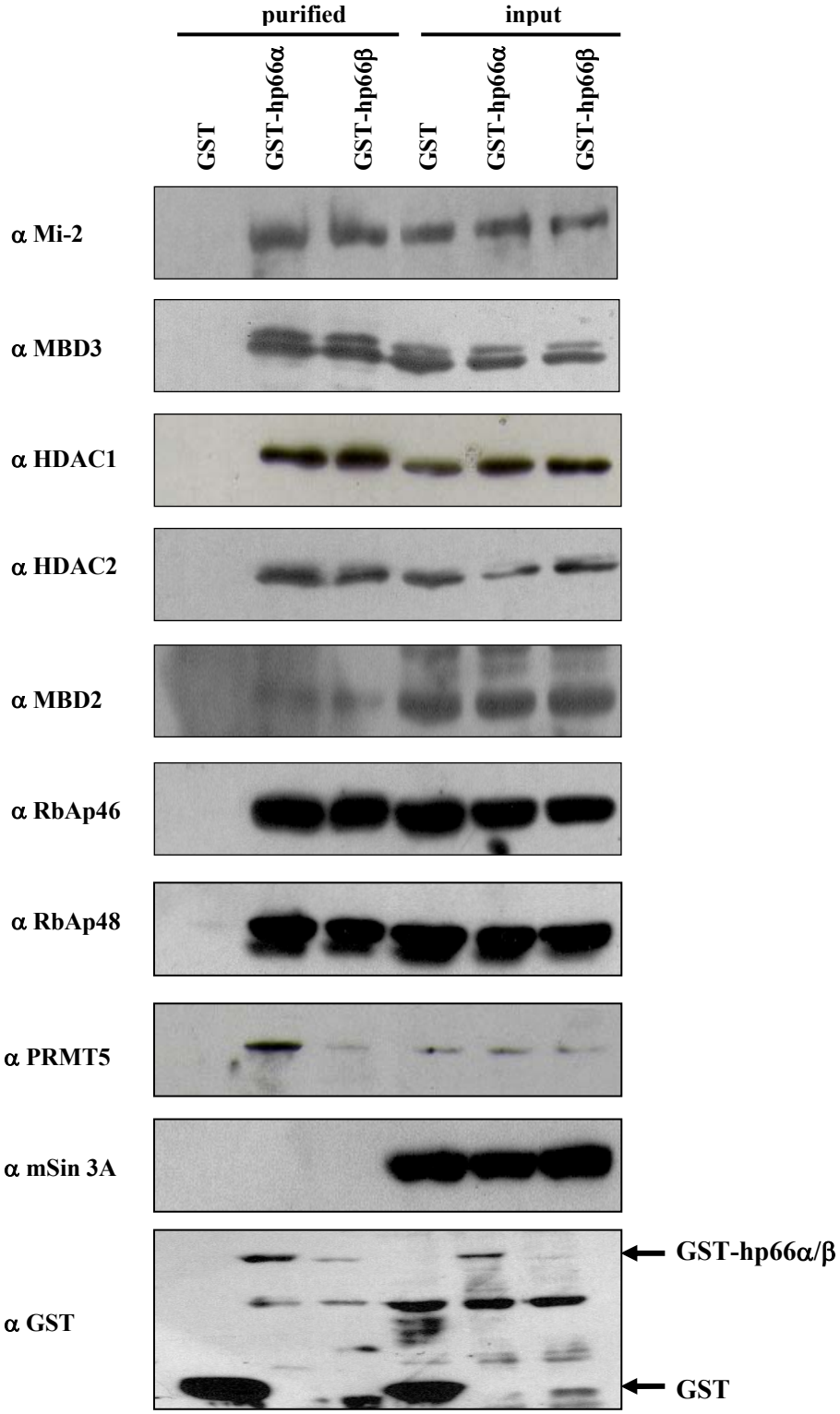

Fig.3.17 hp66 proteins associate with the components of the NuRD complex. GST proteins or GST fusions of hp66 proteins were expressed in HEK293 cells. Forty-eight hours after transfection, nuclear extract was prepared and incubated with glutathione beads. After washing of the beads, the bound proteins were separated on 10% SDS-PAGE. The interacting proteins were analyzed by Western blotting using antibodies against mSin3A, MBD2, PRMT5 and the known components of the NuRD complex.

4 DISCUSSION

Methylation of cytosine at the carbon 5 position of CpG dinucleotides is an epigenetic modification that is implicated in transcriptional silencing. It has long been known that histone deacetylation is a major mechanism in DNA methylation-mediated transcriptional repression (Bird and Wolffe, 1999). In general, acetylated histone tails correlate with active gene transcription and an open chromatin conformation, whereas deacetylated histone tails correlate with inactive gene transcription and a closed chromatin conformation (Wu and Grunstein, 2000). It has been proposed that the bridge between DNA methylation and histone deacetylation are methyl-CpG binding domain (MBD) proteins that are components of multi-protein repressor complexes such as Mi-2/NuRD (Wu and Grunstein, 2000). The MBD3 protein is an integral component of the multi-subunit protein complex Mi-2/NuRD, that contains nucleosomal remodeling activity as well as histone deacetylases that affect chromatin conformation resulting in gene silencing (Wade et al., 1999; Xue et al., 1998). While MBD3 of the Mi-2/NuRD complex can not be directly recruited to methylated DNA, interaction with MBD2, which has an intrinsic affinity for methylated DNA, targets Mi-2/NuRD to methyl-CpG (Boeke et al., 2000; Hendrich and Bird, 1998). This MBD2 containing Mi-2/NuRD complex has also been called MeCP1 (Feng and Zhang, 2001; Ng et al., 1999). It seems that there is an overlap for MBD2 and MBD3 binding sites (Ballestar and Wolffe, 2001; Le Guezennec et al., 2006), whereas complex purification revealed the existence of distinct MBD2/NuRD and MBD3/NuRD complex (Le Guezennec et al., 2006).

Two highly related human p66 proteins, referred to as hp66α and hp66β, have been shown to interact with MBD2 and with MBD3 and to enhance MBD2-mediated transcriptional repression. Both interact with histone tails and reside within the MBD2/NuRD and MBD3/NuRD complexes (Brackertz et al., 2002; Brackertz et al., 2006; Feng et al., 2002; Le Guezennec et al., 2006). Both hp66 proteins colocalize with MBD2 in a speckled nuclear pattern. A comparison between different species revealed two conserved regions, CR1 and CR2. CR1 of hp66β is required for interaction with MBD2, MBD3, MTA2, HDAC1, HDAC2, RbAp46 and RbAp48, whereas CR2 was reported to target hp66 and MBD3 to specific nuclear loci and to mediate histone tail interaction (Brackertz et al., 2006; Feng et al., 2002).

4.1 Transcriptional repression of hp66α and hp66β

4.1.1 Both hp66α and hp66β differ in transcriptional repression and in their repression domains

Both hp66α and hp66β are two closely related proteins with similar CR1 and CR2. The sequence similarity as well as their ubiquitous expression suggest that they have similar properties and exert similar functions (Brackertz et al., 2002). In this study we asked whether both hp66 proteins are functionally equivalent or whether each may have unique molecular features. Here I show that the transcriptional repression of hp66α is much stronger than that of hp66β based on analysis of protein expression level (see section 3.1.1). These finding show for the first time different functional properties of both related proteins.

In addition, I demonstrated that hp66α contains two major repression domains, the C-terminus including CR2 and the N-terminus including CR1, whereas in hp66β only the N-terminal domain including CR1 is functionally equivalent to hp66α (see section 3.1.2), a finding which is consistent with previous study (Feng et al., 2002). I propose that combined domains may act in synergy to mediate the transcriptional repression activity of hp66α.

Since hp66 proteins has been shown to be part of the NuRD complex, which harbor HDAC1 and HDAC2 (Feng et al., 2002; Le Guezennec et al., 2006), I tested hp66 paralogs mediated transcriptional repression in the presence of the HDAC-inhibitor TSA. As expected, inhibition of histone deacetylases by TSA relieves the transcriptional repression of both hp66 proteins, suggesting that one or both hp66 paralogs recruit a protein complex containing HDAC activity. By comparing hp66α with hp66β, no qualitative difference in TSA sensitivity was observed. In particular, the transcriptional repression activity of C-terminus of hp66α and N-terminus of hp66β are partially abolished in the presence of TSA, indicating that both major repression domains are at least partially acting of hp66 protein paralogs through histone deacetylation.

4.1.2 Functional interplay between MBD2 and hp66α

Previous data provided evidence that both hp66α and hp66β are interaction partners of MBD2,

and are capable of enhancing MBD2-mediated transcriptional repression (Brackertz et al., 2002; Brackertz et al., 2006; Feng et al., 2002). In this work, I identified a SUMOylation consensus site at position K149, but not SUMO modification site of hp66α, is within CR1, which is not present in hp66β. Further investigation revealed that the interaction between MBD2 with hp66α requires an intact site K149 amino acid within hp66α. The mutant hp66αK149R protein is unable to enhance MBD2-mediated transcriptional repression (see section 3.1.4). Furthermore, I observed that the mutant hp66αK149R fused to EGFP results in overall loss of the typical speckle pattern but rather displays a diffuse nuclear localization (see section 3.1.5), indicating that nuclear distribution of hp66α may depend on hp66-interaction with MBD2. Thus the interaction between MBD2 and hp66α is essential for both, the functional enhancement of MBD2-mediated transcriptional repression and the nuclear localization of hp66α. This interaction is dependent on the integrity of the specific site at K149 of hp66α. However, according to the experimental observation from MBD2 knockout MEF cells (Brackertz et al., 2006) and knockdown of endogenous MBD2 with RNAi (see section 3.1.4), it seems that MBD2 is not essential for the transcriptional repression by either hp66α or hp66β, and thus does not function as a downstream factor for hp66 paralogs-mediated transcriptional repression.

4.1.3 Concluding remarks and perspectives on transcriptional repression

Human p66α and p66β are two potent transcriptional repressors that interact with the MBD2 and MBD3. In the current work, hp66-mediated transcriptional repression is partially dependent on HDAC activity. Analysis of the molecular mechanisms mediating transcriptional repression resulted in the identification of two major repression domains in hp66α, and one in hp66β. Moreover, amino acid K149 of hp66α, which is a SUMO consensus site, is responsible for functional interaction with MBD2 (Fig.4.4). In contrast, MBD2 seems to be dispensable for hp66-mediated transcriptional repression. Future experiment should be addressed to the biological functions of hp66 for instance by creating a hp66 null mice. Can the Mi-2/NuRD complex be targeted to methylated DNA in hp66$^{-/-}$ mice? Is the MBD3- MBD2 interaction upregulated in hp66$^{-/-}$ mice? An attempt to identify target genes of hp66 proteins would be helpful, thereby to further investigate the subsequent consequences of hp66 action and strengthen the understanding on functions of hp66 proteins.

4.2 SUMO modification of both hp66α and hp66β

4.2.1 Both hp66α and hp66β are substrates for SUMO modification

Post-translational modification of transcription factors is a mechanism widely used to achieve regulation of gene expression. Over the past 10 years, SUMOylation has been shown to be a reversibly modification of many target proteins identified as regulators of gene expression including transcription factors, cofactors and regulators of the chromatin structure. Some of the target proteins by SUMO are shown in Fig.4.1.

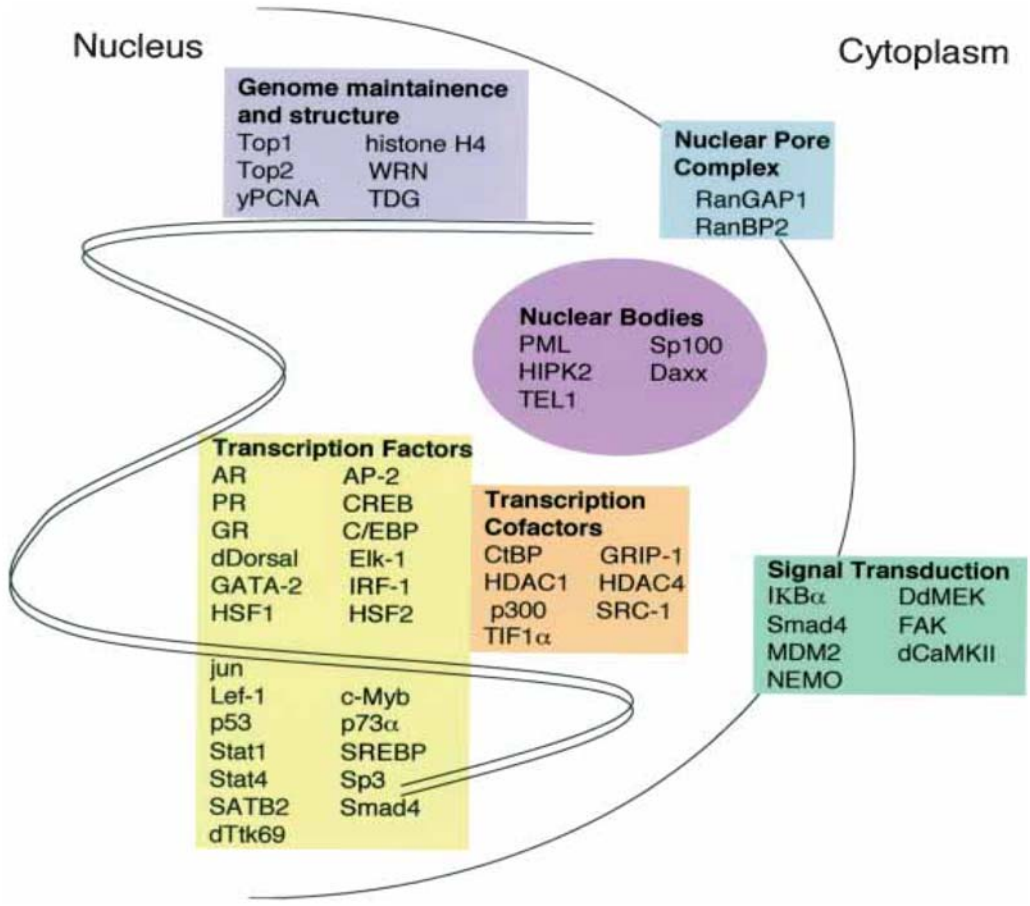

Fig.4.1 Some SUMO-modified substrates grouped by function/localization. Many SUMO-modified proteins function in regulation of transcription, chromatin structure, maintenance of the genome, and signal transduction. All proteins are of mammalian origin unless specifically indicated. (y) Yeast; (d) *Drosophila*; (Dd) *Dictyostelium.* Modified after (Gill, 2004).

In the present study, different lines of evidence support the idea that both hp66α and hp66β can be SUMOylated *in vivo*. On one hand, SUMO-modified hp66α or hp66β was detected when

FLAG-SUMO-1 and HA-Ubc9 was overexpressed. On the other hand, blocking the SUMOylation pathway with the SUMO mutant SUMO1G97A or with dominant negative Ubc9 (DN-Ubc9) prevents the generation of SUMOylated hp66α and hp66β. Detailed inspection and mutational analysis revealed another difference between hp66α and hp66β in respect to SUMOylation. For hp66α I identified two SUMO modification sites (K30 and K487). Mutation of either site reduced SUMOylation of hp66α to undetectable levels. This suggests that both sites synergize in SUMO modification. In contrast, hp66β harbors only a single SUMO modification site (K33). Despite the presence of two SUMO sites in hp66α and a single site in hp66β, migration of the SUMOylated wild type forms seems to be similar, suggesting that only a single site is modified at a time. Moreover, PIAS1, a E3 ligase, is able to enhance the efficiency of SUMO modification on target substrates *in vivo* (Jackson, 2001; Kahyo et al., 2001). In the case of hp66α, bi-SUMOylated form of hp66α is observed in the presence of PIAS1 protein, further suggesting two major SUMO modification sites in hp66α. However, in the case of hp66β, mono-SUMOylated form is occurring by co-expressing PIAS1 protein, strengthing the finding of only one major SUMO modification site in hp66β (see section 3.1.1). In conclusion, both hp66 protein paralogs are true substrates for SUMO modification.

4.2.2 The SUMO pathway directly regulates transcriptional repression activity of hp66 paralogs

SUMOylation of transcription factors has been reported to have different effects on transcriptional activity in diverse pathways. Emerging evidence indicates that SUMOylation negatively regulates the transcriptional activity of several transcriptional factors such as C-Myb, AR, Elk-1, Sp3 (Bies et al., 2002; Nishida and Yasuda, 2002; Ross et al., 2002; Sapetschnig et al., 2002; Yang et al., 2003; Yang and Sharrocks, 2004). In line with these data, overexpression of FLAG-SUMO-1 and HA-Ubc9 enhance the transcriptional repression activity of both hp66α or hp66β. Moreover, blocking the SUMOylation pathway with SUMO1G97A or with DN-Ubc9 impairs transcriptional repression of hp66 paralogs. In addition, mutations of the SUMO modification sites in hp66α and hp66β result in a reduction of transcriptional repression compared to wild type hp66α and hp66β. Taken together, the SUMO modification sites of

hp66α and hp66β are required for maximal repression. But, how does SUMO modification regulate the transcriptional repression of hp66α and hp66β. Based on our experimental observation, there are several possible mechanisms to explain how SUMO modification has such a large impact on both hp66 proteins-mediated transcriptional repression.

First, I and others demonstrated that SUMO-1 itself exhibits intrinsic transcriptional repressive properties (Ross et al., 2002; Yang et al., 2003). This finding raises the possibility that SUMO-1 conjugation of target proteins could mediate at least in parts of the transcriptional repression activity of target proteins. How this repression is achieved is unknown to this state. One mechanistical possibility is the recruitment of corepressors which contain SUMO-interacting motifs(Hecker et al., 2006; Song et al., 2004)**.**

Second, in some cases, a SUMOylation consensus motif is located within a repression domain. It was recently found that several unrelated proteins, for instance Elk-1 and Sp3, contain such an inhibitory domain responsible for the repressive function of the transcriptional factor (Sapetschnig et al., 2002; Yang et al., 2003). In addition, mutation of the critical lysine residue within a repression domain dramatically enhances the transcriptional activity of such proteins, indicating that SUMOylation is indeed involved in repression function. In this work, I demonstrated that the C-terminal region of hp66α and the N-terminal part of hp66β are major repression domain of hp66α and hp66β, respectively. Most importantly, K487, which is the major SUMO modification site of hp66α, is located within the C-terminal repression domain of hp66α, while K33, which is the major SUMO modification site of hp66β, is located within the N-terminal repression domain of hp66β. Moreover, mutation of both SUMO modification sites strongly abrogate the transcriptional repression compared to wild type p66α and p66β. Thus, I propose that SUMO modification may form complexes with Ubc9 and SUMO on repression domains and thereby creates scaffolds for the assembly of HDAC containing repression complexes, and thereby results in a repressive chromatin state.

Third, another model has been presented that might explain the transcriptional repression function of SUMO in a different way. This model proposes that SUMOylated transcription factors are targeted to the repressive environment of specific subnuclear domains, as documented for the promyelocztic leukemia (PML) nuclear body. PML itself as well as other components of the PML bodies are SUMOylated (Hay, 2005). SUMO conjugation of these

proteins is required for recruitment of HDAC1 or heterochromatin protein 1 into the nuclear bodies (Ishov et al., 1999; Lallemand-Breitenbach et al., 2001; Zhong et al., 2000). In addition, SUMOylation or inhibition of SUMO conjugation results in a redistribution of nuclear components within the nucleus. All these findings demonstrated that localization of such target proteins to nuclear bodies by SUMO modification lead to create a local repressive environment within nuclear bodies. This type of SUMO function does not seem to play a role in the context of hp66 proteins. hp66 colocalizes with MBD2 and MBD3 in nuclear speckles (Brackertz et al., 2002; Feng et al., 2002), that are clearly different from PML bodies and that are found at replication foci (Tatematsu et al., 2000). Furthermore, mutation of the SUMO modification sites in hp66α or hp66β does not lead to a redistribution in comparison to wild type hp66.

Fourth, additional mechanism for SUMO function is exemplified by p300 and by Elk-1. In both cases SUMOylation allows HDAC binding and mediates transcriptional repression by histone deacetylation (Girdwood et al., 2003; Yang et al., 2003). Recently, lines of evidence revealed that HDACs play an essential role in SUMOylation-mediated transcriptional repression (Gill, 2005). It has been reported that HDACs are able to enhance the efficiency of SUMO modification of some substrates. Furthermore, several HDACs have been reported to be substrates for SUMOylation. SUMO-modification of HDAC1 is found to increase both deacetylase activity and transcriptional repression activity (Cheng et al., 2004; David et al., 2002). This is reminiscent of the situation I find with hp66. Mutation of the SUMO modification site (K30) abolishes the interaction between HDAC1 and hp66α, and leads to a loss of TSA sensitivity. This suggests that SUMOylation of this site is required for the interaction. In the case of hp66β, I observed that mutation of the N-terminal SUMO modification site (hp66βK33) abolishes the interaction between hp66β and RbAp46, which is also a component of the Mi-2/NuRD complex. This mutation lead to TSA insensitivity probably caused by the loss of RbAp46 binding, which itself may be bound to HDACs. It is well known that lysine residues can be modified by acetylation and SUMOylation. Thus, I assumed that enzymatic removal of acetyl groups on SUMO modification sites by HDAC1 could increase susceptibility of target consensus lysine for SUMO modification. In addition, previous study showed that both hp66 paralogs interact with hitone tails, whereas acetylation of histone tails by the histone acetyltransferases p300 or PCAF abrogates the association with the hp66 proteins (Brackertz et al., 2006). Taken together, these findings suggest that SUMO-

modified hp66 proteins repress transcription by recruitment of HDACs. The consequence are the efficiency of SUMO modification and the deacetylation of core histones, which in turn create a transcriptional repressive chromatin environment and allow the assembly a stable Mi-2/NuRD complex. In conclusion, crosstalk between deacetylation and SUMOylation might be important for regulation of gene expression (Fig.4.2).

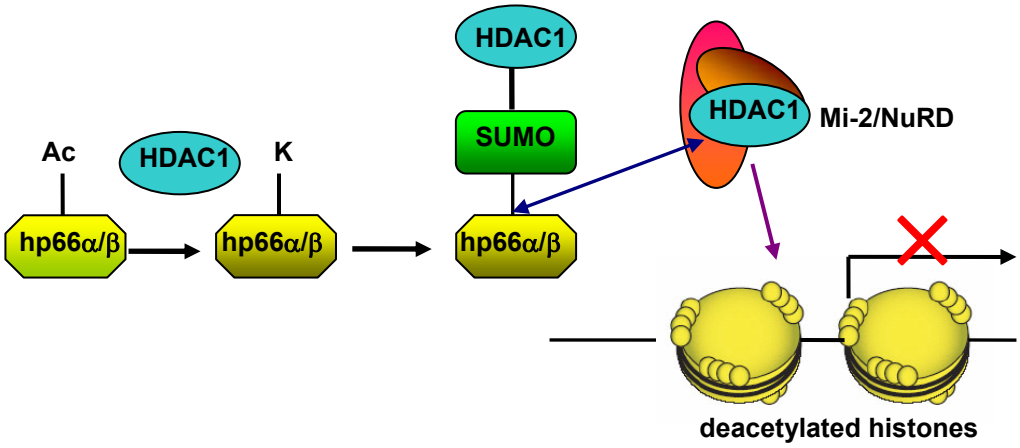

Fig.4.2 Functional interplay between SUMO and HDACs in hp66-mediated transcriptional repression. See text for details.

Although, the above explanations have been proposed for SUMO-mediated transcriptional repression of hp66 proteins, I clearly realized two apparently conflicting observations during SUMO-mediated transcriptional repression, that was recently termed as “SUMO enigma”. This finding describes that in most systems analyzed the proportion of a particular protein found to be SUMOylated is rather small. Indeed, only a small proportion of hp66 proteins appears to be modified by SUMO at the steady state. However, under these conditions SUMO modification is required for maximal repression of hp66 paralogs and mutation of the target lysine residues used for SUMO modification relieves transcriptional repression. A plausible model that accommodates these observations is depicted in Fig.4.3. In this model newly synthesized hp66 paralogs are rapidly SUMOylated and incorporated into a Mi-2/NuRD repression complex in a SUMO-dependent manner. The SUMO peptide could be removed in the presence of constitutively active SUMO specific proteases, but hp66 proteins are retained in the Mi-2/NuRD repression complex in a SUMO-independent manner. Under normal circumstances a relatively slow dissociation of the stable repression complex could release sufficient quantities

of unmodified hp66 proteins to allow basal transcription. Thus, in this model, SUMO is required for the initiation of transcriptional repression, but not for the maintenance of transcriptional repression. Colocalization of enzymes implicated in SUMO conjugation and deconjugation within the cell nucleus (Zhang et al., 2002), suggesting that SUMO modification is a highly dynamic process with substrates undergoing rapid SUMO modification followed by equally rapid deconjugation.

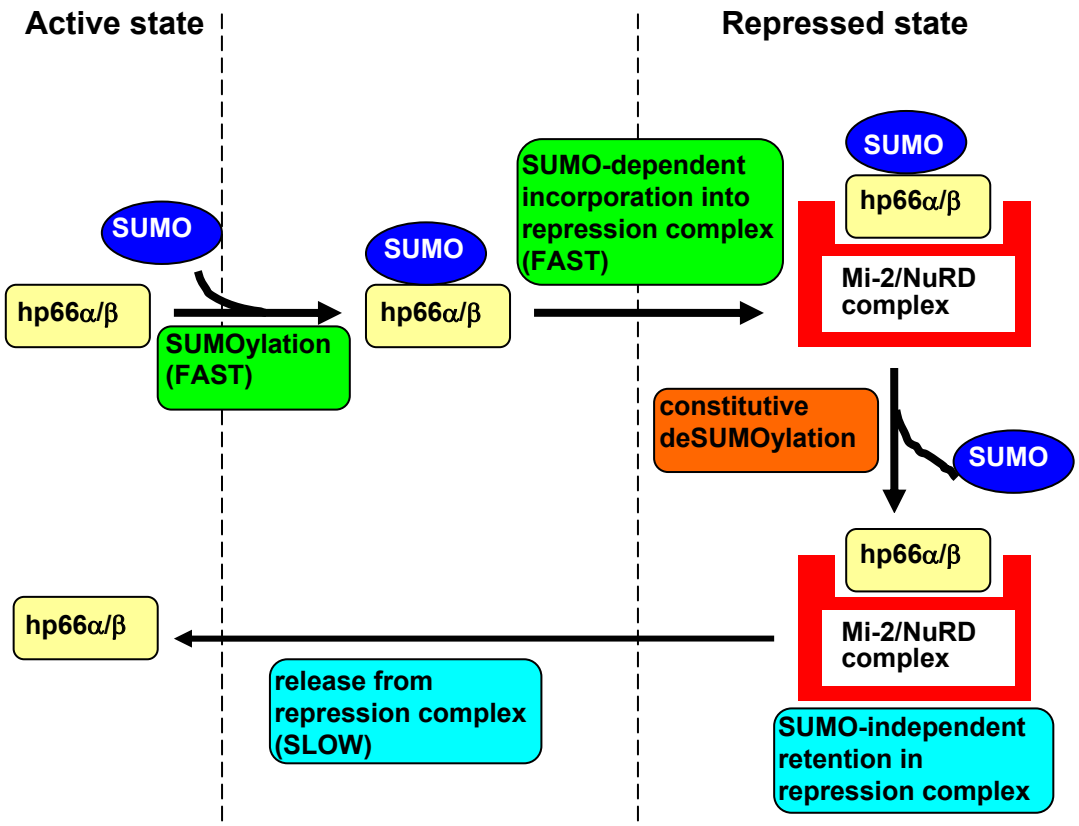

Fig.4.3 Model for transcriptional repression of hp66 proteins by SUMO modification. See text for details. Modified after (Girdwood et al., 2004).

A possible mechanism which explains that SUMO-modified hp66 paralogs incorporate into Mi-2/NuRD repression complex is that SUMO-modified hp66 proteins may recruit chaperonins such as HDAC1 or RbAp46 that assemble the modified hp66 proteins into a stable Mi-2/NuRD complex. Once formed, SUMO can be removed, leaving the once modified hp66 proteins retained with the repressed state in the Mi-2/NuRD repression complex. This model is also consistent with experimental observations where expression of SUMO1G97A mutant or dominant negative Ubc9 relieves SUMO-mediated transcriptional repression of hp66 proteins.

Moreover, mutation of SUMO acceptor lysines of p66 paralogs also results in reduction of SUMO-dependent transcriptional repression of hp66 proteins. These observations revealed that the initial SUMO modification of hp66 proteins would be blocked by SUMO1 mutant, catalytically inactive Ubc9 mutation or by mutation of the target lysine residues of hp66 proteins. As a consequence, hp66 proteins could not be incorporated into Mi-2/NuRD repression complex and would thus fail to be transcriptionally repressed. It has been shown that SUMO modification of transcription factors have diverse functional consequences and can both activate and repress transcripton. This model could fit to many different situations. Thus, SUMO modification of transcription factors could recruit chaperonins to assembly or disassembly a wide variety of multiprotein complexes, which in turn switch transcription factors between different states to regulate transcription. If SUMOylation is indeed only required during a transient phase of complex formation, the amount of protein that needs to be modified at any given time point would then only be a small fraction of the total amount of this protein present in the cell.

4.2.3 Concluding remarks and perspectives on SUMOylation

In the current work, I provided evidence that both hp66α and hp66β are modified by SUMO *in vivo*, hp66α at two sites (K30 and K487) and hp66β at one site (K33). The Mi-2/NuRD components MBD3, RbAp46, RbAp48 and HDAC1 were found to bind to both hp66α and hp66β *in vivo*. Most of the interactions were not affected by the SUMO site mutations in hp66α or hp66β, with two exceptions. HDAC1 binding to hp66α was lost in the case of a hp66αK30R mutant and RbAp46 binding was reduced in the case of a hp66βK33R mutant (Fig.4.4). These results suggest that interactions within the Mi-2/NuRD complex as well as optimal repression are mediated by SUMOylation. SUMO modification is a dynamic, reversible process, which might explain that only a small proportion of modified proteins can be detected under physiological conditions. It is also possible that the *bona fide* effects of SUMO modification is different from what is found with an overexpression system. Analyzing the stable cell lines which stably integrated mutants impaired in SUMOylation of hp66 proteins, or transgenic mice, which express these mutants, will likely provide more findings considering the function of endogenous hp66 proteins, for instance, interactions with associated proteins such as HDAC1,

and the effect of SUMO-modified hp66 proteins in living animals. Since SUMO modification of hp66 proteins is implicated in recruitment of the NuRD complex through interaction with HDAC1 or RbAp46, it would be also worth to try whether SUMO modification of hp66 proteins could alter the protein composition of the Mi-2/NuRD complex. Moreover, it is also interesting to know whether a knockdown of components of the NuRD complex could influence the function of SUMO-modified hp66 proteins.

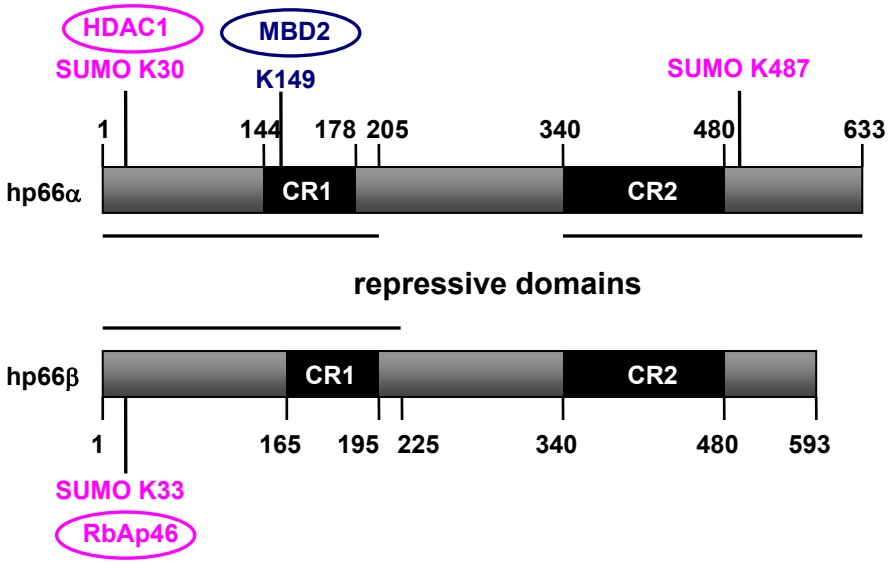

Fig.4.4 The major repression domains, relevant amino acid positions, and SUMO modification sites of hp66α and hp66β. SUMO modification sites affecting interaction with HDAC1 and RbAp46, as well as the CR1 and CR2 regions that are conserved between different species (Brackertz et al., 2002; Feng et al., 2002), are indicated.

4.3 Complex formation of hp66α and hp66β

4.3.1 hp66α/NuRD complex and hp66β/NuRD complex: distinct or same?

The vertebrate Mi-2/NuRD complex is a multisubunit complex containing nucleosome remodeling and histone deacetylase activity (Tong et al., 1998; Tyler and Kadonaga, 1999; Wade et al., 1998; Xue et al., 1998; Zhang et al., 1998). The histone deacetylases HDAC1 and HDAC2 and the histone-binding proteins RbAp46 and RbAp48 form a core complex which is shared between the Mi-2/NuRD complex and the Sin3-histone deacetylase complex (Guschin et al., 2000; Le Guezennec et al., 2006; Yao and Yang, 2003). It has been reported that Mi-2, MTA1/2 and MBD3 are present in the Mi-2/NuRD complex. Although MBD3 is not able to

recognize the methylated DNA, the Mi-2/NuRD complex can be targeted to methylated DNA through an interaction with MBD2. Thus, the Mi-2/NuRD complex associated with MBD2 form the so-called "MeCP1 complex", which provides an important link between DNA methylation and histone deacetylation (Feng et al., 2002; Feng and Zhang, 2001). It has been described that the MeCP1 complex contains 10 major polypeptides including MBD2, all seven subunits of Mi-2/NuRD complex, and possibly hp66β (p66/p68) (Fig.4.5). I also identified a novel protein, hp66α, which is highly related to hp66β. A recent study clearly demonstrated that hp66α and hp66β are components of the MBD2/NuRD complex and the MBD3/NuRD complex (Le Guezennec et al., 2006). In fact, it seems that different known subunit may form unique complexes.

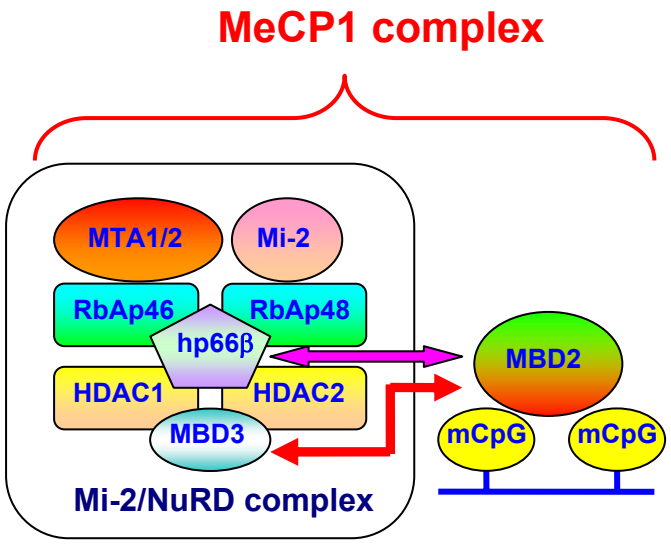

Fig.4.5 Model of the MeCP1-NuRD complex. The complex consists of the indicated proteins. Recruitment of the MeCP1-NuRD complex to CpG-methylated DNA occurs via interaction of the NuRD complex with MBD2, mediated by direct binding of MBD3 or hp66β.

Both hp66α and hp66β proteins are highly related, and have similar properties and exert similar functions. In addition, previous data and results presumed in this work revealed that both hp66 proteins are involved in distinct molecular functions. It has been shown that several subunits of the Mi-2/NuRD complex are found in pairs, nevertheless, these duplicated subunits form different complexes. Since hp66α and hp66β are highly related, I further investigated whether both hp66 proteins are within the same complex or form distinct complexes. To purify the hp66 proteins containing complexes, stable cell lines expressing hp66 proteins were established. The

cell extract was precleared with ion-exchange chromatography, and those fractions containing FLAG-hp66 proteins were eluted mainly at estimated 0.4-0.5M KCl. To determine the size of both hp66 proteins containing complexes, the pooled fraction were passed through gel filtration chromatography. Interestingly, the results revealed two different molecular mass on both hp66 complexes, 1.8MDa and 600-700KDa, respectively, indicating that both hp66 proteins may form distinct complexes with different compositions. As expected, the known subunits of the Mi-2/NuRD complex as well as Sin3A are associated with hp66 proteins, suggesting that these proteins may be components of hp66 proteins complexes. However, the data also demonstrate that there is no significant difference between the high molecular weight and the low molecular weight fractions containing hp66 proteins. I assumed that there are additional subunits in the high molecular weight complex. Further purification with FLAG M2 beads revealed that the known components of the Mi-2/NuRD complex as well as MBD2 and PRMT5 are associated with hp66 proteins on both beads and elution fraction with FLAG peptide. Although MBD2 is not associated with the fractions from gel filtration chromatography, I argue that the amount of MBD2 may not be sufficient for detection by Western blotting. It is also interesting that PRMT5 was previously identified as a component of the MBD2/NuRD complex, but not of the MBD3/NuRD complex, which is retained with hp66 proteins, indicating that PRMT5 may be one of unknown subunit of the hp66 complexes. In contrast, Sin3A, which is a subunit of the Sin3A/HDAC complex, coelutes with FLAG-hp66 proteins after gel filtration chromatography. However, Sin3A is not retained with hp66 proteins after purification with FLAG beads, indicating that Sin3A is not a component of the hp66 proteins complexes. Taken together, so far, our results from the initial protein complex purifications suggest that both hp66α and hp66β may form similar complexes, these are probably not be mutually exclusive. In other words, both hp66α and hp66β may be within the same complex.

4.3.2 Concluding remarks and perspectives on complex formation

A number of evidence have revealed that different components of the Mi-2/NuRD complex may constitute specific Mi-2/NuRD complex. Our results summarized here leads us to propose a new model of the Mi-2/NuRD complex, which further uncovers the link between DNA methylation and transcriptional repression. Recent evidence clearly showed that MBD2 and MBD3 form distinct complex, that the MBD2/NuRD complex contains additionally PRMT5,

and the MBD2/NuRD complex and the MBD3/NuRD complex are mutally exclusive (Fig.4.6). Based on our observation, the MBD2-NuRD complex is recruited to CpG methylated DNA through interaction with MBD2, achieved by hp66α/hp66β-MBD2 and PRMT5-MBD2 interaction, whereas the MBD3-NuRD complex is targeted to methyl-CpG sites via interaction with MBD2, mediated by two different interactions: MBD3-MBD2 and hp66α/hp66β-MBD2. There is another possible mechanism that MBD3/NuRD complex can be recruited to unmethylated DNA by transcription factors such as CTIP2, FOG-1 (Hong et al., 2005; Topark-Ngarm et al., 2006). The different enzymatic activities may act synergistically to regulate transcriptional repression within the hp66-NuRD complex: deacetylation of nucleosomes by HDAC1/HDAC2 surrounding the target gene in combination with chromatin remodeling activity by the ATPase Mi-2, or the addition of transcriptional repressive arginine methyl marks in the histone H3 and H4 tails by the associated PRMT5 (Pal et al., 2004), which in turn leads to closed chromatin structure and gene silencing. As described to date, both hp66α and hp66β may be within the same complex containing HDAC1/HDAC2, MBD2/MBD3, RbAp46/RbAp48, hp66α/hp66β, Mi-2 and PRMT5, which may in fact be the mixture of the hp66-MBD2-NuRD complex and the hp66-MBD3-NuRD complex.

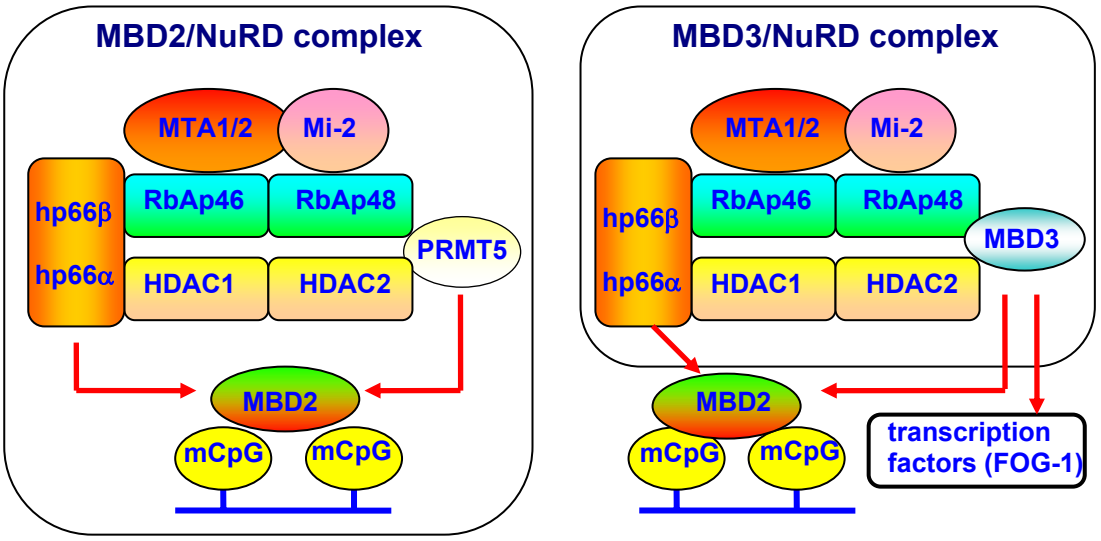

Fig.4.6 Model of the hp66-MBD2-NuRD and the hp66-MBD3-NuRD complexws. The complex consists of the indicated proteins. Recruitment of the hp66-MBD2-NuRD complex to CpG-methylated DNA occurs via interaction of the NuRD complex with MBD2 mediated by direct binding of hp66 paralogs or PRMT5, whereas recruitment of the hp66-MBD3-NuRD complex to CpG-methylated DNA mediated by direct binding of MBD3, or hp66 paralogs with MBD2. MBD3/NuRD complex can also be recruited to unmethylated DNA by transcription factors such as FOG-1.

Nevertheless, the story of complex purification is not sufficient to draw a conclusion. Since a high molecular weight complex is observed, I assumed that there are additional components which are not identified within the hp66-NuRD complex to date. The future experiment is to identify these unknown subunits with mass spectrometry, and these results will further reveal the complete hp66-NuRD complex.

5 REFERENCE

Amir, R. E., Van den Veyver, I. B., Wan, M., Tran, C. Q., Francke, U., and Zoghbi, H. Y. (1999). Rett syndrome is caused by mutations in X-linked MECP2, encoding methyl-CpG-binding protein 2. Nat Genet *23*, 185-188.

Archer, H. L., Whatley, S. D., Evans, J. C., Ravine, D., Huppke, P., Kerr, A., Bunyan, D., Kerr, B., Sweeney, E., Davies, S. J., *et al.* (2006). Gross rearrangements of the MECP2 gene are found in both classical and atypical Rett syndrome patients. J Med Genet *43*, 451-456.

Ausubel, F. M., R.Brent, R.E.Kingston, D.D.Moore, G.Seidman, J.A.Smith and K.Struhl. (1989). Current protocols in molecular biology).

Azuma, Y., Arnaoutov, A., and Dasso, M. (2003). SUMO-2/3 regulates topoisomerase II in mitosis. J Cell Biol *163*, 477-487.

Bachant, J., Alcasabas, A., Blat, Y., Kleckner, N., and Elledge, S. J. (2002). The SUMO-1 isopeptidase Smt4 is linked to centromeric cohesion through SUMO-1 modification of DNA topoisomerase II. Mol Cell *9*, 1169-1182.

Bai, S., Ghoshal, K., Datta, J., Majumder, S., Yoon, S. O., and Jacob, S. T. (2005). DNA methyltransferase 3b regulates nerve growth factor-induced differentiation of PC12 cells by recruiting histone deacetylase 2. Mol Cell Biol *25*, 751-766.

Bailey, D., and O'Hare, P. (2004). Characterization of the localization and proteolytic activity of the SUMO-specific protease, SENP1. J Biol Chem *279*, 692-703.

Baldwin, A. S., Jr. (1996). The NF-kappa B and I kappa B proteins: new discoveries and insights. Annu Rev Immunol *14*, 649-683.

Ballestar, E., and Wolffe, A. P. (2001). Methyl-CpG-binding proteins. Targeting specific gene repression. Eur J Biochem *268*, 1-6.

Bellacosa, A., Cicchillitti, L., Schepis, F., Riccio, A., Yeung, A. T., Matsumoto, Y., Golemis, E. A., Genuardi, M., and Neri, G. (1999). MED1, a novel human methyl-CpG-binding endonuclease, interacts with DNA mismatch repair protein MLH1. Proc Natl Acad Sci U S A *96*, 3969-3974.

Bernier-Villamor, V., Sampson, D. A., Matunis, M. J., and Lima, C. D. (2002). Structural basis for E2-mediated SUMO conjugation revealed by a complex between ubiquitin-conjugating enzyme Ubc9 and RanGAP1. Cell *108*, 345-356.

Best, J. L., Ganiatsas, S., Agarwal, S., Changou, A., Salomoni, P., Shirihai, O., Meluh, P. B., Pandolfi, P. P., and Zon, L. I. (2002). SUMO-1 protease-1 regulates gene transcription through PML. Mol Cell *10*, 843-855.

Bestor, T. H. (2000). The DNA methyltransferases of mammals. Hum Mol Genet *9*, 2395-2402.

Bhattacharya, S. K., Ramchandani, S., Cervoni, N., and Szyf, M. (1999). A mammalian protein with specific demethylase activity for mCpG DNA. Nature *397*, 579-583.

Bienvenu, T., and Chelly, J. (2006). Molecular genetics of Rett syndrome: when DNA methylation goes unrecognized. Nat Rev Genet *7*, 415-426.

Bies, J., Markus, J., and Wolff, L. (2002). Covalent attachment of the SUMO-1 protein to the negative regulatory domain of the c-Myb transcription factor modifies its stability and transactivation capacity. J Biol Chem *277*, 8999-9009.

Bird, A. (2002). DNA methylation patterns and epigenetic memory. Genes Dev *16*, 6-21.

Bird, A. P., and Wolffe, A. P. (1999). Methylation-induced repression--belts, braces, and chromatin. Cell *99*, 451-454.

Birnboim, H. C., and Doly, J. (1979). A rapid alkaline extraction procedure for screening recombinant plasmid DNA. Nucleic Acids Res *7*, 1513-1523.

Boeke, J., Ammerpohl, O., Kegel, S., Moehren, U., and Renkawitz, R. (2000). The minimal repression domain of MBD2b overlaps with the methyl-CpG-binding domain and binds directly to Sin3A. J Biol Chem *275*, 34963-34967.

Bohren, K. M., Nadkarni, V., Song, J. H., Gabbay, K. H., and Owerbach, D. (2004). A M55V polymorphism in a novel SUMO gene (SUMO-4) differentially activates heat shock transcription factors and is associated with susceptibility to type I diabetes mellitus. J Biol Chem *279*, 27233-27238.

Bossis, G., Malnou, C. E., Farras, R., Andermarcher, E., Hipskind, R., Rodriguez, M., Schmidt, D., Muller, S., Jariel-Encontre, I., and Piechaczyk, M. (2005). Down-regulation of c-Fos/c-Jun AP-1 dimer activity by sumoylation. Mol Cell Biol *25*, 6964-6979.

Bossis, G., and Melchior, F. (2006). SUMO: regulating the regulator. Cell Div *1*, 13.

Bouras, T., Fu, M., Sauve, A. A., Wang, F., Quong, A. A., Perkins, N. D., Hay, R. T., Gu, W., and Pestell, R. G. (2005). SIRT1 deacetylation and repression of p300 involves lysine residues 1020/1024 within the cell cycle regulatory domain 1. J Biol Chem *280*, 10264-10276.

Bowen, N. J., Fujita, N., Kajita, M., and Wade, P. A. (2004). Mi-2/NuRD: multiple complexes for many purposes. Biochim Biophys Acta *1677*, 52-57.

Brackertz, M., Boeke, J., Zhang, R., and Renkawitz, R. (2002). Two highly related p66 proteins comprise a new family of potent transcriptional repressors interacting with MBD2 and MBD3. J Biol Chem *277*, 40958-40966.

Brackertz, M., Gong, Z., Leers, J., and Renkawitz, R. (2006). p66alpha and p66beta of the Mi-2/NuRD complex mediate MBD2 and histone interaction. Nucleic Acids Res *34*, 397-406.

Bradford, M. M. (1976). A rapid and sensitive method for the quantitation of microgram quantities of protein utilizing the principle of protein-dye binding. Anal Biochem *72*, 248-254.

Brenner, C., Deplus, R., Didelot, C., Loriot, A., Vire, E., De Smet, C., Gutierrez, A., Danovi, D., Bernard, D., Boon, T., *et al.* (2005). Myc represses transcription through recruitment of DNA methyltransferase corepressor. Embo J *24*, 336-346.

Chandler, S. P., Guschin, D., Landsberger, N., and Wolffe, A. P. (1999). The methyl-CpG binding transcriptional repressor MeCP2 stably associates with nucleosomal DNA. Biochemistry *38*, 7008-7018.

Chen, R. Z., Akbarian, S., Tudor, M., and Jaenisch, R. (2001). Deficiency of methyl-CpG binding protein-2 in CNS neurons results in a Rett-like phenotype in mice. Nat Genet *27*, 327-331.

Cheng, J., Wang, D., Wang, Z., and Yeh, E. T. (2004). SENP1 enhances androgen receptor-dependent transcription through desumoylation of histone deacetylase 1. Mol Cell Biol *24*, 6021-6028.

Choi, C. Y., Kim, Y. H., Kwon, H. J., and Kim, Y. (1999). The homeodomain protein NK-3 recruits Groucho and a histone deacetylase complex to repress transcription. J Biol Chem *274*, 33194-33197.

Chung, C. D., Liao, J., Liu, B., Rao, X., Jay, P., Berta, P., and Shuai, K. (1997). Specific inhibition of Stat3 signal transduction by PIAS3. Science *278*, 1803-1805.

Collins, T., Stone, J. R., and Williams, A. J. (2001). All in the family: the BTB/POZ, KRAB, and SCAN domains. Mol Cell Biol *21*, 3609-3615.

Comerford, K. M., Leonard, M. O., Karhausen, J., Carey, R., Colgan, S. P., and Taylor, C. T. (2003). Small ubiquitin-related modifier-1 modification mediates resolution of CREB-dependent responses to hypoxia. Proc Natl Acad Sci U S A *100*, 986-991.

Cross, S. H., Meehan, R. R., Nan, X., and Bird, A. (1997). A component of the transcriptional repressor MeCP1 shares a motif with DNA methyltransferase and HRX proteins. Nat Genet *16*, 256-259.

Daniel, J. M., Spring, C. M., Crawford, H. C., Reynolds, A. B., and Baig, A. (2002). The p120(ctn)-binding partner Kaiso is a bi-modal DNA-binding protein that recognizes both a sequence-specific consensus and methylated CpG dinucleotides. Nucleic Acids Res *30*, 2911-2919.

David, G., Neptune, M. A., and DePinho, R. A. (2002). SUMO-1 modification of histone deacetylase 1 (HDAC1) modulates its biological activities. J Biol Chem *277*, 23658-23663.

Del Sal, G., Manfioletti, G., and Schneider, C. (1989). The CTAB-DNA precipitation method: a common mini-scale preparation of template DNA from phagemids, phages or plasmids suitable for sequencing. Biotechniques *7*, 514-520.

Desterro, J. M., Rodriguez, M. S., and Hay, R. T. (1998). SUMO-1 modification of IkappaBalpha inhibits NF-kappaB activation. Mol Cell *2*, 233-239.

Desterro, J. M., Rodriguez, M. S., Kemp, G. D., and Hay, R. T. (1999). Identification of the enzyme required for activation of the small ubiquitin-like protein SUMO-1. J Biol Chem *274*, 10618-10624.

Dohmen, R. J. (2004). SUMO protein modification. Biochim Biophys Acta *1695*, 113-131.

Duprez, E., Saurin, A. J., Desterro, J. M., Lallemand-Breitenbach, V., Howe, K., Boddy, M. N., Solomon, E., de The, H., Hay, R. T., and Freemont, P. S. (1999). SUMO-1 modification of the acute promyelocytic leukaemia protein PML: implications for nuclear localisation. J Cell Sci *112 (Pt 3)*, 381-393.

Eaton, E. M., and Sealy, L. (2003). Modification of CCAAT/enhancer-binding protein-beta by the small ubiquitin-like modifier (SUMO) family members, SUMO-2 and SUMO-3. J Biol Chem *278*, 33416-33421.

Eisen, J. A., Sweder, K. S., and Hanawalt, P. C. (1995). Evolution of the SNF2 family of proteins: subfamilies with distinct sequences and functions. Nucleic Acids Res *23*, 2715-2723.

Eloranta, J. J., and Hurst, H. C. (2002). Transcription factor AP-2 interacts with the SUMO-conjugating enzyme UBC9 and is sumolated in vivo. J Biol Chem *277*, 30798-30804.

Feinberg, A. P., and Tycko, B. (2004). The history of cancer epigenetics. Nat Rev Cancer *4*, 143-153.

Feng, Q., Cao, R., Xia, L., Erdjument-Bromage, H., Tempst, P., and Zhang, Y. (2002). Identification and functional characterization of the p66/p68 components of the MeCP1 complex. Mol Cell Biol *22*, 536-546.

Feng, Q., and Zhang, Y. (2001). The MeCP1 complex represses transcription through preferential binding, remodeling, and deacetylating methylated nucleosomes. Genes Dev *15*, 827-832.

Fujita, H., Fujii, R., Aratani, S., Amano, T., Fukamizu, A., and Nakajima, T. (2003). Antithetic effects of MBD2a on gene regulation. Mol Cell Biol *23*, 2645-2657.

Fujita, N., Jaye, D. L., Kajita, M., Geigerman, C., Moreno, C. S., and Wade, P. A. (2003). MTA3, a Mi-2/NuRD complex subunit, regulates an invasive growth pathway in breast cancer. Cell *113*, 207-219.

Fujita, N., Shimotake, N., Ohki, I., Chiba, T., Saya, H., Shirakawa, M., and Nakao, M. (2000). Mechanism of transcriptional regulation by methyl-CpG binding protein MBD1. Mol Cell Biol *20*, 5107-5118.

Fujita, N., Takebayashi, S., Okumura, K., Kudo, S., Chiba, T., Saya, H., and Nakao, M. (1999). Methylation-mediated transcriptional silencing in euchromatin by methyl-CpG binding protein MBD1 isoforms. Mol Cell Biol *19*, 6415-6426.

Fuks, F., Burgers, W. A., Brehm, A., Hughes-Davies, L., and Kouzarides, T. (2000). DNA methyltransferase Dnmt1 associates with histone deacetylase activity. Nat Genet *24*, 88-91.

Fuks, F., Burgers, W. A., Godin, N., Kasai, M., and Kouzarides, T. (2001). Dnmt3a binds deacetylases and is recruited by a sequence-specific repressor to silence transcription. Embo J *20*, 2536-2544.

Fuks, F., Hurd, P. J., Deplus, R., and Kouzarides, T. (2003). The DNA methyltransferases associate with HP1 and the SUV39H1 histone methyltransferase. Nucleic Acids Res *31*, 2305-2312.

Fuks, F., Hurd, P. J., Wolf, D., Nan, X., Bird, A. P., and Kouzarides, T. (2003). The methyl-CpG-binding protein MeCP2 links DNA methylation to histone methylation. J Biol Chem *278*, 4035-4040.

Gavin, A. C., Bosche, M., Krause, R., Grandi, P., Marzioch, M., Bauer, A., Schultz, J., Rick, J. M., Michon, A. M., Cruciat, C. M., *et al.* (2002). Functional organization of the yeast proteome by systematic analysis of protein complexes. Nature *415*, 141-147.

Ge, Q., Nilasena, D. S., O'Brien, C. A., Frank, M. B., and Targoff, I. N. (1995). Molecular analysis of a major antigenic region of the 240-kD protein of Mi-2 autoantigen. J Clin Invest *96*, 1730-1737.

Geiman, T. M., Sankpal, U. T., Robertson, A. K., Zhao, Y., and Robertson, K. D. (2004). DNMT3B interacts with hSNF2H chromatin remodeling enzyme, HDACs 1 and 2, and components of the histone methylation system. Biochem Biophys Res Commun *318*, 544-555.

Gill, G. (2004). SUMO and ubiquitin in the nucleus: different functions, similar mechanisms? Genes Dev *18*, 2046-2059.

Gill, G. (2005). Something about SUMO inhibits transcription. Curr Opin Genet Dev *15*, 536-541.

Girdwood, D., Bumpass, D., Vaughan, O. A., Thain, A., Anderson, L. A., Snowden, A. W., Garcia-Wilson, E., Perkins, N. D., and Hay, R. T. (2003). P300 transcriptional repression is mediated by SUMO modification. Mol Cell *11*, 1043-1054.

Girdwood, D. W., Tatham, M. H., and Hay, R. T. (2004). SUMO and transcriptional regulation. Semin Cell Dev Biol *15*, 201-210.

Gomez-del Arco, P., Koipally, J., and Georgopoulos, K. (2005). Ikaros SUMOylation: switching out of repression. Mol Cell Biol *25*, 2688-2697.

Gong, L., Li, B., Millas, S., and Yeh, E. T. (1999). Molecular cloning and characterization of human AOS1 and UBA2, components of the sentrin-activating enzyme complex. FEBS Lett *448*, 185-189.

Gong, L., Millas, S., Maul, G. G., and Yeh, E. T. (2000). Differential regulation of sentrinized proteins by a novel sentrin-specific protease. J Biol Chem *275*, 3355-3359.

Gong, L., and Yeh, E. T. (2006). Characterization of a family of nucleolar SUMO-specific proteases with preference for SUMO-2 or SUMO-3. J Biol Chem *281*, 15869-15877.

Gong, Z., Brackertz, M., and Renkawitz, R. (2006). SUMO modification enhances p66-mediated transcriptional repression of the Mi-2/NuRD complex. Mol Cell Biol *26*, 4519-4528.

Goodson, M. L., Hong, Y., Rogers, R., Matunis, M. J., Park-Sarge, O. K., and Sarge, K. D. (2001). Sumo-1 modification regulates the DNA binding activity of heat shock transcription factor 2, a promyelocytic leukemia nuclear body associated transcription factor. J Biol Chem *276*, 18513-18518.

Gregoire, S., Tremblay, A. M., Xiao, L., Yang, Q., Ma, K., Nie, J., Mao, Z., Wu, Z., Giguere, V., and Yang, X. J. (2006). Control of MEF2 transcriptional activity by coordinated phosphorylation and sumoylation. J Biol Chem *281*, 4423-4433.

Guschin, D., Wade, P. A., Kikyo, N., and Wolffe, A. P. (2000). ATP-Dependent histone octamer mobilization and histone deacetylation mediated by the Mi-2 chromatin remodeling complex. Biochemistry *39*, 5238-5245.

Guy, J., Hendrich, B., Holmes, M., Martin, J. E., and Bird, A. (2001). A mouse Mecp2-null mutation causes neurological symptoms that mimic Rett syndrome. Nat Genet *27*, 322-326.

Hanahan, D. (1983). Studies on transformation of Escherichia coli with plasmids. J Mol Biol *166*, 557-580.

Hang, J., and Dasso, M. (2002). Association of the human SUMO-1 protease SENP2 with the nuclear pore. J Biol Chem *277*, 19961-19966.

Hardeland, U., Steinacher, R., Jiricny, J., and Schar, P. (2002). Modification of the human thymine-DNA glycosylase by ubiquitin-like proteins facilitates enzymatic turnover. Embo J *21*, 1456-1464.

Hay, R. T. (2005). SUMO: a history of modification. Mol Cell *18*, 1-12.

Hay, R. T. (2005). SUMO: a history of modification. *18*, 1-12.

Hecker, C. M., Rabiller, M., Haglund, K., Bayer, P., and Dikic, I. (2006). Specification of SUMO1- and SUMO2-interacting motifs. J Biol Chem *281*, 16117-16127.

Hendrich, B., Abbott, C., McQueen, H., Chambers, D., Cross, S., and Bird, A. (1999). Genomic structure and chromosomal mapping of the murine and human Mbd1, Mbd2, Mbd3, and Mbd4 genes. Mamm Genome *10*, 906-912.

Hendrich, B., and Bird, A. (1998). Identification and characterization of a family of mammalian methyl-CpG binding proteins. Mol Cell Biol *18*, 6538-6547.

Hendrich, B., Guy, J., Ramsahoye, B., Wilson, V. A., and Bird, A. (2001). Closely related proteins MBD2 and MBD3 play distinctive but interacting roles in mouse development. Genes Dev *15*, 710-723.

Hendrich, B., Hardeland, U., Ng, H. H., Jiricny, J., and Bird, A. (1999). The thymine glycosylase MBD4 can bind to the product of deamination at methylated CpG sites. Nature *401*, 301-304.

Hendrich, B., and Tweedie, S. (2003). The methyl-CpG binding domain and the evolving role of DNA methylation in animals. Trends Genet *19*, 269-277.

Herman, J. G., and Baylin, S. B. (2003). Gene silencing in cancer in association with promoter hypermethylation. N Engl J Med *349*, 2042-2054.

Hershko, A., and Ciechanover, A. (1998). The ubiquitin system. Annu Rev Biochem *67*, 425-479.

Hochstrasser, M. (1996). Ubiquitin-dependent protein degradation. Annu Rev Genet *30*, 405-439.

Hoege, C., Pfander, B., Moldovan, G. L., Pyrowolakis, G., and Jentsch, S. (2002). RAD6-dependent DNA repair is linked to modification of PCNA by ubiquitin and SUMO. Nature *419*, 135-141.

Holmes, D. S., and Quigley, M. (1981). A rapid boiling method for the preparation of bacterial plasmids. Anal Biochem *114*, 193-197.

Holmstrom, S., Van Antwerp, M. E., and Iniguez-Lluhi, J. A. (2003). Direct and distinguishable inhibitory roles for SUMO isoforms in the control of transcriptional synergy. Proc Natl Acad Sci U S A *100*, 15758-15763.

Hong, W., Nakazawa, M., Chen, Y. Y., Kori, R., Vakoc, C. R., Rakowski, C., and Blobel, G. A. (2005). FOG-1 recruits the NuRD repressor complex to mediate transcriptional repression by GATA-1. Embo J *24*, 2367-2378.

Hong, Y., Rogers, R., Matunis, M. J., Mayhew, C. N., Goodson, M. L., Park-Sarge, O. K., and Sarge, K. D. (2001). Regulation of heat shock transcription factor 1 by stress-induced SUMO-1 modification. J Biol Chem *276*, 40263-40267.

Horike, S., Cai, S., Miyano, M., Cheng, J. F., and Kohwi-Shigematsu, T. (2005). Loss of silent-chromatin looping and impaired imprinting of DLX5 in Rett syndrome. Nat Genet *37*, 31-40.

Huang, T. T., Wuerzberger-Davis, S. M., Wu, Z. H., and Miyamoto, S. (2003). Sequential modification of NEMO/IKKgamma by SUMO-1 and ubiquitin mediates NF-kappaB activation by genotoxic stress. Cell *115*, 565-576.

Humphrey, G. W., Wang, Y., Russanova, V. R., Hirai, T., Qin, J., Nakatani, Y., and Howard, B. H. (2001). Stable histone deacetylase complexes distinguished by the presence of SANT domain proteins CoREST/kiaa0071 and Mta-L1. J Biol Chem *276*, 6817-6824.

Iniguez-Lluhi, J. A., and Pearce, D. (2000). A common motif within the negative regulatory regions of multiple factors inhibits their transcriptional synergy. Mol Cell Biol *20*, 6040-6050.

Ishov, A. M., Sotnikov, A. G., Negorev, D., Vladimirova, O. V., Neff, N., Kamitani, T., Yeh, E. T., Strauss, J. F., 3rd, and Maul, G. G. (1999). PML is critical for ND10 formation and recruits the PML-interacting protein daxx to this nuclear structure when modified by SUMO-1. J Cell Biol *147*, 221-234.

Jackson, P. K. (2001). A new RING for SUMO: wrestling transcriptional responses into nuclear bodies with PIAS family E3 SUMO ligases. Genes Dev *15*, 3053-3058.

Jeffery, L., and Nakielny, S. (2004). Components of the DNA methylation system of chromatin control are RNA-binding proteins. J Biol Chem *279*, 49479-49487.

Johnson, E. S. (2004). Protein modification by SUMO. Annu Rev Biochem *73*, 355-382.

Johnson, E. S., and Gupta, A. A. (2001). An E3-like factor that promotes SUMO conjugation to the yeast septins. Cell *106*, 735-744.

Johnson, E. S., Schwienhorst, I., Dohmen, R. J., and Blobel, G. (1997). The ubiquitin-like protein Smt3p is activated for conjugation to other proteins by an Aos1p/Uba2p heterodimer. Embo J *16*, 5509-5519.

Jones, P. A., and Baylin, S. B. (2002). The fundamental role of epigenetic events in cancer. Nat Rev Genet *3*, 415-428.

Jones, P. L., Veenstra, G. J., Wade, P. A., Vermaak, D., Kass, S. U., Landsberger, N., Strouboulis, J., and Wolffe, A. P. (1998). Methylated DNA and MeCP2 recruit histone deacetylase to repress transcription. Nat Genet *19*, 187-191.

Kagey, M. H., Melhuish, T. A., and Wotton, D. (2003). The polycomb protein Pc2 is a SUMO E3. Cell *113*, 127-137.

Kahyo, T., Nishida, T., and Yasuda, H. (2001). Involvement of PIAS1 in the sumoylation of tumor suppressor p53. Mol Cell *8*, 713-718.

Kaji, K., Caballero, I. M., MacLeod, R., Nichols, J., Wilson, V. A., and Hendrich, B. (2006). The NuRD component Mbd3 is required for pluripotency of embryonic stem cells. Nat Cell Biol *8*, 285-292.

Kaludov, N. K., and Wolffe, A. P. (2000). MeCP2 driven transcriptional repression in vitro: selectivity for methylated DNA, action at a distance and contacts with the basal transcription machinery. Nucleic Acids Res *28*, 1921-1928.

Kamitani, T., Kito, K., Nguyen, H. P., Wada, H., Fukuda-Kamitani, T., and Yeh, E. T. (1998). Identification of three major sentrinization sites in PML. J Biol Chem *273*, 26675-26682.

Kang, J., Gocke, C. B., and Yu, H. (2006). Phosphorylation-facilitated sumoylation of MEF2C negatively regulates its transcriptional activity. BMC Biochem *7*, 5.

Karin, M., and Ben-Neriah, Y. (2000). Phosphorylation meets ubiquitination: the control of NF-[kappa]B activity. Annu Rev Immunol *18*, 621-663.

Kass, S. U., Landsberger, N., and Wolffe, A. P. (1997). DNA methylation directs a time-dependent repression of transcription initiation. Curr Biol *7*, 157-165.

Kawasaki, H., and Taira, K. (2004). Induction of DNA methylation and gene silencing by short interfering RNAs in human cells. Nature *431*, 211-217.

Kerr, A. M., Nomura, Y., Armstrong, D., Anvret, M., Belichenko, P. V., Budden, S., Cass, H., Christodoulou, J., Clarke, A., Ellaway, C.*, et al.* (2001). Guidelines for reporting clinical features in cases with MECP2 mutations. Brain Dev *23*, 208-211.

Kim, J., Cantwell, C. A., Johnson, P. F., Pfarr, C. M., and Williams, S. C. (2002). Transcriptional activity of CCAAT/enhancer-binding proteins is controlled by a conserved inhibitory domain that is a target for sumoylation. J Biol Chem *277*, 38037-38044.

Kim, K. I., Baek, S. H., and Chung, C. H. (2002). Versatile protein tag, SUMO: its enzymology and biological function. J Cell Physiol *191*, 257-268.

Kim, K. I., Baek, S. H., Jeon, Y. J., Nishimori, S., Suzuki, T., Uchida, S., Shimbara, N., Saitoh, H., Tanaka, K., and Chung, C. H. (2000). A new SUMO-1-specific protease, SUSP1, that is highly expressed in reproductive organs. J Biol Chem *275*, 14102-14106.

Kim, Y. H., Choi, C. Y., and Kim, Y. (1999). Covalent modification of the homeodomain-interacting protein kinase 2 (HIPK2) by the ubiquitin-like protein SUMO-1. Proc Natl Acad Sci U S A *96*, 12350-12355.

Klose, R. J., and Bird, A. P. (2006). Genomic DNA methylation: the mark and its mediators. Trends Biochem Sci *31*, 89-97.

Klose, R. J., Sarraf, S. A., Schmiedeberg, L., McDermott, S. M., Stancheva, I., and Bird, A. P. (2005). DNA binding selectivity of MeCP2 due to a requirement for A/T sequences adjacent to methyl-CpG. Mol Cell *19*, 667-678.

Kondo, E., Gu, Z., Horii, A., and Fukushige, S. (2005). The thymine DNA glycosylase MBD4 represses transcription and is associated with methylated p16(INK4a) and hMLH1 genes. Mol Cell Biol *25*, 4388-4396.

Kouzarides, T. (2002). Histone methylation in transcriptional control. Curr Opin Genet Dev *12*, 198-209.

Kriaucionis, S., and Bird, A. (2004). The major form of MeCP2 has a novel N-terminus generated by alternative splicing. Nucleic Acids Res *32*, 1818-1823.

Laemmli, U. K. (1970). Cleavage of structural proteins during the assembly of the head of bacteriophage T4. Nature *227*, 680-685.

Lallemand-Breitenbach, V., Zhu, J., Puvion, F., Koken, M., Honore, N., Doubeikovsky, A., Duprez, E., Pandolfi, P. P., Puvion, E., Freemont, P., and de The, H. (2001). Role of promyelocytic leukemia (PML) sumolation in nuclear body formation, 11S proteasome recruitment, and As2O3-induced PML or PML/retinoic acid receptor alpha degradation. J Exp Med *193*, 1361-1371.

Le Guezennec, X., Vermeulen, M., Brinkman, A. B., Hoeijmakers, W. A., Cohen, A., Lasonder, E., and Stunnenberg, H. G. (2006). MBD2/NuRD and MBD3/NuRD, two distinct complexes with different biochemical and functional properties. Mol Cell Biol *26*, 843-851.

Lee, P. S., Chang, C., Liu, D., and Derynck, R. (2003). Sumoylation of Smad4, the common Smad mediator of transforming growth factor-beta family signaling. J Biol Chem *278*, 27853-27863.

Lehembre, F., Muller, S., Pandolfi, P. P., and Dejean, A. (2001). Regulation of Pax3 transcriptional activity by SUMO-1-modified PML. Oncogene *20*, 1-9.

Lehnertz, B., Ueda, Y., Derijck, A. A., Braunschweig, U., Perez-Burgos, L., Kubicek, S., Chen, T., Li, E., Jenuwein, T., and Peters, A. H. (2003). Suv39h-mediated histone H3 lysine 9 methylation directs DNA methylation to major satellite repeats at pericentric heterochromatin. Curr Biol *13*, 1192-1200.

Lewis, J. D., Meehan, R. R., Henzel, W. J., Maurer-Fogy, I., Jeppesen, P., Klein, F., and Bird, A. (1992). Purification, sequence, and cellular localization of a novel chromosomal protein that binds to methylated DNA. Cell *69*, 905-914.

Li, H., Leo, C., Zhu, J., Wu, X., O'Neil, J., Park, E. J., and Chen, J. D. (2000). Sequestration and inhibition of Daxx-mediated transcriptional repression by PML. Mol Cell Biol *20*, 1784-1796.

Li, S. J., and Hochstrasser, M. (1999). A new protease required for cell-cycle progression in yeast. Nature *398*, 246-251.

Li, S. J., and Hochstrasser, M. (2000). The yeast ULP2 (SMT4) gene encodes a novel protease specific for the ubiquitin-like Smt3 protein. Mol Cell Biol *20*, 2367-2377.

Lin, D., Tatham, M. H., Yu, B., Kim, S., Hay, R. T., and Chen, Y. (2002). Identification of a substrate recognition site on Ubc9. J Biol Chem *277*, 21740-21748.

Lin, X., Liang, M., Liang, Y. Y., Brunicardi, F. C., and Feng, X. H. (2003). SUMO-1/Ubc9 promotes nuclear accumulation and metabolic stability of tumor suppressor Smad4. J Biol Chem *278*, 31043-31048.

Lin, X., Liang, M., Liang, Y. Y., Brunicardi, F. C., Melchior, F., and Feng, X. H. (2003). Activation of transforming growth factor-beta signaling by SUMO-1 modification of tumor suppressor Smad4/DPC4. J Biol Chem *278*, 18714-18719.

Lin, X., Sun, B., Liang, M., Liang, Y. Y., Gast, A., Hildebrand, J., Brunicardi, F. C., Melchior, F., and Feng, X. H. (2003). Opposed regulation of corepressor CtBP by SUMOylation and PDZ binding. Mol Cell *11*, 1389-1396.

Liu, B., Liao, J., Rao, X., Kushner, S. A., Chung, C. D., Chang, D. D., and Shuai, K. (1998). Inhibition of Stat1-mediated gene activation by PIAS1. Proc Natl Acad Sci U S A *95*, 10626-10631.

Long, J., Wang, G., He, D., and Liu, F. (2004). Repression of Smad4 transcriptional activity by SUMO modification. Biochem J *379*, 23-29.

Loyola, A., and Almouzni, G. (2004). Histone chaperones, a supporting role in the limelight. Biochim Biophys Acta *1677*, 3-11.

Mahajan, R., Delphin, C., Guan, T., Gerace, L., and Melchior, F. (1997). A small ubiquitin-related polypeptide involved in targeting RanGAP1 to nuclear pore complex protein RanBP2. Cell *88*, 97-107.

Makedonski, K., Abuhatzira, L., Kaufman, Y., Razin, A., and Shemer, R. (2005). MeCP2 deficiency in Rett syndrome causes epigenetic aberrations at the PWS/AS imprinting center that affects UBE3A expression. Hum Mol Genet *14*, 1049-1058.

Matunis, M. J., Coutavas, E., and Blobel, G. (1996). A novel ubiquitin-like modification modulates the partitioning of the Ran-GTPase-activating protein RanGAP1 between the cytosol and the nuclear pore complex. J Cell Biol *135*, 1457-1470.

Matunis, M. J., Wu, J., and Blobel, G. (1998). SUMO-1 modification and its role in targeting the Ran GTPase-activating protein, RanGAP1, to the nuclear pore complex. J Cell Biol *140*, 499-509.

McCutchan, T. F., Hansen, J. L., Dame, J. B., and Mullins, J. A. (1984). Mung bean nuclease cleaves Plasmodium genomic DNA at sites before and after genes. Science *225*, 625-628.

Meehan, R. R., Lewis, J. D., McKay, S., Kleiner, E. L., and Bird, A. P. (1989). Identification of a mammalian protein that binds specifically to DNA containing methylated CpGs. Cell *58*, 499-507.

Mendoza, H. M., Shen, L. N., Botting, C., Lewis, A., Chen, J., Ink, B., and Hay, R. T. (2003). NEDP1, a highly conserved cysteine protease that deNEDDylates Cullins. J Biol Chem *278*, 25637-25643.

Millar, C. B., Guy, J., Sansom, O. J., Selfridge, J., MacDougall, E., Hendrich, B., Keightley, P. D., Bishop, S. M., Clarke, A. R., and Bird, A. (2002). Enhanced CpG mutability and tumorigenesis in MBD4-deficient mice. Science *297*, 403-405.

Mnatzakanian, G. N., Lohi, H., Munteanu, I., Alfred, S. E., Yamada, T., MacLeod, P. J., Jones, J. R., Scherer, S. W., Schanen, N. C., Friez, M. J., *et al.* (2004). A previously unidentified MECP2 open reading frame defines a new protein isoform relevant to Rett syndrome. Nat Genet *36*, 339-341.

Moilanen, A. M., Karvonen, U., Poukka, H., Yan, W., Toppari, J., Janne, O. A., and Palvimo, J. J. (1999). A testis-specific androgen receptor coregulator that belongs to a novel family of nuclear proteins. J Biol Chem *274*, 3700-3704.

Morris, K. V., Chan, S. W., Jacobsen, S. E., and Looney, D. J. (2004). Small interfering RNA-induced transcriptional gene silencing in human cells. Science *305*, 1289-1292.

Muller, S., Berger, M., Lehembre, F., Seeler, J. S., Haupt, Y., and Dejean, A. (2000). c-Jun and p53 activity is modulated by SUMO-1 modification. J Biol Chem *275*, 13321-13329.

Nakao, M., Matsui, S., Yamamoto, S., Okumura, K., Shirakawa, M., and Fujita, N. (2001). Regulation of transcription and chromatin by methyl-CpG binding protein MBD1. Brain Dev *23 Suppl 1*, S174-176.

Nan, X., Campoy, F. J., and Bird, A. (1997). MeCP2 is a transcriptional repressor with abundant binding sites in genomic chromatin. Cell *88*, 471-481.

Nan, X., Meehan, R. R., and Bird, A. (1993). Dissection of the methyl-CpG binding domain from the chromosomal protein MeCP2. Nucleic Acids Res *21*, 4886-4892.

Nan, X., Ng, H. H., Johnson, C. A., Laherty, C. D., Turner, B. M., Eisenman, R. N., and Bird, A. (1998). Transcriptional repression by the methyl-CpG-binding protein MeCP2 involves a histone deacetylase complex. Nature *393*, 386-389.

Ng, H. H., Jeppesen, P., and Bird, A. (2000). Active repression of methylated genes by the chromosomal protein MBD1. Mol Cell Biol *20*, 1394-1406.

Ng, H. H., Zhang, Y., Hendrich, B., Johnson, C. A., Turner, B. M., Erdjument-Bromage, H., Tempst, P., Reinberg, D., and Bird, A. (1999). MBD2 is a transcriptional repressor belonging to the MeCP1 histone deacetylase complex. Nat Genet *23*, 58-61.

Nishida, T., Kaneko, F., Kitagawa, M., and Yasuda, H. (2001). Characterization of a novel mammalian SUMO-1/Smt3-specific isopeptidase, a homologue of rat axam, which is an axin-binding protein promoting beta-catenin degradation. J Biol Chem *276*, 39060-39066.

Nishida, T., Tanaka, H., and Yasuda, H. (2000). A novel mammalian Smt3-specific isopeptidase 1 (SMT3IP1) localized in the nucleolus at interphase. Eur J Biochem *267*, 6423-6427.

Nishida, T., and Yasuda, H. (2002). PIAS1 and PIASxalpha function as SUMO-E3 ligases toward androgen receptor and repress androgen receptor-dependent transcription. J Biol Chem *277*, 41311-41317.

Nuber, U. A., Kriaucionis, S., Roloff, T. C., Guy, J., Selfridge, J., Steinhoff, C., Schulz, R., Lipkowitz, B., Ropers, H. H., Holmes, M. C., and Bird, A. (2005). Up-regulation of glucocorticoid-regulated genes in a mouse model of Rett syndrome. Hum Mol Genet *14*, 2247-2256.

Okano, M., Bell, D. W., Haber, D. A., and Li, E. (1999). DNA methyltransferases Dnmt3a and Dnmt3b are essential for de novo methylation and mammalian development. Cell *99*, 247-257.

Okano, M., Xie, S., and Li, E. (1998). Cloning and characterization of a family of novel mammalian DNA (cytosine-5) methyltransferases. Nat Genet *19*, 219-220.

Okuma, T., Honda, R., Ichikawa, G., Tsumagari, N., and Yasuda, H. (1999). In vitro SUMO-1 modification requires two enzymatic steps, E1 and E2. Biochem Biophys Res Commun *254*, 693-698.

Pal, S., Vishwanath, S. N., Erdjument-Bromage, H., Tempst, P., and Sif, S. (2004). Human SWI/SNF-associated PRMT5 methylates histone H3 arginine 8 and negatively regulates expression of ST7 and NM23 tumor suppressor genes. Mol Cell Biol *24*, 9630-9645.

Park, J. I., Kim, S. W., Lyons, J. P., Ji, H., Nguyen, T. T., Cho, K., Barton, M. C., Deroo, T., Vleminckx, K., Moon, R. T., and McCrea, P. D. (2005). Kaiso/p120-catenin and TCF/beta-catenin complexes coordinately regulate canonical Wnt gene targets. Dev Cell *8*, 843-854.

Peterson, C. L., and Laniel, M. A. (2004). Histones and histone modifications. Curr Biol *14*, R546-551.

Pichler, A., Gast, A., Seeler, J. S., Dejean, A., and Melchior, F. (2002). The nucleoporin RanBP2 has SUMO1 E3 ligase activity. Cell *108*, 109-120.

Pickart, C. M. (2001). Mechanisms underlying ubiquitination. Annu Rev Biochem *70*, 503-533.

Polly, P., Herdick, M., Moehren, U., Baniahmad, A., Heinzel, T., and Carlberg, C. (2000). VDR-Alien: a novel, DNA-selective vitamin D(3) receptor-corepressor partnership. Faseb J *14*, 1455-1463.

Poukka, H., Karvonen, U., Janne, O. A., and Palvimo, J. J. (2000). Covalent modification of the androgen receptor by small ubiquitin-like modifier 1 (SUMO-1). Proc Natl Acad Sci U S A *97*, 14145-14150.

Prokhortchouk, A., Hendrich, B., Jorgensen, H., Ruzov, A., Wilm, M., Georgiev, G., Bird, A., and Prokhortchouk, E. (2001). The p120 catenin partner Kaiso is a DNA methylation-dependent transcriptional repressor. Genes Dev *15*, 1613-1618.

Rigaut, G., Shevchenko, A., Rutz, B., Wilm, M., Mann, M., and Seraphin, B. (1999). A generic protein purification method for protein complex characterization and proteome exploration. Nat Biotechnol *17*, 1030-1032.

Robertson, K. D., Ait-Si-Ali, S., Yokochi, T., Wade, P. A., Jones, P. L., and Wolffe, A. P. (2000). DNMT1 forms a complex with Rb, E2F1 and HDAC1 and represses transcription from E2F-responsive promoters. Nat Genet *25*, 338-342.

Rodriguez, M. S., Dargemont, C., and Hay, R. T. (2001). SUMO-1 conjugation in vivo requires both a consensus modification motif and nuclear targeting. J Biol Chem *276*, 12654-12659.

Roloff, T. C., and Nuber, U. A. (2005). Chromatin, epigenetics and stem cells. Eur J Cell Biol *84*, 123-135.

Ross, S., Best, J. L., Zon, L. I., and Gill, G. (2002). SUMO-1 modification represses Sp3 transcriptional activation and modulates its subnuclear localization. Mol Cell *10*, 831-842.

Rountree, M. R., Bachman, K. E., and Baylin, S. B. (2000). DNMT1 binds HDAC2 and a new co-repressor, DMAP1, to form a complex at replication foci. Nat Genet *25*, 269-277.

Rountree, M. R., Bachman, K. E., Herman, J. G., and Baylin, S. B. (2001). DNA methylation, chromatin inheritance, and cancer. Oncogene *20*, 3156-3165.

Ruzov, A., Dunican, D. S., Prokhortchouk, A., Pennings, S., Stancheva, I., Prokhortchouk, E., and Meehan, R. R. (2004). Kaiso is a genome-wide repressor of transcription that is essential for amphibian development. Development *131*, 6185-6194.

Saitoh, H., and Hinchey, J. (2000). Functional heterogeneity of small ubiquitin-related protein modifiers SUMO-1 versus SUMO-2/3. J Biol Chem *275*, 6252-6258.

Samaco, R. C., Hogart, A., and LaSalle, J. M. (2005). Epigenetic overlap in autism-spectrum neurodevelopmental disorders: MECP2 deficiency causes reduced expression of UBE3A and GABRB3. Hum Mol Genet *14*, 483-492.

Sapetschnig, A., Rischitor, G., Braun, H., Doll, A., Schergaut, M., Melchior, F., and Suske, G. (2002). Transcription factor Sp3 is silenced through SUMO modification by PIAS1. Embo J *21*, 5206-5215.

Sarraf, S. A., and Stancheva, I. (2004). Methyl-CpG binding protein MBD1 couples histone H3 methylation at lysine 9 by SETDB1 to DNA replication and chromatin assembly. Mol Cell *15*, 595-605.

Schwartz, D. C., and Hochstrasser, M. (2003). A superfamily of protein tags: ubiquitin, SUMO and related modifiers. Trends Biochem Sci *28*, 321-328.

Schwienhorst, I., Johnson, E. S., and Dohmen, R. J. (2000). SUMO conjugation and deconjugation. Mol Gen Genet *263*, 771-786.

Seeler, J. S., and Dejean, A. (2003). Nuclear and unclear functions of SUMO. Nat Rev Mol Cell Biol *4*, 690-699.

Seeler, J. S., Marchio, A., Losson, R., Desterro, J. M., Hay, R. T., Chambon, P., and Dejean, A. (2001). Common properties of nuclear body protein SP100 and TIF1alpha chromatin factor: role of SUMO modification. Mol Cell Biol *21*, 3314-3324.

Seeler, J. S., Marchio, A., Sitterlin, D., Transy, C., and Dejean, A. (1998). Interaction of SP100 with HP1 proteins: a link between the promyelocytic leukemia-associated nuclear bodies and the chromatin compartment. Proc Natl Acad Sci U S A *95*, 7316-7321.

Sekimata, M., and Homma, Y. (2004). Sequence-specific transcriptional repression by an MBD2-interacting zinc finger protein MIZF. Nucleic Acids Res *32*, 590-597.

Sekimata, M., Takahashi, A., Murakami-Sekimata, A., and Homma, Y. (2001). Involvement of a novel zinc finger protein, MIZF, in transcriptional repression by interacting with a methyl-CpG-binding protein, MBD2. J Biol Chem *276*, 42632-42638.

Shanklin, J., Jabben, M., and Vierstra, R. D. (1987). Red light-induced formation of ubiquitin-phytochrome conjugates: Identification of possible intermediates of phytochrome degradation. Proc Natl Acad Sci U S A *84*, 359-363.

Shcherbik, N., and Haines, D. S. (2004). Ub on the move. J Cell Biochem *93*, 11-19.

Shiio, Y., and Eisenman, R. N. (2003). Histone sumoylation is associated with transcriptional repression. Proc Natl Acad Sci U S A *100*, 13225-13230.

Shirohzu, H., Kubota, T., Kumazawa, A., Sado, T., Chijiwa, T., Inagaki, K., Suetake, I., Tajima, S., Wakui, K., Miki, Y., *et al.* (2002). Three novel DNMT3B mutations in Japanese patients with ICF syndrome. Am J Med Genet *112*, 31-37.

Siegfried, Z., Eden, S., Mendelsohn, M., Feng, X., Tsuberi, B. Z., and Cedar, H. (1999). DNA methylation represses transcription in vivo. Nat Genet *22*, 203-206.

Song, J., Durrin, L. K., Wilkinson, T. A., Krontiris, T. G., and Chen, Y. (2004). Identification of a SUMO-binding motif that recognizes SUMO-modified proteins. Proc Natl Acad Sci U S A *101*, 14373-14378.

Standke, G. J., Meier, V. S., and Groner, B. (1994). Mammary gland factor activated by prolactin on mammary epithelial cells and acute-phase response factor activated by interleukin-6 in liver cells share DNA binding and transactivation potential. Mol Endocrinol *8*, 469-477.

Stelter, P., and Ulrich, H. D. (2003). Control of spontaneous and damage-induced mutagenesis by SUMO and ubiquitin conjugation. Nature *425*, 188-191.

Sternsdorf, T., Jensen, K., Reich, B., and Will, H. (1999). The nuclear dot protein sp100, characterization of domains necessary for dimerization, subcellular localization, and modification by small ubiquitin-like modifiers. J Biol Chem *274*, 12555-12566.

Subramanian, L., Benson, M. D., and Iniguez-Lluhi, J. A. (2003). A synergy control motif within the attenuator domain of CCAAT/enhancer-binding protein alpha inhibits transcriptional synergy through its PIASy-enhanced modification by SUMO-1 or SUMO-3. J Biol Chem *278*, 9134-9141.

Tabor, S., and Richardson, C. C. (1987). DNA sequence analysis with a modified bacteriophage T7 DNA polymerase. Proc Natl Acad Sci U S A *84*, 4767-4771.

Takahashi, Y., Kahyo, T., Toh, E. A., Yasuda, H., and Kikuchi, Y. (2001). Yeast Ull1/Siz1 is a novel SUMO1/Smt3 ligase for septin components and functions as an adaptor between conjugating enzyme and substrates. J Biol Chem *276*, 48973-48977.

Tan, J. A., Hall, S. H., Hamil, K. G., Grossman, G., Petrusz, P., and French, F. S. (2002). Protein inhibitors of activated STAT resemble scaffold attachment factors and function as interacting nuclear receptor coregulators. J Biol Chem *277*, 16993-17001.

Tatematsu, K. I., Yamazaki, T., and Ishikawa, F. (2000). MBD2-MBD3 complex binds to hemi-methylated DNA and forms a complex containing DNMT1 at the replication foci in late S phase. Genes Cells *5*, 677-688.

Tatham, M. H., Jaffray, E., Vaughan, O. A., Desterro, J. M., Botting, C. H., Naismith, J. H., and Hay, R. T. (2001). Polymeric chains of SUMO-2 and SUMO-3 are conjugated to protein substrates by SAE1/SAE2 and Ubc9. J Biol Chem *276*, 35368-35374.

Terui, Y., Saad, N., Jia, S., McKeon, F., and Yuan, J. (2004). Dual role of sumoylation in the nuclear localization and transcriptional activation of NFAT1. J Biol Chem *279*, 28257-28265.

Tiefenbach, J., Novac, N., Ducasse, M., Eck, M., Melchior, F., and Heinzel, T. (2006). SUMOylation of the corepressor N-CoR modulates its capacity to repress transcription. Mol Biol Cell *17*, 1643-1651.

Tong, J. K., Hassig, C. A., Schnitzler, G. R., Kingston, R. E., and Schreiber, S. L. (1998). Chromatin deacetylation by an ATP-dependent nucleosome remodelling complex. Nature *395*, 917-921.

Topark-Ngarm, A., Golonzhka, O., Peterson, V. J., Barrett, B., Jr., Martinez, B., Crofoot, K., Filtz, T. M., and Leid, M. (2006). CTIP2 associates with the NuRD complex on the promoter of p57KIP2, a newly identified CTIP2 target gene. J Biol Chem.

Tudor, M., Akbarian, S., Chen, R. Z., and Jaenisch, R. (2002). Transcriptional profiling of a mouse model for Rett syndrome reveals subtle transcriptional changes in the brain. Proc Natl Acad Sci U S A *99*, 15536-15541.

Tyler, J. K., and Kadonaga, J. T. (1999). The "dark side" of chromatin remodeling: repressive effects on transcription. Cell *99*, 443-446.

Ulrich, H. D. (2005). Mutual interactions between the SUMO and ubiquitin systems: a plea of no contest. Trends Cell Biol *15*, 525-532.

van Roy, F. M., and McCrea, P. D. (2005). A role for Kaiso-p120ctn complexes in cancer? Nat Rev Cancer *5*, 956-964.

Verger, A., Perdomo, J., and Crossley, M. (2003). Modification with SUMO. A role in transcriptional regulation. EMBO Rep *4*, 137-142.

Vertegaal, A. C., Ogg, S. C., Jaffray, E., Rodriguez, M. S., Hay, R. T., Andersen, J. S., Mann, M., and Lamond, A. I. (2004). A proteomic study of SUMO-2 target proteins. J Biol Chem *279*, 33791-33798.

Wade, P. A. (2001). Methyl CpG-binding proteins and transcriptional repression. Bioessays *23*, 1131-1137.

Wade, P. A., Gegonne, A., Jones, P. L., Ballestar, E., Aubry, F., and Wolffe, A. P. (1999). Mi-2 complex couples DNA methylation to chromatin remodelling and histone deacetylation. Nat Genet *23*, 62-66.

Wade, P. A., Jones, P. L., Vermaak, D., and Wolffe, A. P. (1998). A multiple subunit Mi-2 histone deacetylase from Xenopus laevis cofractionates with an associated Snf2 superfamily ATPase. Curr Biol *8*, 843-846.

Wakefield, R. I., Smith, B. O., Nan, X., Free, A., Soteriou, A., Uhrin, D., Bird, A. P., and Barlow, P. N. (1999). The solution structure of the domain from MeCP2 that binds to methylated DNA. J Mol Biol *291*, 1055-1065.

Watt, F., and Molloy, P. L. (1988). Cytosine methylation prevents binding to DNA of a HeLa cell transcription factor required for optimal expression of the adenovirus major late promoter. Genes Dev *2*, 1136-1143.

Westermarck, J., Weiss, C., Saffrich, R., Kast, J., Musti, A. M., Wessely, M., Ansorge, W., Seraphin, B., Wilm, M., Valdez, B. C., and Bohmann, D. (2002). The DEXD/H-box RNA helicase RHII/Gu is a co-factor for c-Jun-activated transcription. Embo J *21*, 451-460.

Wigler, M., Pellicer, A., Silverstein, S., and Axel, R. (1978). Biochemical transfer of single-copy eucaryotic genes using total cellular DNA as donor. Cell *14*, 725-731.

Wong, E., Yang, K., Kuraguchi, M., Werling, U., Avdievich, E., Fan, K., Fazzari, M., Jin, B., Brown, A. M., Lipkin, M., and Edelmann, W. (2002). Mbd4 inactivation increases Cright-arrowT transition mutations and promotes gastrointestinal tumor formation. Proc Natl Acad Sci U S A *99*, 14937-14942.

Wu, J., and Grunstein, M. (2000). 25 years after the nucleosome model: chromatin modifications. Trends Biochem Sci *25*, 619-623.

Wu, K., Yamoah, K., Dolios, G., Gan-Erdene, T., Tan, P., Chen, A., Lee, C. G., Wei, N., Wilkinson, K. D., Wang, R., and Pan, Z. Q. (2003). DEN1 is a dual function protease capable of processing the C terminus of Nedd8 and deconjugating hyper-neddylated CUL1. J Biol Chem *278*, 28882-28891.

Xue, Y., Wong, J., Moreno, G. T., Young, M. K., Cote, J., and Wang, W. (1998). NURD, a novel complex with both ATP-dependent chromatin-remodeling and histone deacetylase activities. Mol Cell *2*, 851-861.

Yang, S. H., Jaffray, E., Hay, R. T., and Sharrocks, A. D. (2003). Dynamic interplay of the SUMO and ERK pathways in regulating Elk-1 transcriptional activity. Mol Cell *12*, 63-74.

Yang, S. H., and Sharrocks, A. D. (2004). SUMO promotes HDAC-mediated transcriptional repression. Mol Cell *13*, 611-617.

Yang, X. J., and Seto, E. (2003). Collaborative spirit of histone deacetylases in regulating chromatin structure and gene expression. Curr Opin Genet Dev *13*, 143-153.

Yao, Y. L., and Yang, W. M. (2003). The metastasis-associated proteins 1 and 2 form distinct protein complexes with histone deacetylase activity. J Biol Chem *278*, 42560-42568.

Yeh, E. T., Gong, L., and Kamitani, T. (2000). Ubiquitin-like proteins: new wines in new bottles. Gene *248*, 1-14.

Yoon, H. G., Chan, D. W., Reynolds, A. B., Qin, J., and Wong, J. (2003). N-CoR mediates DNA methylation-dependent repression through a methyl CpG binding protein Kaiso. Mol Cell *12*, 723-734.

Young, J. I., Hong, E. P., Castle, J. C., Crespo-Barreto, J., Bowman, A. B., Rose, M. F., Kang, D., Richman, R., Johnson, J. M., Berget, S., and Zoghbi, H. Y. (2005). Regulation of RNA splicing by the methylation-dependent transcriptional repressor methyl-CpG binding protein 2. Proc Natl Acad Sci U S A *102*, 17551-17558.

Yu, F., Thiesen, J., and Stratling, W. H. (2000). Histone deacetylase-independent transcriptional repression by methyl-CpG-binding protein 2. Nucleic Acids Res *28*, 2201-2206.

Zhang, H., Saitoh, H., and Matunis, M. J. (2002). Enzymes of the SUMO modification pathway localize to filaments of the nuclear pore complex. Mol Cell Biol *22*, 6498-6508.

Zhang, H., Smolen, G. A., Palmer, R., Christoforou, A., van den Heuvel, S., and Haber, D. A. (2004). SUMO modification is required for in vivo Hox gene regulation by the Caenorhabditis elegans Polycomb group protein SOP-2. Nat Genet *36*, 507-511.

Zhang, Y., LeRoy, G., Seelig, H. P., Lane, W. S., and Reinberg, D. (1998). The dermatomyositis-specific autoantigen Mi2 is a component of a complex containing histone deacetylase and nucleosome remodeling activities. Cell *95*, 279-289.

Zhang, Y., Ng, H. H., Erdjument-Bromage, H., Tempst, P., Bird, A., and Reinberg, D. (1999). Analysis of the NuRD subunits reveals a histone deacetylase core complex and a connection with DNA methylation. Genes Dev *13*, 1924-1935.

Zhong, S., Muller, S., Ronchetti, S., Freemont, P. S., Dejean, A., and Pandolfi, P. P. (2000). Role of SUMO-1-modified PML in nuclear body formation. Blood *95*, 2748-2752.

Plasmids

pAB-Gal$_{94}$-hp66α$_{1-205}$.

This vector was generated by in-frame insertion of the *Eco*RI/*Hind*III fragment from pSG5-hp66α into the pAB-Gal$_{94}$ linker opened with *Sal*I/*Hind*III.

pAB-Gal$_{94}$-hp66α$_{205-345}$.

This vector was created by subclonting the *Hind*III/*Not*I fragment from pSG5-hp66α and in-frame ligation into the pAB-Gal$_{94}$ linker digested with *Cfr*9I.

pAB-Gal$_{94}$-hp66α$_{205-475}$.

This vector was cloned by excision of the *Hind*III/*Eco47*III fragment out of pSG5-hp66α into the pAB-Gal$_{94}$ linker cut with *Eco47*III.

pAB-Gal$_{94}$-hp66α$_{345-475}$.

This vector was created by in-frame insertion of the *Not*I/*Eco47*III fragment from pSG5-hp66α into the pAB-Gal$_{94}$ linker opened with *SalI/Eco47*III.

pAB-Gal$_{94}$-hp66α$_{345-633}$.

This vector was generated by in-frame ligation of the *Not*I/*Bgl*II fragment from pSG5-hp66α into the pAB-Gal$_{94}$ linker cut with *Sal*I/*BamH*I.

pAB-Gal$_{94}$-hp66α$_{475-633}$.

This vector was constructed by cutting the *Eco47*III/*Bgl*II fragment from pSG5-hp66α and in-frame insertion into the pAB-Gal$_{94}$ linker digested with *Eco47*III/*BamH*I.

pAB-Gal$_{94}$-hp66αK30R.

This vector was created via mutagenesis PCR with the sense primers 5'-GTGGAGAGCAAGAAAAT A**A**G**A**ATGGAGAGAGGATTGTTG -3' and antisense primers 5'- CAACAATCCTCTCTCCATTCT TATTTTCTTGCTCTCCAC -3' on pAB-Gal$_{94}$-hp66α by using the QuikChange site-directed mutagenesis kit according to the manufacturer's instructions.

pAB-Gal$_{94}$-hp66αK149R.

This vector was generated via mutagenesis PCR with the sense primers 5'-GGATGATCAAGC

AGCTGAGGGAAGAATTGAGGTTAG-3' and antisense primers 5'-CTAACCTCAATTC TTCCCTCAGCT GCTTGATCATCC-3' on pAB-Gal_{94}-hp66α by using the QuikChange site-directed mutagenesis kit.

pAB-Gal_{94}-hp66αK451R.

This vector was made via mutagenesis PCR with the sense primers 5'- GAAGAAGGCGCT CAGGGTGGAGCACACC-3' and antisense primers 5'- GGTGTGCTCCACCCTGAGCGCC TTCTTC -3' on pAB-Gal_{94}-hp66α by using the QuikChange site-directed mutagenesis kit.

pAB-Gal_{94}-hp66αK487R.

This vector was generated via mutagenesis PCR with the sense primers 5'- CCTGCACAGGC CAGGGCCGAGCCCACC -3' and antisense primers 5'- GGTGGGCTCGGCCCTGGCCTGT GCAGG -3' on pAB-Gal_{94}-hp66α by using the QuikChange site-directed mutagenesis kit.

pAB-Gal_{94}-hp66αK30RK149R.

This vector was created via mutagenesis PCR with the K149R mutagenesis primers on pAB-Gal_{94}-hp66αK30R by using the QuikChange site-directed mutagenesis kit.

pAB-Gal_{94}-hp66αK30RK451R.

This vector was made via mutagenesis PCR with the K451R mutagenesis primers on pAB-Gal_{94}-hp66αK30R by using the QuikChange site-directed mutagenesis kit.

pAB-Gal_{94}-hp66αK149RK451R.

This vector was created via mutagenesis PCR with the K451R mutagenesis primers on pAB-Gal_{94}-hp66αK149R by using the QuikChange site-directed mutagenesis kit.

pAB-Gal_{94}-hp66αK451RK487R.

This vector was generated via mutagenesis PCR with the K487R mutagenesis primers on pAB-Gal_{94}-hp66αK451R by using the QuikChange site-directed mutagenesis kit.

pAB-Gal_{94}-hp66αK30RK149RK451R.

This vector was made via mutagenesis PCR with the K451R mutagenesis primers on pAB-Gal_{94}-hp66αK30RK149R by using the QuikChange site-directed mutagenesis kit.

pAB-Gal$_{94}$-hp66αK30RK149RK451RK487R.

This vector was constructed by ligation of the *Not*I/*BamH*I fragment from pAB-Gal$_{94}$-hp66αK451RK487R into the pAB-Gal$_{94}$-hp66αK30RK149R digested with *Not*I/*BamH*I.

pAB-Gal$_{94}$-hp66β$_{1-225}$.

This vector was created by in-frame ligation of the *EcoR*I/*Hind*III fragment out of pSG5-hp66β into the pAB-Gal$_{94}$ linker opened with Eco47III/*Hind*III.

pAB-Gal$_{94}$-hp66β$_{225-349}$.

This vector was generated by excision of the *Hind*III/*Not*I fragment from pSG5-hp66β into the pAB-Gal$_{94}$ linker cut with *Cfr9*I.

pAB-Gal$_{94}$-hp66β$_{225-479}$.

This vector was cloned by cutting *Hind*III/*Eco47*III fragment from pSG5-hp66β and in-frame insertion into the pAB-Gal$_{94}$ linker digested with *Eco47*III.

pAB-Gal$_{94}$-hp66β$_{349-479}$.

This vector was created by subcloning the *Not*I/*Eco47*III fragment from pSG5-hp66β into the pAB-Gal$_{94}$ linker cut with *SalI/Eco47*III.

pAB-Gal$_{94}$-hp66β$_{349-593}$.

This vector was generated by in-frame insertion of the *Not*I/*BamH*I fragment from pSG5-hp66β into the pAB-Gal$_{94}$ linker opened with *Sal*I/*BamH*I.

pAB-Gal$_{94}$-hp66β$_{479-593}$.

This vector was constructed by excision of the *Eco47*III/*BamH*I fragment out of pSG5-hp66β and in-frame ligation into the pAB-Gal$_{94}$ linker digested with *Eco47*III/*BamH*I.

pAB-Gal$_{94}$-hp66βK33R.

This vector was generated via mutagenesis PCR with the sense primers 5'-GGCAAAGCGAC TC**A**G**A**ATGGAGGGGCATG -3' and antisense primers 5'- CATGCCCCTCCATTCTGAGT CGCTTTGCC -3' on pAB-Gal$_{94}$-hp66β by using the QuikChange site-directed mutagenesis kit.

pAB-Gal$_{94}$-hp66βK454R.

This vector was created via mutagenesis PCR with the sense primers 5'- CCAGAAAAAGGCT CTAAGAGCTGAACACACCAACC -3' and antisense primers 5'- GGTTGGTGTGTTCAG CTCTTAGAGCCTTTTTCTGG -3' on pAB-Gal$_{94}$-hp66β by using the QuikChange site-directed mutagenesis kit.

pAB-Gal$_{94}$-hp66βK33RK454R.

This vector was made via mutagenesis PCR with the K454R mutagenesis primers on pAB-Gal$_{94}$-hp66βK33R by using the QuikChange site-directed mutagenesis kit.

pEGFPC2-hp66αK30R.

The EGFP fusions of hp66αK30R was generated by subcloning the *Sal*I/*BamH*I fragment of pAB-Gal$_{94}$-hp66αK30R followed by insertion into pEGFP-hp66α opened with *Sal*I/*BamH*I.

pEGFPC2-hp66αK149R.

The EGFP fusions of hp66αK149R was constructed by excision of the *Sal*I/*BamH*I fragment out of pAB-Gal$_{94}$-hp66αK149R and insertion into pEGFP-hp66α digested with *Sal*I/*BamH*I.

pEGFPC2-hp66αK487R.

The EGFP fusions of hp66αK487R was created by ligation of the *Sal*I/*BamH*I fragment of pAB-Gal-p66αK487R into pEGFP-p66α opened with *Sal*I/*BamH*I.

pEGFPC2-hp66βK33R.

The EGFP fusions of hp66βK33R was generated by insertion of the *Sal*I/*BamH*I fragment of pAB-Gal$_{94}$-hp66βK33R into pEGFP-hp66β digested with *Sal*I/*BamH*I.

pEGFPC2-hp66βK454R.

The EGFP fusions of hp66βK454R was made by cutting the *Sal*I/*BamH*I fragment of pAB-Gal$_{94}$-hp66βK454R followed by insertion into pEGFP-hp66β cut with *Sal*I/*BamH*I.

pSG5-hp66α mutants for cloning of deletion constructs.

pSG5-hp66α*Hind*III$_{mut}$ at position aa205 was created by using sense primer:5'-CATTCCTG CTGGCAAGCTTTCACTCCAGACCTCTTC-3' and antisense primer: 5'-GAAGAGGTCTG GAGTGAAA GCTTGCCAGCAGGAATG-3'. pSG5-hp66α*Eco47*III$_{mut}$ at position aa475 was generated by using sense primer: 5'-GAGATTGAGCAGCGCTTGCTGCAGCAGGGCACG-

3’ and antisense primer: 5’-CGTGCCCTGCTGCAGCAAGCGCTGCTCAATCTC-3’. pSG5-hp66α*Eco47*III$_{del}$, the naturally occurring *Eco47*III site at position aa14 was deleted via using sense primer: 5’-GGAGTCAGA AACGAGCCCTTGAACGGGACCC-3’ and antisense primer: 5’-GGGTCCCGTTCAAGGGCTC GTTTCTGACTCC-3’.

pSG5-hp66β mutants for cloning of deletion constructs.

pSG5-hp66β*Not*I$_{mut}$ at position aa349 was generated via using sense primer: 5’-GCCAACTCA CAGGCGGCCGCCAAATTGGCTC-3’ and antisense primer: 5’-GAGCCAATTTGGCGGC CGCCTGTGAGTTGGC-3’. pSG5-hp66β*Eco47*III$_{mut}$ at position aa479 was created by using sense primer:5’-AGGAAATTGAACAGCGCTTACAGCAGCAGGCAGC-3’ and antisense primer: 5’-GCTGCCTGC TGCTGTAAGCGCTGTTCAATTTCCT-3’.

pSG5-hp66αK149R.

This vector was created by ligation of the *Sal*I/*BamH*I fragment from pAB-Gal$_{94}$-hp66αK149R into pSG5-hp66β digested with *Sal*I/*BamH*I.

pcDNA3-FLAG-hp66α$_{mut}$/hp66β$_{mut}$-CBP.

This vector were generated with PCR from pBK-CMV-FLAG-hp66α/hp66ß-CBP. The PCR products were digested with *BamH*I/*Xba*I and ligated into pcDNA3-FLAG-hp66α.

pcDNA3-FLAG-CBP.

Control plasmid pcDNA3-FLAG-CBP was constructed with PCR from pBS1479, and cut with *BamH*I/*Xba*I and ligated into pcDNA3-FLAG-hp66α.

pBK-CMV-FLAG.

This vector was generated by digesting the annealed double strand oligos, (sense strand: CTAGAGCCACCATGGACTACAAGGACGACGATGACAAGGCTAGCGAATTCGCTCG AGGGGATCCGAT, antisense strand: ATCGGATCCCCTCGAGCGAATTCGCTAGCCTTG TCATCGTCGTCCTTGTAGTCCATGGTGGCT) with *Spe*I/*Sma*I and inserted into pBK-CMV vector.

pBK-CMV-FLAG-hp66α$_{mut}$/hp66β$_{mut}$-CBP.

pBK-CMV-FLAG-hp66α/hp66ß-CBP was amplified by PCR from pSG5-hp66α/hp66β,

respectively. Products were then digested with *EcoR*I, *EcoR*I/*Xho*I and ligated into pBK-CMV-FLAG-CBP, respectively.

pBK-CMV-FLAG-CBP.

CBP(calmodulin binding peptide) was amplified by PCR from pBS1479 vector (Euroscarf), cut with *Xho*I/*BamH*I and inserted into pBK-CMV-FLAG.

pSilencer hMBD2

This vector was generated by annealing oligos 5'-GATCCGGGTAAACCAGACTTGAATTT CAAGAG AATTCAAGTCTGGTTTACCCTTTTTTGGAAA-3' and 5'-AGCTT TTCCAAA AAAGGGTAAAC CAGACTTGAATTCTCTTGAAATTCAAGTCTG GTTTACCCG-3' and ligating the product into pSilencer 2.1-U6 neo digested with *BamH*I/*Hind*III.

pN3-FLAG-SUMO1G97A

This vector was generated via mutagenesis PCR with the sense primers 5'-CAGGAACAAA CGGGGGCTCATTCAACAGTTTAG-3' and antisense primers 5'- CTAAACTGTTGAATGA GCCCCCGTTTGTTCCTG-3' on pN3-FLAG-SUMO1 by using the QuikChange site-directed mutagenesis kit.

pcDNA3-HA-Dominant negative Ubc9 (DN-Ubc9).

This vector was generated via mutagenesis PCR with the sense primers 5'- CTTCGGGG ACAGTGTCCCTGTCCATCTTAGAG-3' and antisense primers 5'- CTCTAAGATGGACA GGGACACTGTCCCCGAAG -3' on pcDNA3-HA-Ubc9 by using the QuikChange site-directed mutagenesis kit.

pCMV-GST-hp66α.

This eukaryotic expression vectors was generated by cutting the *Bgl*II/*BamH*I fragment of pEGFP-C1-hp66α and insertion into pCMV-GST cut with *Sal*I/NotI.

pCMV-GST-hp66β.

This eukaryotic expression vectors was cloned by ligation of the *Bgl*II/*BamH*I fragment of pEGFP-C1-hp66β into pCMV-GST digested with *Sal*I/*Not*I.

pCMV-GST-MBD3.

This eukaryotic expression vectors was constructed by subcloning the *BamH*I/*Sal*I fragment of c-Myc-MBD3 into pCMV-GST cut with *BamH*I/*Sal*I.

pCMV-GST-HDAC1.

The eukaryotic expression vectors pCMV-GST-HDAC1 was cloned by cutting the *BamH*I/*Sal*I fragments of pcDNA3-HDAC1 and insertion into pCMV-GST digested with *BamH*I/*Sal*I.

pCMV-GST-RbAp46.

This vector was generated by in-frame ligation of the *Nco*I/*BamH*I fragment of RbAp46 into pCMV-GST opened with *BamH*I/*Xho*I.

pCMV-GST-RbAp48.

This vector was created by in-frame insertion of the *Nco*I/*Xho*I fragment of RbAp48 pCMV-GST cut with *BamH*I/*Not*I.

Abbreviations

%	percent
ºC	centigrade
A	adenosine
α	anti
Amp	ampicillin
APS	ammonium persulfate
ATP	adenosine triphosphate
bp	base pairs
BSA	bovine serum albumin
C	cytosine
$CaCl_2$	calcium chloride
$CaPO_4$	calcium phosphate
CBP	calmodulin binding peptide
cm	centimeter
CpG, CpGs	cytosine guanine dinucleotide
CR1, CR2	conserved region 1, 2
CsCl	caesium chloride
CTAB	cetyl trimethyl ammonium bromide
C-terminus	carboxyl-terminus
DBD	DNA Binding Domain
ddH_2O	double distilled water
dNTP	deoxynucleotide triphosphate
DMEM	Dulbecco's modified Eagle's medium
DMSO	dimethylformamide
DNA	deoxyribonucleic acid
DTT	dithiothreitol
E.coli	*Escherichia coli*
ECL	enhanced chemoluminescence
EDTA	ethylenediamine tetraacetic acid
et al.	*Et alli* (=and others)
FCS	fetal calf serum
Fig	Figure
g	gram
g	acceleration of gravity
G	guanosine
Gal_{94}	N-terminal 1-94 amino acids of yeast Gal_4 activator
GFP	green fluorescent protein
EGFP	enhanced green fluorescent protein
G3PDH / GAPDH	Glycerinaldehyd-3-phosphat Dehydrogenase
GST	glutathione-S-transferase
HATs	histone acetyltransferases
HBS	HEPES-buffered saline
HDAC	histondeacetylase
HEPES	n-2-Hydroxyethylpiperazine
HRP	horseradish peroxidase
k	kilo (10^3)

K	lysine
kDa	kilodalton
l	liter
LacZ	β-galactosidase
LB Medium	*Luria Bertani* Medium
ml	milliliter (10^{-3} liter)
M	molar; mol/l
mg	milligram
µl	microliter (10^{-6} liter)
MBD	methyl CpG binding domain
MBPs	methyl CpG binding proteins
MeCP1	methyl CpG binding protein complex 1
MeCP2	methyl CpG binding protein 2
Mi-2	dermatomyositis specific antigen
mRNA	messenger RNA
MTA	metastasis associated protein
MW	molecular weight
ng	nanogram (10^{-9} gram)
NaCl	sodium chloride
NaAc	sodium acetate
NaOH	sodium hydroxide
NEM	N-ethylmaleimide
NP-40	Nonidet P-40
N-terminus	amino-terminus
NuRD complex	nucleosome remodeling and deacetylase complex
OD_{600} (OD_{420})	optical density at 600 nm (420 nm)
ONPG	ortho-Nitrophenyl β-D-galactopyranoside
ORF	open reading frame
pmol	picomolar (10^{-12} molar)
PBS	phosphate buffered saline
PAGE	polyacrylamide gel electrophoresis
PCR	polymerase chain reaction
PIAS	protein inhibitor of activated STAT
PIC	protein inhibitor cocktail
PMSF	phenylmethylsulfonyl fluoride
PVDF	polyvinzlidene difluoride
R	arginine
RbAp46/48	retinoblastoma protein (Rb) associated protein 46/48
RLU	relative light unit
RNA	ribonucleic acid
RNase	ribonuclease
RNasin	ribonuclease inhibitor
RNAi	RNA interference
rpm	revolutions per minute
RT	room temperature
RT	reverse transcription
SDS	sodium dodecyl sulfate
SUMO	small ubiquitin related modifier

T	thymine
TAE	Tris-Acetate-EDTA buffer
TB-Medium	*Terrific-Broth*-Medium
TE	Tris-EDTA buffer
TEMED	n,n,n',n'-Tetramethylethylenediamine
T_m	melting temperature
Tris	Tris-hydroxymethylaminomethane
TSA	trichostatin A
Tween 20	polyoxyethylenesorbiten monolaurate
U	units
UAS	activating upstream sequence
Ubc9	ubiquitin conjugating enzyme 9units
UV	ultraviolet
V	volt
vol	volume
v /v	volume pencentage
wt	wild type
w/v	weight pencentage

Acknowledgement

I would like to express deep sense of gratitude to my supervisor Prof. Renkawitz for giving the opportunity to work in his outstanding department as a Ph.D student. It was only with his constant support, excellent guidance, creative discussions, and permanent encouragement which were the key to my success to finish my work. Moreover, I am also grateful for his careful and critical review of my thesis.

Further I would like to thank Prof. Dr. Ewald Beck for being my co-supervisor of this work and for his scientific advice and friendly inspiration on my study.

Special thanks are addressed to Dr. Brackertz, who creates friendly and scientific atmosphere in the Lab322. His patience and encouragement helped me to settle down at the beginning of my study. His invaluable insight and scientific criticism encouraged me to make progress in my study. My sincere thanks to Sonja for her excellent technical assistance during this work.

I am eternally grateful to the countless people who have helped me along the way. I would like to say "Vielen Dank" to Aria, Jörg, Ölle, Man, Tine, Imke, Marek, Christine Paprotka, Les Burke, Angela, Magada, Leona, Maria, Oli, Maren, Frauke, Asim, Christina, for your kindly helps and the great scientific and social environment you created. Moreover, I would like to thank Doris, Leni, Briggit and Crista for your kindly assistant in preparation of experimental materials. I am so great with all of you in the parties, travels and game nights.

I thank the academic programs (Graduiertenkolleg) "Biochemistry of Nucleoprotein Complexes" for financial support of my experiment in Giessen University.

I would like to thank Anna and Jamilah for the great helps on administrative work throughout my stay at the department.

I am grateful to my Chinese friends Ru, Ying, Xinjiang, Yuchen, Shaojun, Yutong, Pingping, Yunbin, Jingyi, Zhengyu, Zhiguo, Feng, Junfeng, Ganhua for your friendship and kind help.

I am forever indebted to my parents and my younger sisters for providing me all their love, understanding and encouragement. I am forever grateful to Yan for her love, understanding and support during all these years.

Curriculum Vitae

Zi-Hua GONG

Personal Data

Name	Gong
First name	Zi-Hua
Date of birth	Dec,07,1974
Place of birth	Anhui, China
Nationality	P.R.China
Marital status	Single

Contact information

Institute for genetics
Justus-Liebig-University, Giessen,
Heinrich buff ring 58-62
D-35392, Germany
Phone: 0049-641-9935473 (office)
E-mail: zihua.gong@gen.bio.uni-giessen.de

SCIENTIFIC EDUCATION

Doctor of Philosophy 2003-present (candidate)	Institut for Genetics, Justus-Liebig-University, Giessen, Germany Major in Biology
Master of Science 1997-2000	Ruijin Hospital, Shanghai Second Mecical University Shanghai, China Major in gastroenterology of internal medicine
Bachelor of Medicine 1992-1997	Bengbu Medical College Anhui, China Major in clinical medicine
1989-1992	Chaohu No.1 high school Anhui, China

EMPLOYMENT EXPERIENCE

2000-2003	Worked as *resident* and *attending* doctor in the department of Gastroenterology in Shanghai First People's Hospital affiliated to Shanghai Jiaotong University

ACADEMIC CONFERENCES

Annual meeting of the German Genetics Society
Kassel, Germany, Sep. 26-28, 2003

International meeting ''Chromatin mediated biological decisions''
Marburg, Germany, Oct. 5-7, 2006

Erklärung

Ich versichere an Eides statt, daß ich die vorliegende Arbeit eigenständig ausgeführt und keine anderen als die angegebenen Hilfsmittel verwendet habe.

Alle Stellen, die in Wortlaut oder dem Sinn entsprechend aus anderen Arbeiten übernommen wurden, sind mit Quellenangaben als Zitat kenntlich gemacht.

Diese Arbeit wurde in dieser oder veränderter Form noch kneiner anderen Prüfungsbehörder vorgelegt.

Gießen, den 2006

Zihua Gong